



Fondo Sociale Europeo - FSE  
Programma Operativo Nazionale 2000/06  
"Ricerca, Sviluppo tecnologico ed Alta Formazione  
nelle regioni dell'Obiettivo 1" - Misura 1.1 (F.S.E)



**Università degli Studi della Calabria**

**Dottorato di Ricerca in Ingegneria Chimica e dei Materiali**

**Tesi**

**Development of new polymeric functional membranes for  
applications in catalysis and fuel cells**

**Settore Scientifico Disciplinare CHIM07 – Fondamenti chimici delle tecnologie**

*Supervisore*

Ch.mo Prof. Enrico Drioli

*Candidata*

Enrica Fontananova

Ciclo XX

*Il Coordinatore del Corso di Dottorato*

Ch.mo Prof. Rosario Aiello

---

**A.A. 2006-2007**

## SUMMARY

<b>Introduction</b>	I
<b>Chapter 1: Integration of molecular separation and chemical conversion in a catalytic membrane reactor (CMR)</b>	
1.1 Catalysis, sustainable growth and membrane technology	2
1.2 Integration of molecular separation and chemical conversion in a catalytic membrane reactor (CMR): advantages and limitations	3
1.3 Different types of CMRs	4
1.3.1 Extractor, distributor and contactor type membranes	4
1.3.2 Organic and inorganic CMRs	5
1.3.3 Biocatalytic membrane reactors	22
1.3.4 Catalytically active and catalytically passive membranes	25
1.4 Basic aspects for the heterogenization of catalysts in polymeric membranes	25
References	
1.5 Transport mechanism in porous and dense polymeric membranes	28
References	33
<b>Chapter 2: Integration of molecular separation and energy conversion in a fuel cell (FC)</b>	
2.1 Basic aspect of fuel cells technology	36
2.2 Thermodynamics fundamentals	40
2.3 Proton exchange membranes for PEMFC applications	43
2.3.1 Nafion and other polymers used in PEMFCs	43
2.3.2 Sulfonated PEEK and sulfonated PEEK-WC membranes	53
2.3.3 Mechanisms of proton transport in PEMs	59
References	62
<b>Chapter 3: Functionalization of polymeric membranes with transition metals-oxygen clusters: experimental, results and discussion</b>	
3.1 Heterogenization of polyoxometallates in polymeric membrane for oxidation reactions with a low environmental impact	66

3.1.1 Preparation and characterization of PVDF membranes containing decatungstate	69
3.1.2 Preparation and characterization of Hyflon membranes containing decatungstate	92
3.2 Heterogenization of heteropolyacids in proton exchange membranes for energy conversion	106

## **CONCLUSIONS**

v

## **Introduction**

Membrane science and technology has led to significant innovations in both processes and products particularly appropriate for a sustainable industrial growth. The basic properties of the membrane operations, i.e. simplicity in concept and operations, efficiency, modularity, reduced energy consumptions, make them very attractive for a more rational utilization of raw materials and waste minimization. The most interesting developments for industrial applications of membrane technology are related to the possibility to integrate various membrane operations in the same industrial cycle and/or to integrate membrane operations with traditional operations, with important benefits in product quality, plant compactness, environmental impact, and energy use.

Membrane technology has well established applications in many industrial processes (water desalination, wastewater treatments, fruit juices concentration, etc.) and more progresses can be anticipated in various sectors including catalytic reactions and energy production. The needs for fundamentals changes in these two strategic fields in term of sustainable development is the driving force of the impressive worldwide research effort in membrane technology applied to catalytic reactions (catalytic membrane reactors (CMRs)) and energy conversion systems (fuel cells (FCs)).

In the CMRs, the integration of molecular separation and chemical conversion is realized in a one unit in which the membrane can be catalytically active (catalyst entrapped in the membrane, or membrane made of an intrinsically catalytic material) or can serve to compartmentalize the catalyst in the reaction environment. Moreover in some CMRs the membrane function is to selectively supply reagents and/or to selectively remove products (membrane-assisted catalysis).

Catalytic reactions are intensively used in chemical industry, wastewater treatments and many other processes; however the necessity to realize a sustainable growth calls for additional and substantial developments in this field.

The main requirements that must be considered to produce an “ideal catalyst” are the following: low costs, high selectivity, high stability under reaction conditions, non-toxicity, “green properties”, first of all recoverability, i.e. the possibility to recover and reuse the catalyst.

In this perspective, the heterogenization of catalysts has interesting implications because it allows the reuse several time of the same catalyst. Among the different heterogenization methods, the entrapping of catalysts in membranes, or in general the use of a catalyst confined in a catalytic membrane reactor, offers new possibility for the design of new catalytic

processes. The CMRs have many advantages in comparison with traditional reactors. They are integrated processes; the catalyst can be easily recycled; the selective transport properties of the membranes can be used to shift the equilibrium conversion, to remove selectively products and by-products from the reaction mixture, to supply selectively the reagents. Moreover in a CMR with a suitable membrane it is possible to control the concentration profile of the reactants and, as a consequence, improved reactor performance can be obtained.

In the fuel cells the integration of molecular separation and energy conversion is instead carried out in an electrochemical device in which the selective transport of ions through an electrolyte occurs in combination with a redox reaction in order to convert chemical energy in electrical energy.

Fuel cell technology has many advantages in comparison with traditional energy conversion systems: high energy efficiency, zero- or near-zero emissions, very low noise emissions, reliability and simplicity, modularity and easy up- and down scaling.

The membranes have a central role in fuel cell technology not only in hydrogen production (by CMRs) and purification (by gas separation), but also as ion conducting electrolyte.

In a polymer electrolyte membrane fuel cell (PEMFC) the electrolyte is a proton exchange membrane which allows the transport of the protons (but not the electrons) from the anode, where they are produced in the oxidation of the fuel, typically  $H_2$  or methanol, to the cathode where the protons react with  $O_2$  to produce water. The electrons travel through the external circuit.

The desirable characteristics of a proton exchange membrane for PEMFCs are, not only high proton conductivity, but also low permeability to gases (in particular  $H_2$  and  $O_2$ ), low permeability to methanol and water, absence of electronic conductivity, chemical and mechanical stability under the operative condition over long time.

The aim of the present work is the design and development of new polymeric functional membranes for application in catalysis and fuel cell.

Although inorganic membranes are characterized by high chemical and thermal stability, they have also important drawbacks: high cost, limited lifetime, difficulties in manufacturing.

On the other hand, the use of polymeric membranes is of increasing interest. The cost of polymeric membranes is lower in comparison with inorganic ones and the preparation protocols allow a better reproducibility.

Polymeric membranes are generally less resistant to high temperatures and aggressive chemicals than inorganic, however, polymeric materials resistant under rather harsh conditions – such as. polyvinylidene fluoride, Hyflon and polydimethylsiloxane - are today available.

A very interesting alternative to polymeric and inorganic membranes are the composite membranes in which organic and inorganic phases coexisting in order to have synergistic effect on transport properties, mechanic and thermal stability, as well as to introduce new functionality.

In this work various polymeric membranes have been functionalized with inorganic additives in order to have composite membranes with catalytic activity or with improved proton conductivity for application respectively in CMRs and FCs.

Fluorinated polymeric membranes have been functionalized with polyoxometalates (POMs), polyanionic metal oxide clusters of early transition metals, having interesting properties for application in oxidation catalysis for fine chemistry and wastewater treatments. We have carried out the heterogenization of the decatungstate ( $W_{10}O_{32}^{4-}$ ), a photocatalyst, in polymeric membranes of PVDF. The polymeric catalytic membranes prepared by phase inversion technique, have been successfully applied in the aerobic mineralization of the phenol in water as model of organic pollutant.

In order to evaluate the effect of the polymeric environment on the catalyst activity, we also heterogenized the decatungstate (opportunely functionalized) also in perfluorinated membrane made of Hyflon<sup>®</sup>.

The Hyflon-based membranes embedding decatungstate have been used in the aerobic photo-oxidation of ethylbenzene.

Particular relevance have been given to the chemical-physical characterization of the membranes prepared because the understanding of the properties and behavior of these functionalized materials is fundamental in order to exploit their use as heterogeneous catalysts.

The POMs in the acid form or heteropolyacids (HPAs), have interesting properties, not only as oxidation or acid catalysts, but also as proton conductors for fuel cells applications. For this reason we have used some HPAs for the functionalization of cation exchange membranes.

Perfluorosulfonic acid based membranes (e.g. Nafion from Du Pont) still today dominate the market of the PEMFCs. These systems are characterized by an high proton conductivity and

good chemical, mechanical and thermal stability; however they have also relevant limitations: high cost, loss of proton conductivity at relative high temperature because of dehumidification problems and high methanol and water crossover which limit the efficiency of the FC.

In this work we have investigated a new engineered materials, the sulfonated derivative of an amorphous polyetheretherketone known as PEEK-WC (SPEEK-WC), as possible alternative to the Nafion membranes. SPEEK-WC polymers with different degree of sulfonation have been used for the preparation of dense membranes by phase inversion technique induced by solvent evaporation.

We developed also composite membranes entrapping the following HPAs in the polymeric matrix: tungstophosphoric acid ( $\text{H}_3\text{PW}_{12}\text{O}_{40}$ ), silicotungstic acid ( $\text{H}_4\text{SiW}_{12}\text{O}_{40}$ ) and phosphomolybdic acid ( $\text{H}_3\text{PMo}_{12}\text{O}_{40}$ ).

The polymeric and composite membranes have been characterized by chemical-physical and electrochemical characterization. The results obtained with each membrane have been compared with those obtained with a commercial Nafion 117 membrane, used as reference.

## **Chapter 1:**

# **Integration of molecular separation and chemical conversion in a catalytic membrane reactor (CMR)**



## 1.1 Catalysis, sustainable growth and membrane technology

Catalysis is today one of chemistry's most important and powerful technologies. Currently, about 90% of chemical manufacturing processes and more than 20% of all industrial products involve catalytic steps<sup>1</sup>. Catalytic reactions are intensively used in chemical industry, energy conversion, wastewater treatment, and in many other processes (Fig.1); however the necessity to realize a *sustainable growth* calls for additional and substantial developments in this field.

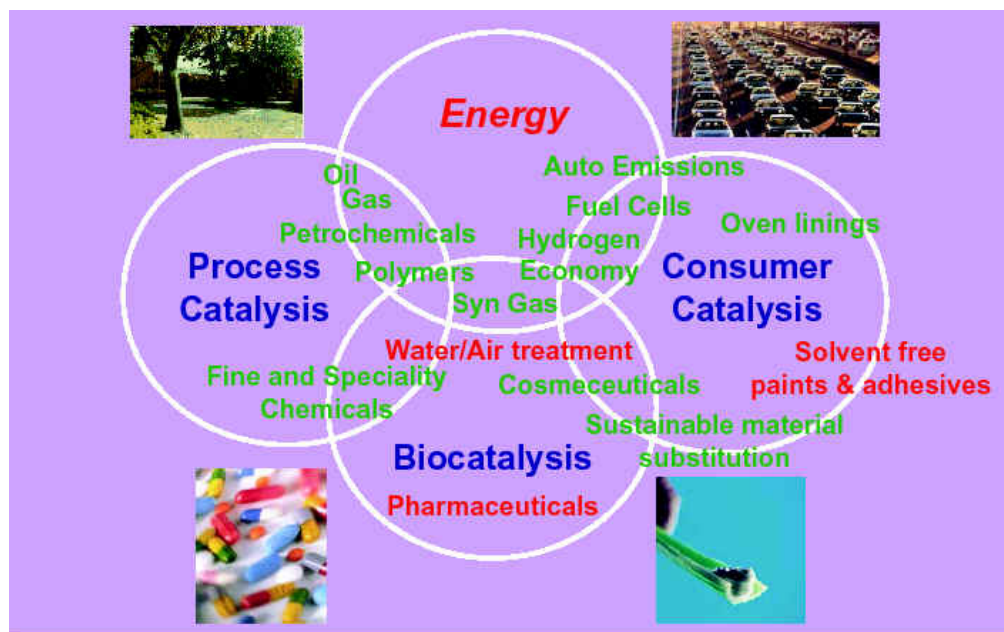


**Figure 1.** The European Technology Platform for Sustainable Chemistry individuated catalysis as a key technology in our society ([www.suschem.org](http://www.suschem.org))

Sustainable growth focuses on making progress to satisfy global human needs without damaging the environment. A promising way for the realization of a sustainable growth, is the strategy of the *process intensification*.<sup>2</sup> It consists of innovative equipments design and process development methods that are expected to bring substantial improvements manufacturing and processing, decreasing production costs, equipment size, energy consumption, waste generation and improving remote control, information fluxes and process flexibility.<sup>2</sup>

Membrane science and technology, whose basic aspects satisfy the requirements of the process intensification strategy, has led to significant innovation in both processes and products, particularly appropriate for sustainable industrial growth, over the past few decades.<sup>3</sup>

In this perspective, the application of membrane technology in integrated catalytic processes offers interesting opportunities.

## **1.2 Integration of molecular separation and chemical conversion in a catalytic membrane reactor (CMR): advantages and limitations**

The main characteristics of an “ideal catalyst” are the following: low cost, high selectivity, high stability under reaction conditions, non-toxicity and “green properties” first of all recoverability (possibility to reuse more times the same catalyst).

Most of these requirements can be addressed by the heterogenization of the catalyst using appropriate support materials.

Among the different heterogenization strategies, the entrapping of catalysts in membranes or, in general, the use of a catalyst confined by a membrane in the reactor, offers new possibility for the design of new catalytic processes.

In addition to the expected advantages typical of an integrated system (synergic effects on processing and economic aspects), the combination of advanced molecular separation and chemical conversion realized in a catalytic membrane reactor (CMR), has many advantages in comparison to traditional systems.<sup>4</sup>

CMRs can offer viable solutions to the main drawback of the homogeneous catalysis: the catalyst recycling. The catalyst can be heterogenized within or on the membrane surface (catalytically active membranes), otherwise the membrane simply compartmentalizes the catalyst in the reaction environment (catalytically passive membrane). In both cases is possible to reuse more times the same catalyst.

In addition, the membrane can actively take part in the reactive processes by controlling the concentration profiles thanks to the possibility to have membrane with well defined properties by the modulation of the membrane materials and structures.

Moreover, the selective transport properties of the membranes can be used to shift the equilibrium conversion by the removal of one product from the reaction mixture (e.g. hydrogen in in dehydrogenation reactions), or to increase the reaction selectivity by the controlled supply of the reagents (e.g. oxygen for partial oxidation reactions).

The membrane can also define the reaction volume (for example by providing a contacting zone for two immiscible phases, as in phase transfer catalysis) excluding polluting solvents and reducing the environmental impact of the process.

In numerous cases, membrane separation processes operate at much lower temperature, especially when compared with thermal processes such as reactive distillation. As a consequence they might provide a solution for the limited thermal stability of either catalyst and products. Furthermore, by membrane separation processes is possible also to separate non volatile components.

In some specific cases, the heat dissipated in an exothermic reaction can be used in an endothermic reaction, taking place at the opposite side of the membrane (for example in hydrogenation/dehydrogenation reactions).

The downstream processing of the products can be substantially facilitated when they are removed from the reaction mixture by means of a membrane

The still existing limitations in CMRs are related to the:

- manufacturing cost of the membranes and membrane modules,
- limited membrane life time,
- considerable technical complexity of the process which renders modeling and prediction more difficult.

### 1.3 Different types of CMRs

Because there are a lot of different way to combine a catalyst with a membrane, there are numerous possible classifications of the CMRs. Some useful classifications will be presented in the next sections using also examples reported in literature.

#### 1.3.1 Extractor, distributor and contactor type membranes

Depending on the type of selective transport through the membrane, we can have: extractor, distributor and contactor type CMRs (Fig. 2)

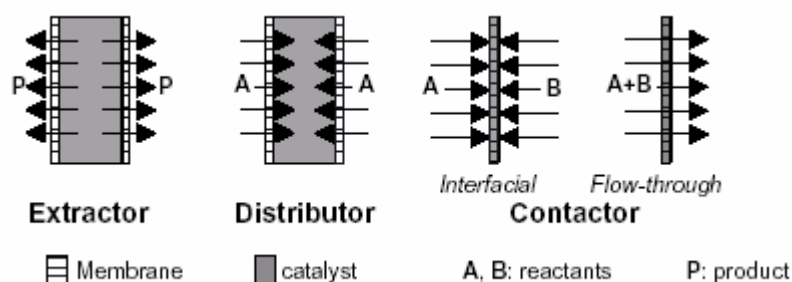


**Figure 2.** Three possible transport functions of the membrane in a CMR (from ref. 5)

In the **membrane extractor** the membrane is used to remove a reaction product from the reaction zone.

Typical advantages: increasing the reaction yields in equilibrium limited reactions; improving the selectivity towards a primary product in possible consecutive reactions via its selective

extraction through the membrane.

In the **membrane distributor** the membrane controls the introduction of one of the reactants in the reaction zone.

Main advantages achievable: reactants concentration is kept at a low level in the entire reaction zone increasing selectivity and/or reducing the possible dangerous interactions (e.g. with flammable or explosive mixtures)

In the **membrane contactor**: the membrane is used to facilitate the contact between reactants and catalyst. In the interfacial contactor configuration, reactants are introduced separately from the two side of the membrane. In the flow-trough configuration the reaction mixture is forced from one membrane side (the feed side) to permeate trough the membrane.

Potential advantages: improvements in activity and selectivity also controlling the contact time between catalyst and reagents (in the case of catalytically active membrane) acting on the operative conditions such as transmembrane pressure.

### 1.3.2 Organic and inorganic CMRs

According to the material used for the membrane preparation we can classify the CMRs in organic and inorganic.

Artificial membranes can be prepared starting from different materials: ceramics, metals, polymers, also in combination each other (hybrid or composite materials).

Membrane made of ceramic or metals, are generally indicated as inorganic.

**Inorganic membranes** are typically applied in high temperature reactions. They are characterized by an high thermal stability and resistance to aggressive environments. However inorganic membranes have also some important drawbacks: their cost is generally very high, their lifetime is limited (poisoning and fouling of the membranes), their brittleness is problematic.

The high operative temperature typical of the inorganic CMR led to difficulties in membrane-to-module sealing, moreover in the case of thin supported inorganic membrane, when materials with different thermal expansion coefficients are combined delamination of the membranes toplayer from the support can be a relevant problem.

Membrane characterized by highly selective transport mechanisms, such as palladium membranes for hydrogen purification and perovskite membranes used for oxygen separation, are at the base of the great interest for inorganic membranes used in combination with catalysis.

Pd dense membrane are characterized by a 100% theoretical selectivity towards the hydrogen.

Only hydrogen can permeate by a mechanism involving a series of steps:

- 1) adsorption; 2) dissociation; 3) ionization; 4) diffusion; 5) reassociation; 6) desorption (Fig. 3).

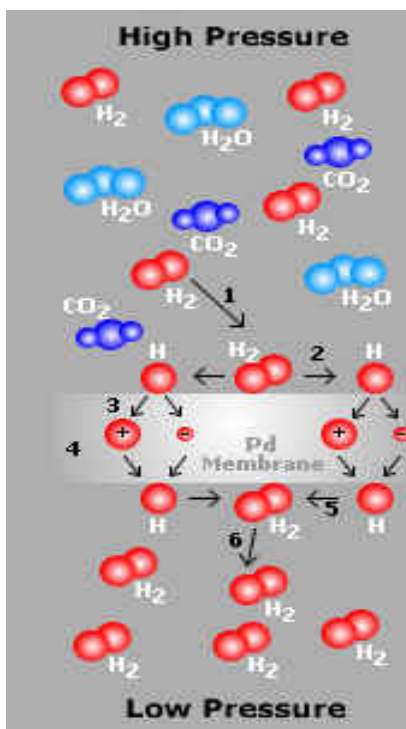


**Figure 3.** Selective transport of H<sub>2</sub> through a Pd membrane (from <http://www.stillwaterpalladium.com/hydrogen.html>)

To reduce the Pd consumption is possible to produced dense palladium alloy layers (Pd-Ag, Pd-Rh, etc.) on thermostable porous support.<sup>6</sup>

Palladium membranes have been extensively investigated for the performance improvement of the dehydrogenation and hydrogenation reactions. Combination of the dehydrogenation on one surface of the Pd-based catalytic membrane and hydrogenation by the diffused hydrogen on the other surface has been also proposed<sup>7</sup>. Thanks to the excellent thermal conductivity of these membranes, the heat released by the hydrogenation can be utilised to drive the endothermic dehydrogenation (Fig. 4).<sup>4</sup>

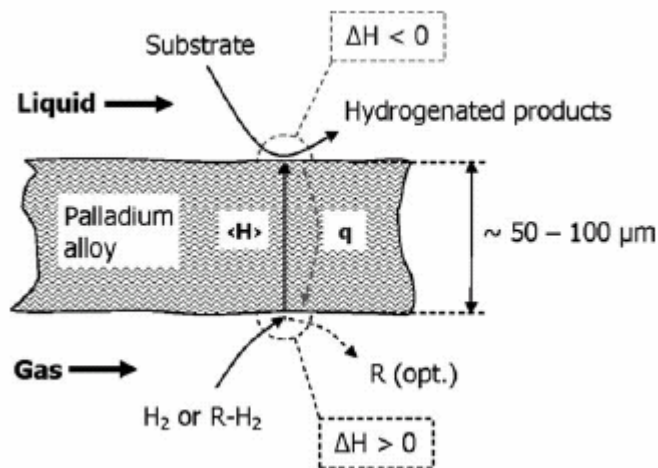


**Figure 4.** Scheme of the combination of a dehydrogenation reaction (endothermic) on one surface of a Pd-based catalytic membrane and a hydrogenation reaction (exothermic) by the diffused hydrogen on the other surface of a dense (from ref. 8).

Perovskites constitute an interesting group of solid state ion conductors for application in oxidation reactions.<sup>9</sup> The general perovskite stoichiometry is  $ABO_3$ . High ionic conductivity in perovskites is achieved by doping with elements that introduce oxygen vacancies.

For example a perovskite-type oxide of  $Ba_{0.5}Sr_{0.5}Co_{0.8}Fe_{0.2}O_{3-\delta}$  (BSCFO) showed mixed (electronic/oxygen ionic) conductivity at high temperatures.<sup>10</sup> Membranes made of this oxide have high oxygen permeability under air/helium oxygen partial pressure gradient.<sup>10</sup>

A membrane reactor made of BSCFO (Fig. 5) using a  $LiLaNiO_x/\gamma-Al_2O_3$  with 10 wt.% Ni loading as packed catalyst, has been successfully operated for partial oxidation of the methane (reaction 1) at 875.C for about 500 h without failure, with methane conversion of >97%, CO selectivity of >95% and oxygen permeation rate of about 11.5 ml/(cm<sup>2</sup> min).<sup>10</sup>



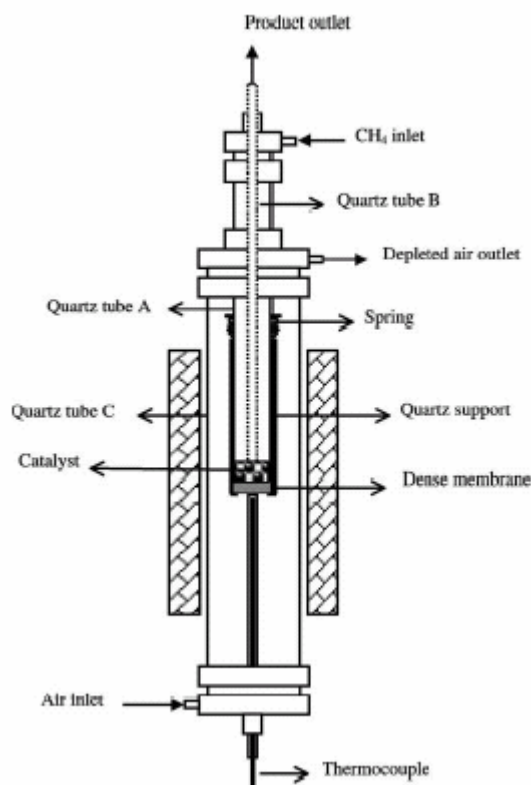


**Figure 5.** Scheme of the catalytic membrane reactor used for the partial oxidation of the methane (from ref. 10).

Also the mixed-conducting  $\text{SrFe}_{0.7}\text{Al}_{0.3}\text{O}_{3-\delta}$  (SFA) perovskite-like oxide, exhibits substantial catalytic activity towards partial oxidation of methane and has been presented as a possible component of monolithic ceramic reactors for synthesis gas generation, where the dense membrane and porous catalyst at the permeate-side surface are made of similar compositions.<sup>11</sup>

It has been suggested that the oxygen species diffusing through the membrane generate at its surface very active and selective oxygen entities that give higher yields than molecular oxygen.<sup>11</sup>

The use of a mixed oxygen ion–electronic conductor for oxygen separation with direct reforming of methane, followed by the use of a mixed protonic–electronic conductor for hydrogen extraction has been also proposed in literature (Fig. 6).<sup>12</sup> The products are thus pure hydrogen and synthesis gas with reduced hydrogen content, the latter suitable for example, in the Fisher–Tropsch synthesis of methanol.<sup>12</sup>

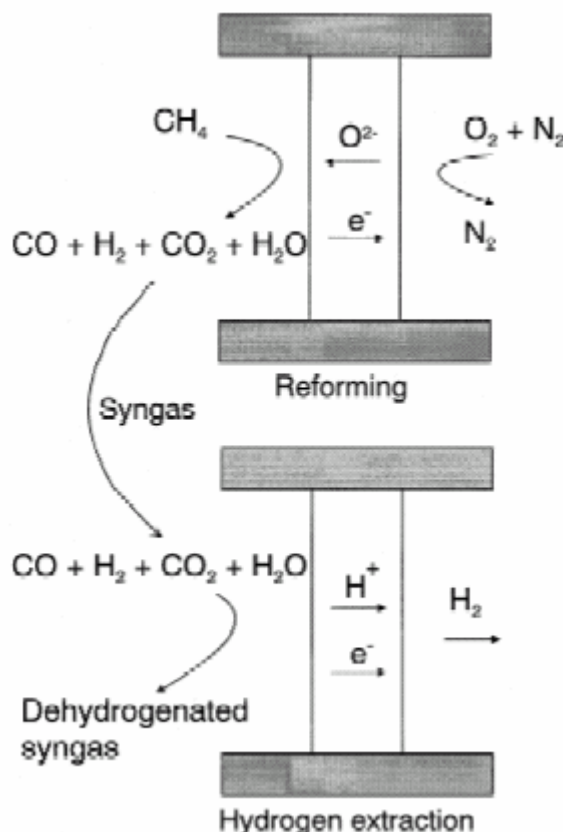
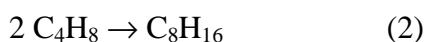


**Figure 6.** Mixed oxygen ion–electronic conductor used for oxygen separation with direct reforming of methane, followed by the use of a mixed protonic–electronic conductor for hydrogen extraction (from ref. 12.)

Because their high selectivity and elevated chemical and thermal resistance, also zeolite membranes are ideal candidates to increase the reaction yield by selective removal of one product.

Improved selectivity in the liquid-phase oligomerization of *i*-butene (reaction 2) by extraction of a primary product (*i*-octene - C<sub>8</sub>) in a zeolite membrane reactor (ZMR; acid resin catalyst bed located on the membrane tube side) respect to a conventional fixed bed reactor (FBR) has been reported<sup>13</sup>.



The MFI (silicalite) membrane selective removes the C<sub>8</sub> product from the reaction environment, thus reducing the formation of other unwanted by-product.



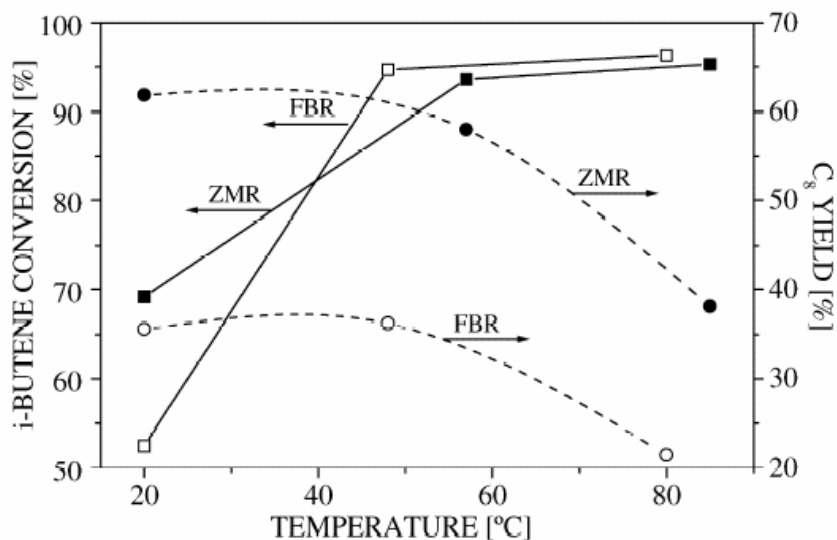


**Figure 7.** The i-butene conversion and i-octene yield as a function of temperature in a zeolite membrane reactor (ZMR) respect to a conventional fixed bed reactor (FBR) (from ref. 13).

Another interesting example is the isobutane (iC<sub>4</sub>) dehydrogenation (reaction 3) carried out in an extractor-type zeolite CMR (including a Pt-based fixed-bed catalyst) in which the removal of the hydrogen allows to overcome the equilibrium limitations.<sup>14</sup> In the same work the reaction was also carried out using a Pd membrane for the hydrogen removal (Fig. 8)

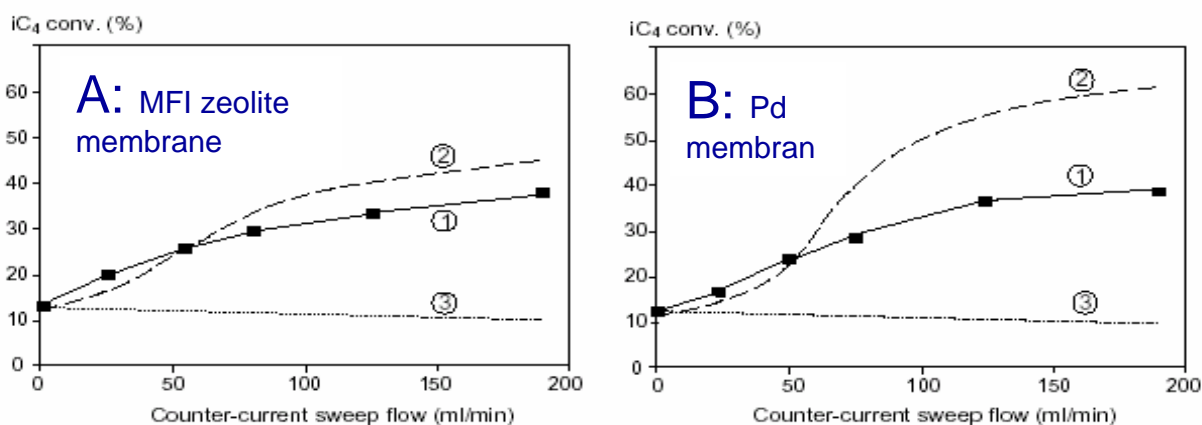
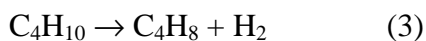


**Figure 8.** Isobutane (iC<sub>4</sub>) dehydrogenation carried out in two different CMRs:

**A:** MFI-zeolite membrane growth on a tubular alumina host material;

**B:** Pd membrane electroless deposited on the same tubular support.

(1) experimental data; (2) modelling; (3) thermodynamic equilibrium in a conventional reactor (From ref. 14)

Many interesting advantages have been also demonstrated in pervaporation (PV) assisted catalysis using both inorganic and organic membranes (Fig. 9).

Pervaporation is today considered as an interesting alternative for the separation of liquid mixtures which are difficult or not possible to separate by conventional distillation methods. PV assisted catalysis in comparison with reactive distillation has many advantages: the separation efficiency is not limited by relative volatility as in distillation; in pervaporation only a fraction of feed is forced to permeate through the membrane and undergoes the liquid-to vapor-phase change, and thus energy consumption is generally low as compared to distillation.

In these integrated processes, pervaporation is usually used to extract continuously one of the formed products in order to improve conversion of the reactants or to increase reaction selectivity.

By far the most studied reaction combined with pervaporation reaction is the esterification. It is a typical example of an equilibrium-limited reaction with industrial relevance.

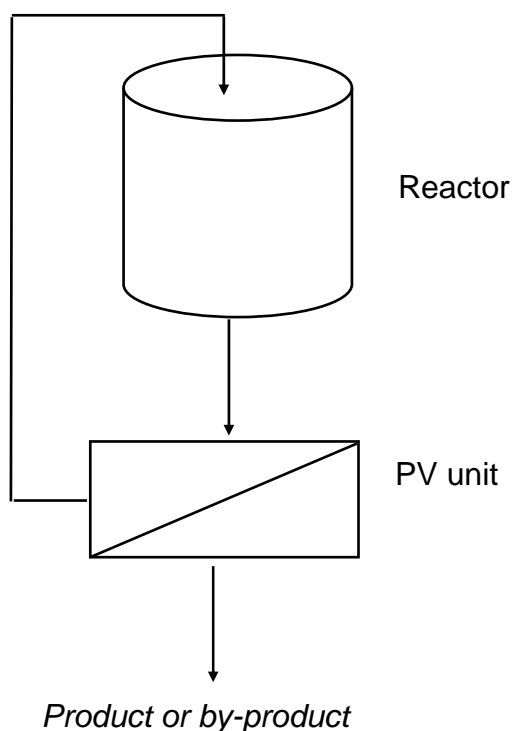
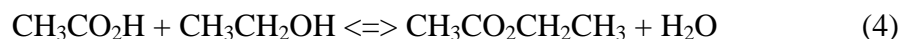


**Figure 9.** Scheme of a pervaporation-assisted catalytic process

The esterification of acetic acid with ethanol (reaction 4) has been investigated using zeolite membranes grown hydrothermally on the surface of a porous cylindrical alumina support (the catalyst used was a cation exchange resin).<sup>15</sup>



The conversion exceeded the equilibrium limit, by the selective removal through the membrane of water, and reached to almost 100% within 8 h (Fig. 10).

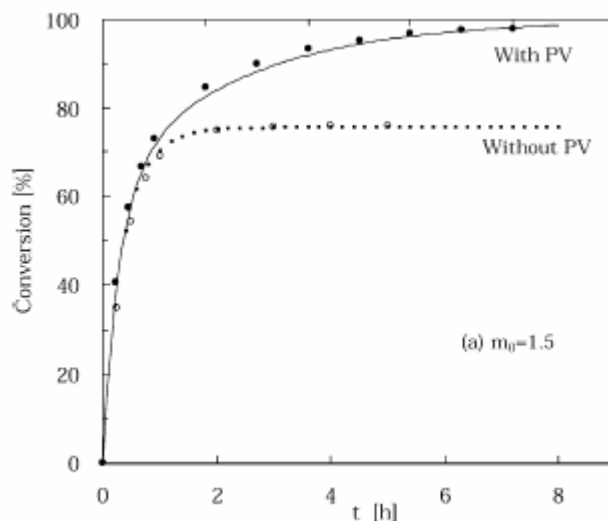


**Figure 10.** Conversion of the acetic acid in a catalytic reactor with and without water removal by PV (from ref. 15).

In the previous example the zeolitic membrane have only a separation function however they can acquire catalytic activity by the loading inside the zeolite pores of catalytic species. For example Pt-loaded catalytic membranes have been prepared by the ion-exchange of FAU (Na-Y) zeolitic membranes synthesized on tubular  $\alpha\text{-Al}_2\text{O}_3$  supports by a secondary growth method.<sup>16</sup> This catalytic zeolitic membrane has been used in the CO selective oxidation (Selox) for the purification of hydrogen-rich streams.<sup>16</sup>

**Organic membranes**, made of polymeric materials, are usually used when the reaction temperatures are lower, i.e. in the field of fine chemicals or when biocatalysts are present.

In a recent review Mathias Ulbricht<sup>17</sup> presented an interesting overview on the development of polymeric membranes having advanced or novel functions in the various membrane separation processes and in other important applications such as biotechnologies, sensors, catalysis and fuel cell systems.

The use of polymeric membranes in catalytic membrane reactors has an increasing interest because a much wider choice of polymeric materials is available as compared with inorganic membranes (Tab. 1) and the cost of polymeric membranes is generally lower, and the preparation protocols allow a better reproducibility. Moreover, the relatively low operating

temperatures, typical of the polymeric membranes, are associated with a less stringent demand for materials used in the reactor construction.<sup>4</sup>

In general, polymeric membranes are less resistant to high temperatures and aggressive chemicals than inorganic or metallic membranes; however, polymeric materials resistant under rather harsh conditions are today available.

One of the polymeric material more used for catalyst heterogenization is the polydimethylsiloxane (PDMS).

PDMS is an high permeable, rubbery polymer, characterized by an elevated chemical resistance also in organic solvent.<sup>18</sup> It is generally prepared from a two component system by a Pt catalysed hydrosilylation reaction (Fig. 11).

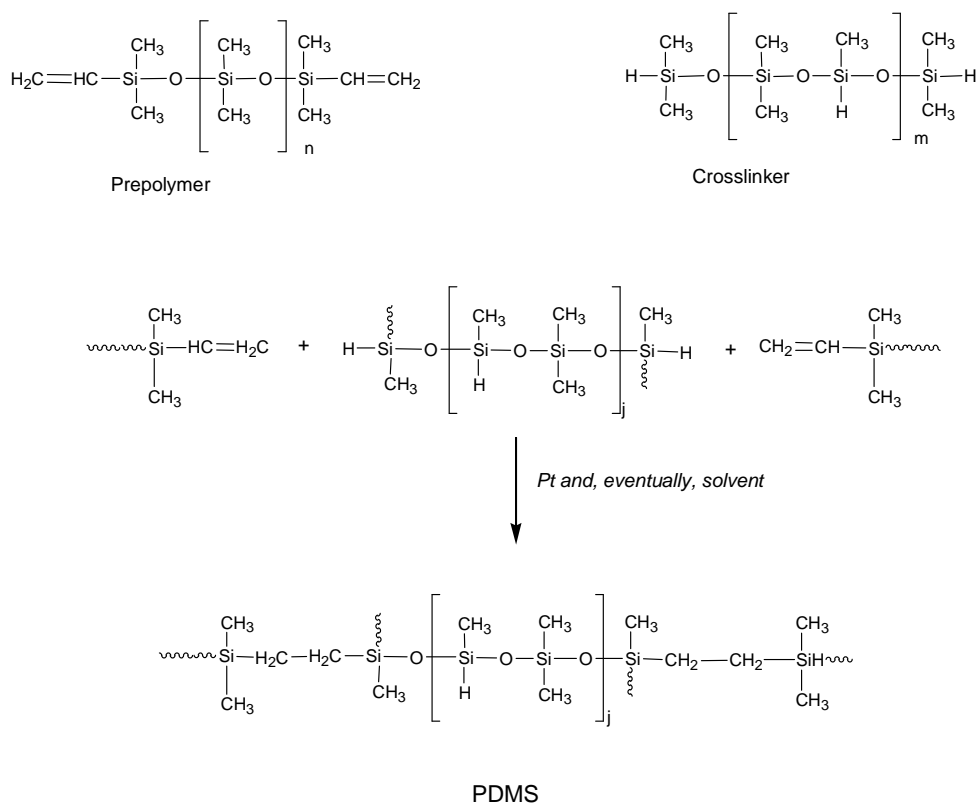


**Figure 11.** Scheme of the synthesis of the PDMS polymer from a prepolymer and a crosslinker (adapted from ref.. 4).

**Table 1.** Polymers materials commonly used for industrially established membranes separation processes(from ref. 17)

Polymer	Morphology			Membrane process
	Barrier type	Cross-section	Barrier thickness ( $\mu\text{m}$ )	
Cellulose acetates	Nonporous	Anisotropic	$\sim 0.1$	GS, RO
	Mesoporous	Anisotropic	$\sim 0.1$	UF
	Macroporous	Isotropic	50–300	MF
Cellulose nitrate	Macroporous	Isotropic	100–500	MF
Cellulose, regenerated	Mesoporous	Anisotropic	$\sim 0.1$	UF, D
Perfluorosulfonic acid polymer	Nonporous	Isotropic	50–500	ED, fuel cell
Polyacrylonitrile	Mesoporous	Anisotropic	$\sim 0.1$	UF
Polyetherimides	Mesoporous	Anisotropic	$\sim 0.1$	UF
Polyethersulfones	Mesoporous	Anisotropic	$\sim 0.1$	UF
	Macroporous	Isotropic	50–300	MF
Polyethylene terephthalate	Macroporous	Isotropic track-etched	6–35	MF
Polyphenylene oxide	Nonporous	Anisotropic	$\sim 0.1$	GS
Poly(styrene- <i>co</i> -divinylbenzene), sulfonated or aminated	Nonporous	Isotropic	100–500	ED
Polytetrafluoroethylene	Macroporous	Isotropic	50–500	MF
	Nonporous		$\sim 0.1$	GS
Polyamide, aliphatic	Macroporous	Isotropic	100–500	MF
Polyamide, aromatic	Mesoporous	Anisotropic	$\sim 0.1$	UF
Polyamide, aromatic, in situ synthesized	Nonporous	Anisotropic/composite	$\sim 0.05$	RO, NF
Polycarbonates, aromatic	Nonporous	Anisotropic	$\sim 0.1$	GS
	Macroporous	Isotropic track-etched	6–35	MF
Polyether, aliphatic crosslinked, in situ synthesized	Nonporous	Anisotropic/composite	$\sim 0.05$	RO, NF
Polyethylene	Macroporous	Isotropic	50–500	MF
Polyimides	Nonporous	Anisotropic	$\sim 0.1$	GS, NF
Polypropylene	Macroporous	Isotropic	50–500	MF
Polysiloxanes	Nonporous	Anisotropic/composite	$\sim 0.1 < 1-10$	GS PV, NF (organophilic)
Polysulfones	Nonporous	Anisotropic	$\sim 0.1$	GS
	Mesoporous	Anisotropic	$\sim 0.1$	UF
Polyvinyl alcohol, crosslinked	Nonporous	Anisotropic/composite	$< 1-10$	PV (hydrophilic)
Polyvinylidene fluoride	Mesoporous	Anisotropic	$\sim 0.1$	UF
	Macroporous	Isotropic	50–300	MF

Iron phthalocyanine in zeolite Y (FePcY, this type of catalysts are also indicated as *zeozyme*) has been occluded in a PDMS membrane (Fig. 12) and successfully used in a catalytic membrane contactor for cyclohexane oxidation by tertiary-butyl hydroperoxide at room temperature (Fig. 11).<sup>19</sup>

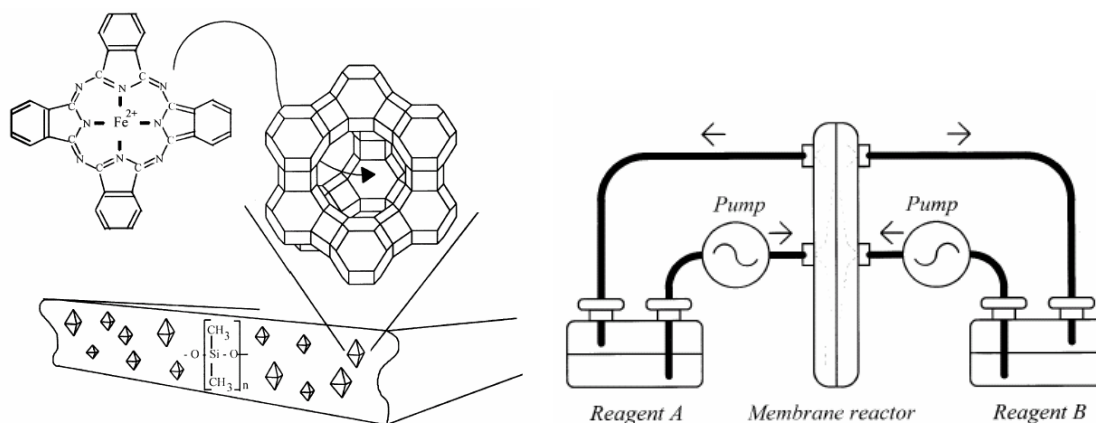


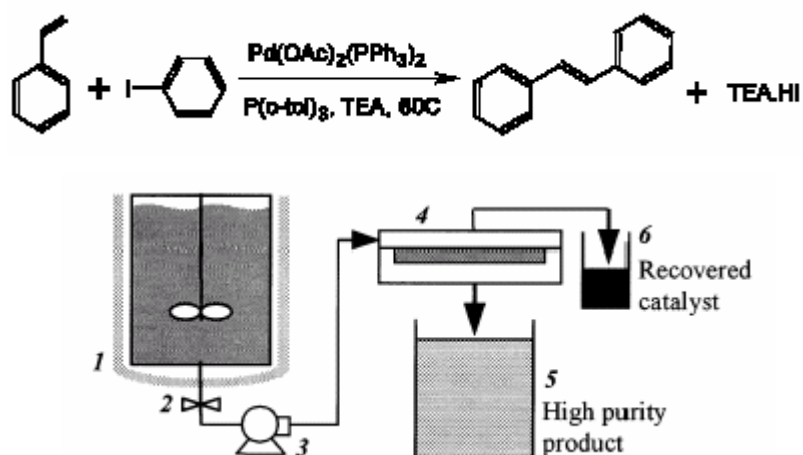
**Figure 12.** Representation of the PDMS membrane occluding the iron phthalocyanine (FePc) included in the supercages of a zeolite Y and scheme of the catalytic membrane contactor (from ref. 19)

Separating the two immiscible reactant phases, the membrane eliminates the need for a solvent and actively controls the concentration of the reactants near the catalytic sites. Moreover the membrane can be regenerate and no significant difference in catalytic behaviour have been observed between the original and the regenerated membrane.<sup>19</sup>

PDMS membranes have been also used to recover gold nanosols stabilized with poly(vinylalcohol), employed as homogeneous oxidation catalysts for the conversion of 1,2-diols to  $\alpha$ -hydroxy-carboxylates in organic phase, by means of a nanofiltration step.<sup>20</sup>

The Au metal colloids can be efficiently recycled and their catalytic activity is largely preserved in consecutive runs. In the same study cellulose acetate membranes are individuated as the most suitable for the Au sol recuperation in aqueous phase.<sup>20</sup>

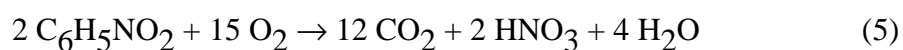
Nanofiltration-coupled catalysis was also used for the arylation of olefins (Heck reaction using as catalyst  $\text{Pd(OAc)}_2(\text{PPh}_3)_2$  with  $\text{P(o-tolyl)}_3$  as stabilising agent) obtaining catalyst recycling, preventing metal contamination of the products and increasing reactor productivity (Fig. 13).<sup>21</sup> In this case polyimide solvent resistant nanofiltration (SRNF) membranes have been used.



**Figure 13.** Scheme of the Heck reaction and the NF-coupled catalytic reactor (from ref. 21)

The coupling of photocatalysis and polymeric membranes has been carried out using  $\text{TiO}_2$  as photocatalyst.<sup>22</sup> Various types of commercial membranes (ranging from UF to NF) and reactor configurations have been investigated.<sup>22</sup>

The configurations with irradiation of the re-circulation tank and catalyst in suspension confined by means of the membrane (Fig. 14), has been reported as the more promising for the 4-nitrophenol mineralization (reaction. 5).<sup>22</sup> The membrane function in this case is the confining of the photocatalyst and maintaining the pollutants in the reaction environment until their complete mineralization.



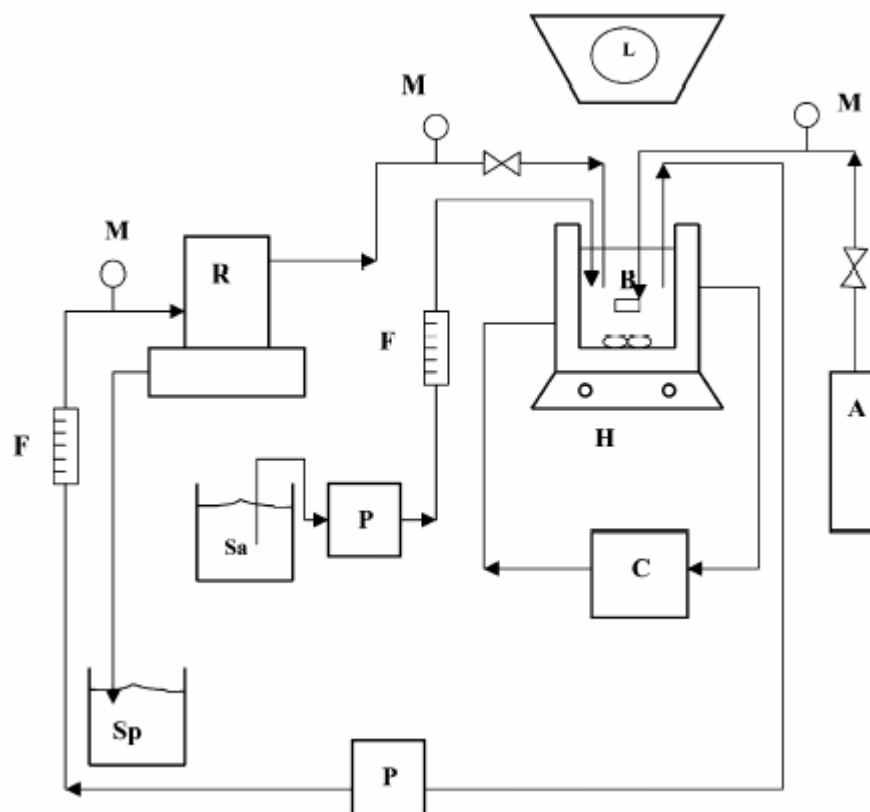


**Figure 14.** Scheme of the membrane photoreactor system with suspended  $\text{TiO}_2$  catalyst (A: oxygen cylinder; B: re-circulation reservoir (reactor); C: thermostating water; L: UV lamp; M: pressure gauge; F: flowmeter; R: membrane cell; H: magnetic stirrer; P: peristaltic pump; Sa: feed reservoir; Sp: permeate reservoir) used for 4-nitrophenol degradation (from ref. 22).

Another field in which the use of polymeric CMRs is very promising is the acid catalysis carried out by cation exchange membranes, i.e. membranes preferentially permeable to cation because the presence of fixed negative charged groups (e.g.,  $-\text{SO}_3^{2-}$ ) on the polymer chains.

Numerous chemical reactions of the petroleum refinery industry (e.g. the cracking processes) and for the production of chemicals (e.g. the hydration of alkenes), are catalyzed by acids. These acid catalysed reactions are often carried out using conventional acids, such as  $\text{H}_2\text{SO}_4$  and  $\text{AlCl}_3$ . However these processes are generally associated with problems of high toxicity, corrosion and catalyst waste.

For these reasons today, one of the priority targets for the green chemistry is the moving from liquid acid to solid acid catalysts.

A more environmentally friendly solution is constituted by the use of a solid acid catalyst such as zeolites, acid oxides, phosphates and, in particular, heteropolyacids.<sup>23</sup>

The most important property which distinguish the HPAs from the other solid acid catalysts, beside the stronger acidity, is their multifunctionality which can be tuned by varying their chemical composition.<sup>24</sup>



Acid catalysis and catalytic oxidation are the two major application areas of HPAs, however interesting uses of HPAs are present also in fuel cell technology because these systems have an high proton conductivity in solid state.<sup>12</sup>

In this work we have functionalized polymeric membranes with various heteropoly anion for applications in oxidation catalysis and as proton exchange membranes for fuel cells.

Although there are many structural types of HPAs in the majority of the catalytic applications the Keggin type HPAs, are used, especially in acid catalysis.<sup>25</sup> The Keggin HPAs comprise heteropoly anions of the formula  $[XM_{12}O_{40}]^{n-}$  where X is the heteroatom ( $P^{5+}$ ,  $Si^{4+}$ , etc.) and M is the addenda atom ( $Mo^{6+}$ ,  $W^{6+}$ , etc.). The structure of the Keggin type anion is composed of a central tetrahedron  $XO_4$  surrounded by 12 edge- and corner-sharing metal-oxygen octahedral  $MO_6$  (Fig. 15)<sup>25</sup>

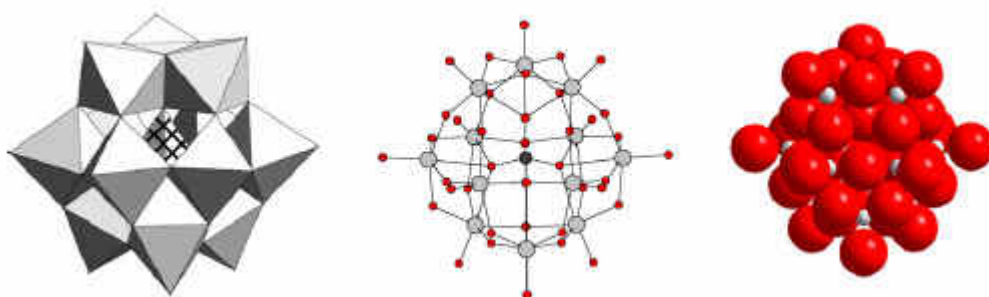


**Figure 15.** Different representations of the of an heteropoly anion with Keggin structure (from ref. 25)

Catalysis by heteropolyacids (HPAs) has well established industrial applications including heterogeneous catalysed selective oxidations (oxidation of methacrolein to methacrylic acid and ethylene to acetic acid) and acid-catalysed reactions (homogeneous liquid-phase hydration of olefins, biphasic polymerisation of THF to poly(tetramethylene glycole) and the gas-phase synthesis of ethyl acetate from ethylene and acetic).<sup>25</sup>

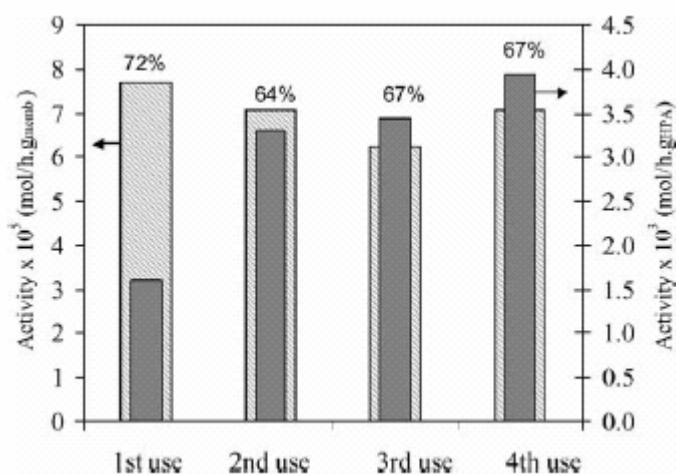
Nevertheless in many processes using HPAs catalysts there are relevant difficulties concerning catalyst separation and recovery and reaction selectivity. In this perspective, the heterogenization of acid catalysts in membranes, or the use of intrinsically catalytic acid membranes can offer important advantages in catalysis by the integration of solid acid catalysis with the selective transport through the membranes.

Hydration of  $\alpha$ -pinene to  $\alpha$ -terpineol over molybdophosphoric acid ( $H_3PMo_{12}O_{40}$ ) entrapped in polyvinyl alcohol (PVA) membranes cross-linked with succinic acid, and molybdophosphoric acid encaged in USY zeolites dispersed in PDMS membrane, have

been reported in literature.<sup>26</sup> In both cases, the catalytic activity of the membranes is quite good in successive runs although a partial catalyst leaching observed (Fig. 16).

Transesterification of soybean oil over Nafion membranes and PVA membranes containing sulfonic groups have been also investigated.<sup>27</sup>

(A)



(B)

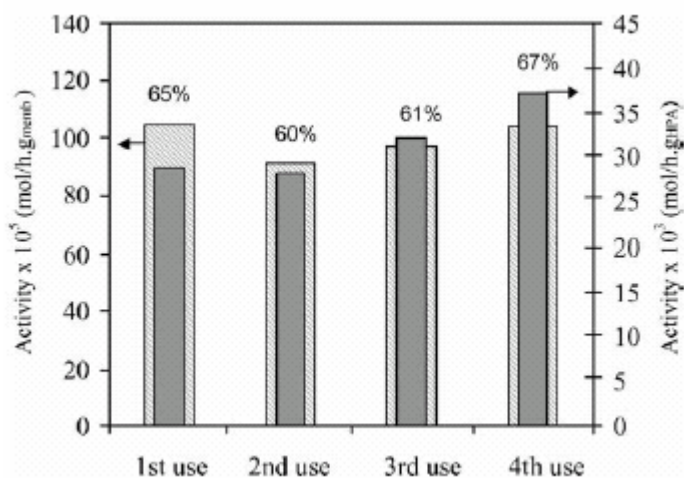


**Figure 16.** Activity of PVA-based (A) and PDMS-based (B) catalytic membranes entrapping  $\text{H}_3\text{PMo}_{12}\text{O}_{40}$ , taken as the maximum reaction rate observed in successive runs, referred to the HPA amount or to the membrane weight (from ref. 26)

Interesting results have been reported for the acid catalysed isobutene dimerisation utilising a forced-flow catalytic membrane reactor (Fig. 17).<sup>28</sup>

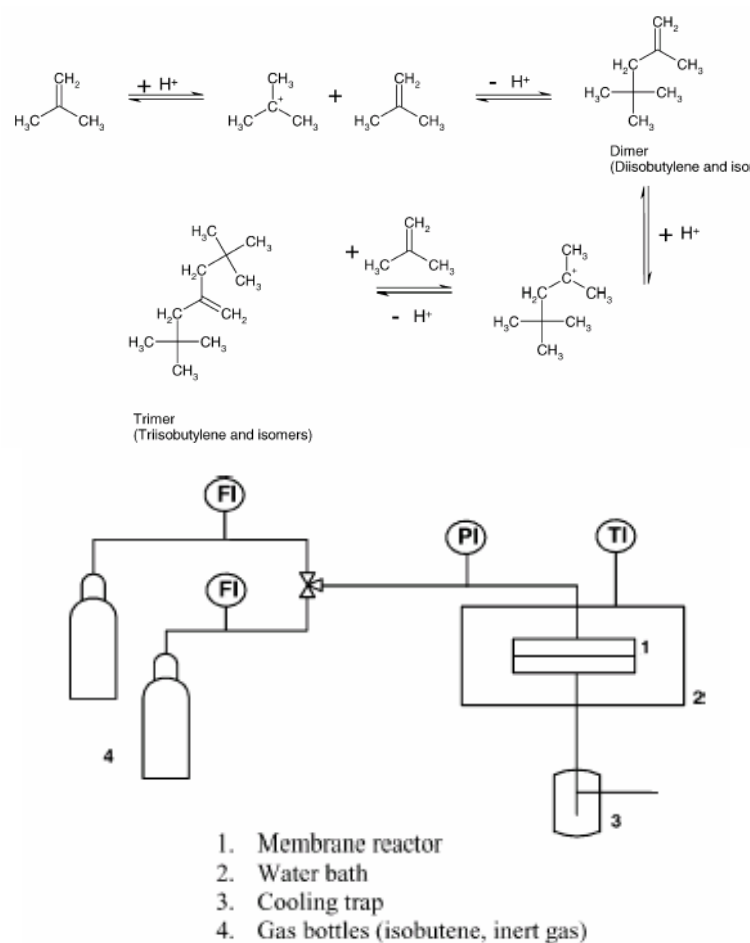


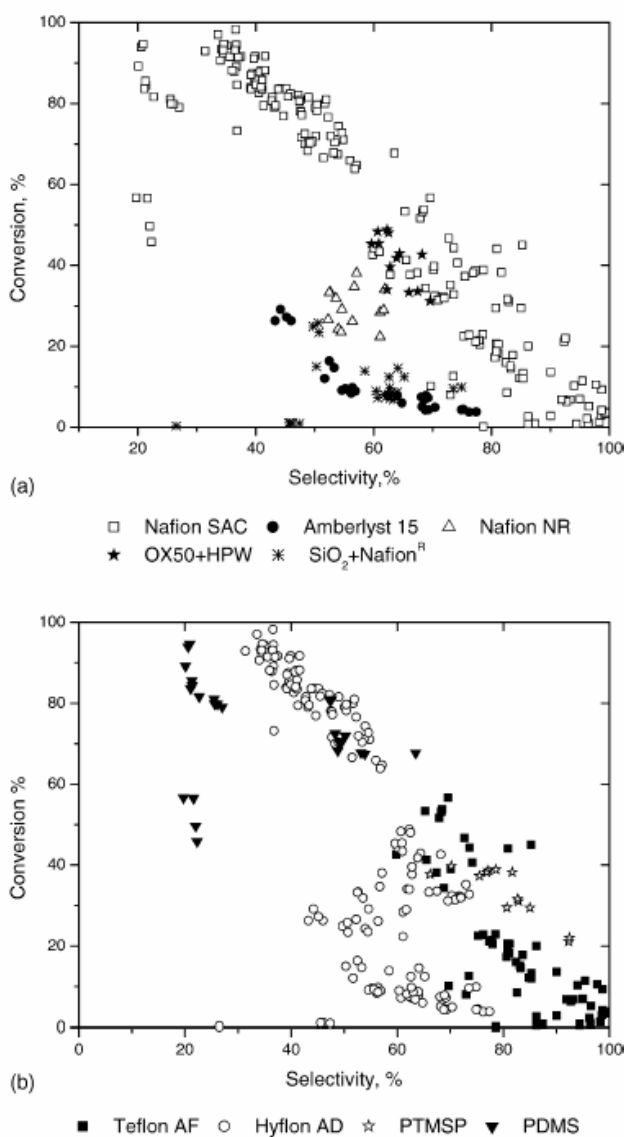
**Figure 17.** Isobutene dimerisation reaction and scheme of the forced-flow catalytic membrane reactor (from ref. 28)

Several acid catalysts, such as silica supported Nafion (Nafion SAC-13), Nafion NR50, Amberlyst<sup>TM</sup> 15, and silica supported phosphotungstic ( $\text{H}_3\text{PW}_{12}\text{O}_{40}$ ) acid have been mixed in solution with a polymeric binder. Teflon AF, Hyflon AD, polytrimethylsilylpropyne, and PDMS have been used as binder to form a porous, reactive layer on top of a porous, polymeric, supporting membrane.<sup>28</sup>

Depending on the type of binder and catalyst high conversions and selectivity to isooctene have been achieved (Tab. 2 and Fig. 18).<sup>28</sup>

**Table 2.** Summary of the results obtained in the acid catalysed isobutene dimerisation utilising a forced-flow composite catalytic membrane

Membrane no.	Catalyst	Polymeric binder	Pressure (bar)	Temperature (°C)	Conversion (%)	Selectivity (mol%)	SV <sup>a</sup> (g <sub>i-C<sub>4</sub></sub> /g <sub>cat</sub> h)
10	Nafion SAC	Hyflon AD	3.5	50	90–98	34–43	500
9	Nafion SAC	PDMS	4.5	50	90–94	20	1300
9	Nafion SAC	PDMS	4.0	50	70	50	1000
13	SiO <sub>2</sub> /HPW <sup>b</sup>	Hyflon AD	4.4	50	50	60	250
7	Nafion SAC	PTMSP <sup>c</sup>	3.7	30	22	86	175
5	Nafion SAC	Teflon AF	3.9	50	45	80	275

<sup>a</sup> Space velocity.<sup>b</sup> Phosphotungstic acid.<sup>c</sup> Poly(trimethylsilylpropine).**Figure 18.** Conversion in relation to selectivity in the isobutene dimerisation as a function of the nature of the catalyst (a) and binder (b) (From ref. 28)

### 1.3.3 Biocatalytic membrane reactors

The nature of the catalyst: artificial (organic or inorganic) or biological (enzymes and microbial cell), is another factor used to distinguish CMRs.

The membrane reactors using biological catalysts are generally called **biocatalytic membrane reactors**.

The immobilization of enzymes and microbial cell in artificial membranes (Fig. 19) is a well accepted technique that reproduces in many aspects the natural operating conditions in living systems.<sup>29</sup>

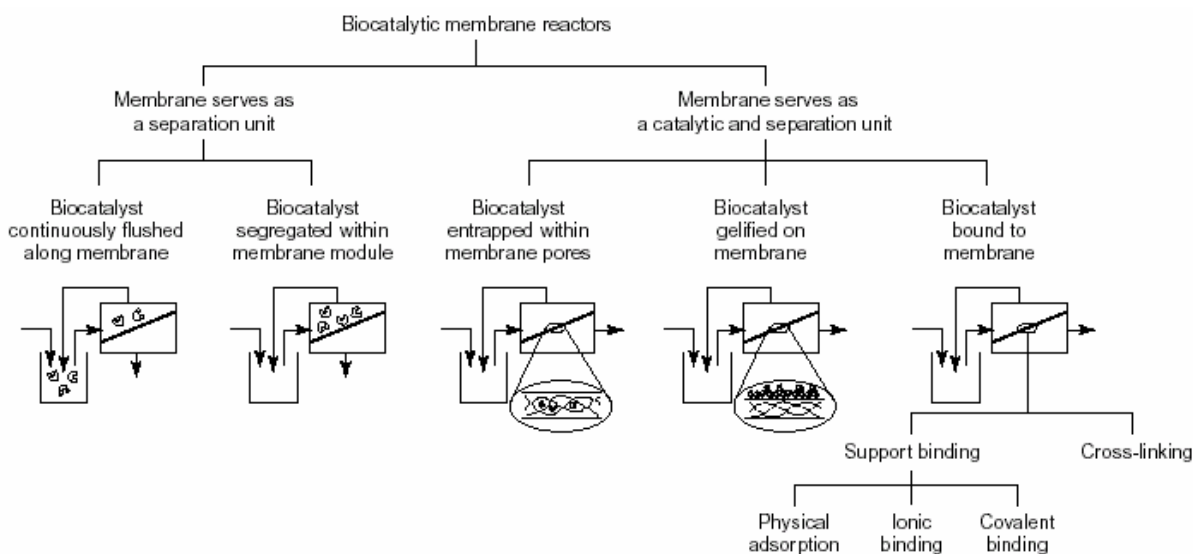


**Figure 19.** Biocatalysts immobilized using different methods (from ref. 30)

The recent trend towards environmentally friendly technologies makes these biocatalytic membrane reactors particularly attractive because of their ability to operate at moderate temperature and pressure, and to reduce the formation of by-products. Enzymes, compared to artificial catalysts, generally permit greater stereospecificity and higher reaction rates under milder reaction conditions.

Thermophilic microbial cells (*Caldariella acidophila* or *Sulfolobus solfataricus*) have been successfully immobilized, without loss of activity, in polymeric artificial membranes prepared by phase inversion technique, since in the early eighties.<sup>31</sup> Dynamically formed gelled enzyme composite membranes in continuous ultrafiltration processes represents another interesting methodology to produce catalytic membranes.<sup>32</sup>

A new multiphase enzyme membrane reactor has been developed by immobilizing the lipase from *Candida rugosa* in a polymeric membrane in presence of a stable and uniform oil-in-water emulsion prepared by membrane emulsification.<sup>33</sup> The kinetic resolution of the naproxen esters (Fig. 20) has been investigated showing that the presence of an emulsion

within the membrane improved the catalytic activity and the enantioselectivity of the immobilized enzyme as well as its stability.<sup>33</sup>

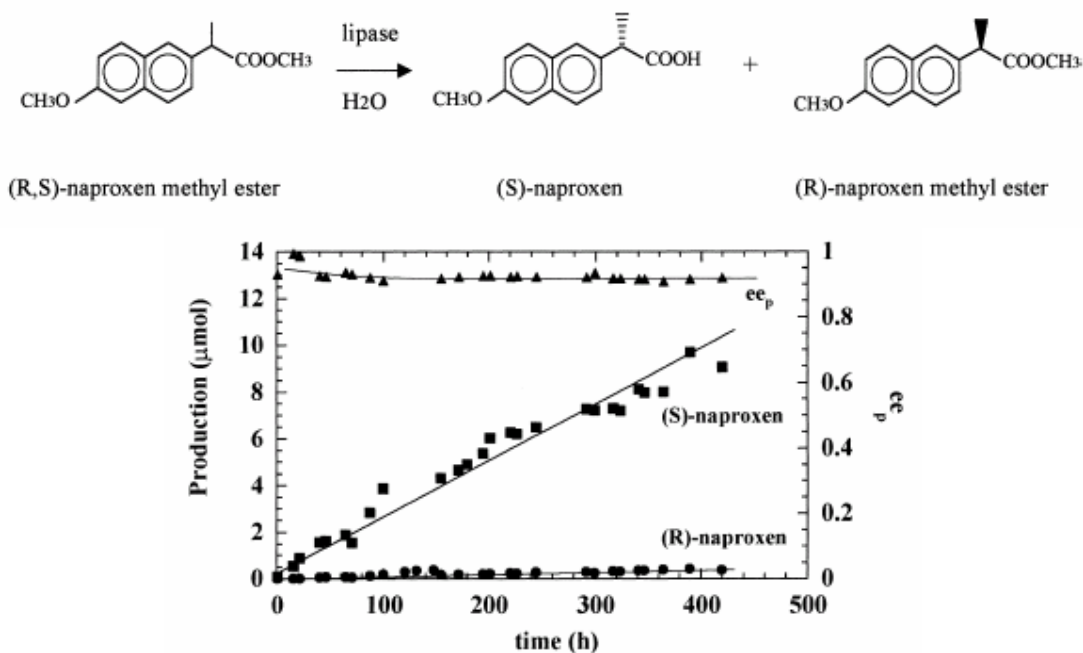


**Figure 20.** Scheme of the enantioselective hydrolysis of (R, S)-naproxen methyl ester catalyzed by lipase and time-course of naproxen production and enantio-excess in biphasic enzyme membrane reactor (from ref 33)

Biocatalytic membrane reactors have been also successfully applied in wastewater treatment by integrating biological treatment with membrane filtration in the **membrane bioreactors (MBRs)** and providing an effective alternative to conventional processes such as activated sludge for municipal and industrial effluents.<sup>29</sup>

Membrane bioreactors are composed of two primary parts, the biological reactor in which the reaction occurs (active sludge containing purifying bacteria) and the membrane module for the physical separation of the different compounds. Only the treated effluent passes through the membrane.

Membrane bioreactors can be classified into two main groups according to their configurations. The first group, commonly known as the **integrated** or **submerged MBR** (Fig. 21), involves outer skin membranes that are internal to the bioreactor. The second configuration is the **recirculated** or **external MBR** (Figure 22), that involves the recirculation of the solution through a membrane module that is outside the bioreactor. Both inner-skin and outer-skin membranes can be used in this application.

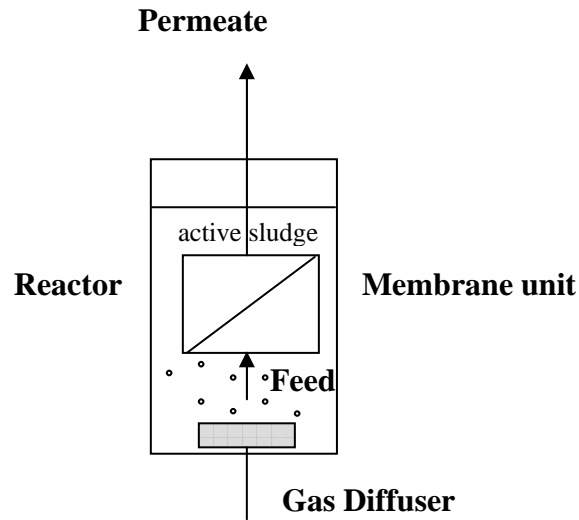


**Figure 21.** Scheme of an integrated or submerged MBR.

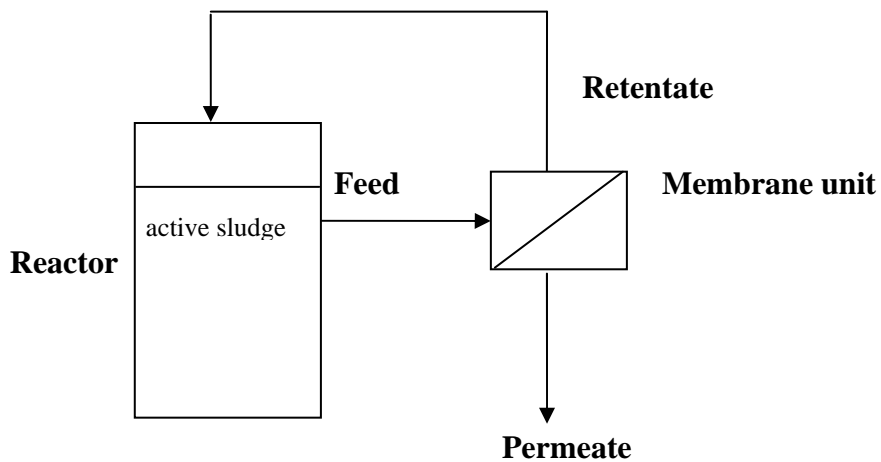


**Figure 22.** Scheme of a recirculated or external MBR

In the submerged MBR the driving force is achieved by pressurizing the bioreactor or creating negative pressure on the permeate side. A diffuser is usually placed directly beneath the membrane module to facilitate scouring on the filtration surface. Aeration and mixing are also achieved by the same unit. In the external MBR the driving force is due to a difference in transmembrane pressure created by high cross-flow velocity along the membrane surface. Several types and configurations of membranes have been used for MBR applications including tubular, plate and frame, rotary disk, hollow fiber; organic, metallic and inorganic (ceramic); microfiltration and ultra-filtration membranes.<sup>34</sup>

The early examples of MBRs operated with tubular membranes placed in external recirculation loops. However, the use of recirculation loops leads to relative high energy costs, depending on the internal diameter of the tubes used. In addition, the high shear stresses in the tubes and recirculation pumps can contribute to the loss of biological activity of the system.<sup>35</sup> The submerged MBRs are alternative systems to overcome these limits. This operating mode limits the energy consumption associated with the recirculation cost.<sup>36</sup> Moreover, the use of submerged membranes allow to operate at low transmembrane pressures. This makes them well suited to relatively large-scale applications.

Submerged MBR were first introduced for decentralised sanitation in the US and in building water reuse in Japan, and are now widely applied in different sectors.

The largest membrane bioreactor unit in the world was recently built in Porto Marghera (Venice) in order to extract remaining pollutants in tertiary water prior to disposal into the Venetian Lagoon.<sup>37</sup>

The ultrafiltration unit, containing submerged PVDF hollow fibers membranes (ZeeWeed<sup>®</sup> by Zenon), is designed to treat 1600 m<sup>3</sup>/h of wastewater with a COD/h of 445 kg and the suspended matter of the treated water is <1mg/L.<sup>37</sup>

There are two interconnected UF lines, each line contains 4 unit composed by 9 ZeeWeed<sup>®</sup> modules and the total membrane area is 100.000 m<sup>2</sup>.<sup>37</sup>

### 1.3.4 Catalytically active and catalytically passive membranes

Another possible classification of the CMRs is based on the role of the membrane in the catalytic step: we have a **catalytically active membrane** if the membrane has itself catalytic properties (the membrane is functionalized with a catalyst inside or on the surface, or the material used to prepare the membrane is intrinsically catalytic); otherwise if the only function of the membrane is a separation process (retention of the catalyst in reactor and/or removal of products and/or dosing of reagents) we have a **catalytically passive membrane**. The process carried out with the second type of membrane is also known as **membrane-assisted catalysis**.

Numerous examples of catalytically active polymeric membranes<sup>19, 26, 27, 28, 31-33</sup> and catalytically active inorganic membranes<sup>11, 16</sup> have been presented in the previous sections. Moreover various example of catalytically passive membranes used in membrane-assisted catalysis have been also discussed.

Examples of integration of pervaporation<sup>15</sup>, gas separation<sup>10, 13, 14</sup>, nanofiltration<sup>20-22</sup> and ultrafiltration<sup>22, 37</sup> with catalytic reactions, have been proposed, but catalytic reactions can



be combined with practically all the membrane unit operations today available in integrated process.<sup>38</sup>

#### **1.4 Basic aspects for the heterogenization of catalysts in polymeric membranes**

Because one of the most interesting aspect of the catalytic membrane reactors is the effect of the membrane environment, especially if polymeric, on the catalyst activity, in our opinion the most promising opportunities are in the use of catalytically active polymeric membranes in comparison with catalytically passive membranes.

In this section the basic aspect of catalyst heterogenization in polymeric membranes will be illustrated.

In the experimental part of this thesis (Chapter 3) the developments of new functionalized membranes obtained by heterogenization of inorganic additives in polymeric membranes will be presented.

When a catalyst is heterogenized within or on the surface of a membrane, the membrane composition (characteristics of the membrane material: hydrophobic or hydrophilic, presence of chemical groups with acid or basic properties, etc.) and the membrane structure (dense or porous, symmetric or asymmetric) can positively influence the catalyst performance, not only by the selective sorption and diffusion of reagents and/or products, but also influencing the catalyst activity by electronic (electron donating and electron withdrawing groups) and conformational effects (stabilization of the transition states). These effects are the same occurring in biological membranes.

For this reason, the appropriate choice of the polymeric material used for catalyst heterogenization is fundamental.

Major issue in the polymer selection is its mechanical, thermal, and chemical stability under reaction conditions.<sup>4</sup>

A good affinity for the catalyst is also desirable in order to avoid catalyst leaching and to have a good adhesion between polymer and catalyst with an optimal dispersion of the same.<sup>4</sup>

Different methods for the immobilization of catalysts in membrane can be identified: covalent binding, electrostatic interaction, weak interactions (Van der Waals or hydrogen bonds) and encapsulation.

The polymer/catalyst affinity can be also improved by an appropriate chemical functionalization of one or both components. The choice of a solvent to carry out the reaction, in which the catalyst is not soluble is, in any case, advantageous.

The polymer should also to have good transport properties for the reagents and products. The affinity between a compound and the membrane polymer can anticipated by the calculation of the *affinity parameters*.<sup>39, 40</sup> These parameters reflects the ability to form hydrogen bond, polar and Van der Waals interactions in condensed phase

In the membrane-assisted catalysis, the choice of a membrane with appropriate permeability and selectivity, is more simple in comparison with catalytically active membranes.

In the last case, mass transfer of the reagents to the catalytic sites and of the product away from them, should be fast enough in order to not limit the reaction but, in the same time, the contact time catalyst/reagent should be also appropriate.

Computational strategies and modelling are key tools to be considered to improve and better understand the catalysis by a CMR.

For a porous membrane, the choice of polymer is of less importance for transport properties in comparison with a dense membrane, because permeation does not take place through the polymer matrix but through the membrane pores.<sup>4</sup> However the membrane material is relevant for the stability and surface properties, such as wettability and fouling.

The membrane preparation conditions depend from the membrane material and desired morphology. In the case of a polymeric catalytically active membrane, the presence of the catalyst to be incorporated, complicate the process because the catalyst should be firmly entrapped in the membrane and the catalyst structure and activity has to be preserved during the preparation procedure.

Different technique for polymeric membrane preparation are toady available<sup>38</sup> and can be opportunely employed also to prepare catalytic membranes: phase inversion, coating, sintering, stretching, track-etching, Supercritical Assisted Phase Inversion Method (SAPIM)<sup>41</sup>, are some examples.

The most versatile is the phase inversion technique, in which a polymer is transformed, in a controlled mode, from a liquid to a solid state.

Phase inversion can be induced by different ways, the most used are: precipitation by

solvent evaporation (to obtain dense membrane) and precipitation by immersion in a non-solvent (to obtain porous membrane).

In the phase inversion process induced by solvent evaporation the polymer is dissolved in a solvent having appropriate volatility, the solution is cast in an environment with controlled temperature and humidity. The solvent evaporation cause the polymer precipitation with the concomitant formation of a dense membrane.

In the phase inversion process induced by a non-solvent, a homogeneous polymeric solution, is initially demixed in two liquid phases because of the exchange of the solvent and non-solvent. The phase with the higher polymer concentration will form the solid membrane, the phase with the lower polymer concentration will form the membrane pores. During the process, the exchange of solvent and non-solvent in the demixed phases continues to cause an increase of the polymer concentration in the concentrated phase surrounding the pores. The polymer molecules may rearrange their structure until the solidification (vitrification or crystallization) of the concentrated phase occurs.

By controlling the initial stage of the phase inversion the membrane morphology can be controlled.<sup>42</sup>

### **1.5 Transport mechanism in porous and dense polymeric membranes**

Depending on the pore and molecules sizes, gas molecules can be transported through porous membranes via viscous flow, Knudsen flow or molecular sieving (Fig. 23).

Transport through dense membranes follows the solution-diffusion mechanism, according to which a molecule first is adsorbed in the polymer, after it diffuses through the membrane and finally is desorbed (Fig. 23).

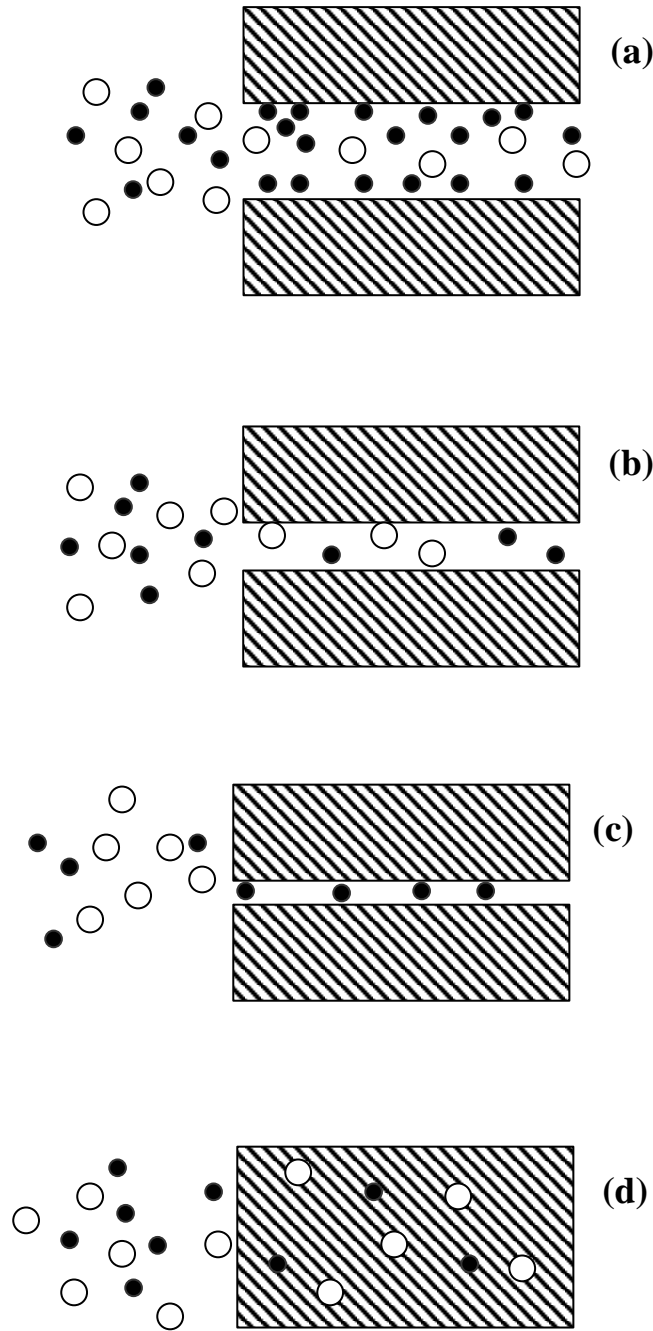


**Figure 23.** Transport mechanisms of gases species through porous (a-c) and dense (d) membranes: (a) viscous flow; (b) Knudsen flow; (c) molecular sieving; (d) solution diffusion (from ref. 34)

The ratio of the pore radius ( $r$ ) to the mean free path ( $\lambda$ ) of the gas molecules, regulates the proportion of Knudsen and viscous mechanism.

The mean free path  $\lambda$  of the gas molecules can be calculated by:

$$\lambda = \frac{3\eta \sqrt{\pi RT}}{2P \cdot 2M_w} \quad (6)$$

where  $\eta$  is the gas viscosity,  $R$  is the universal gas constant ( $8.314 \text{ J mol}^{-1} \text{ K}^{-1}$ ),  $T$  the temperature,  $P$  the pressure and  $M_w$  the molecular weight.

If  $\lambda/r \ll 1$  viscous flow is preponderant and the gas flux through the membrane is described by the following equation:

$$J = \frac{\epsilon^2 \Delta P}{8\eta\tau \Delta x} \quad (7)$$

where  $\Delta P$  is the partial pressure difference,  $r$  is the pores radius,  $\tau$  pores tortuosity and  $\epsilon$  surface porosity defined as:

$$\epsilon = n_p \pi r^2 / A_m \quad (8)$$

where  $n_p$  is the number of the pores,  $A_m$  is the membrane area.

In the viscous flow  $J$  is proportional to  $r^4$  and  $1/\eta$ .

In Knudsen flow  $\lambda/r \ll 1$  and there are more collisions with the pore walls than with the other molecules.

The gas flow in this case is described by the equation:

$$J = \frac{\pi r^2 D_k \Delta P}{RT \tau} \quad (9)$$

where  $D_k$  is the Knudsen diffusion coefficient.

$$D_k = 0.66r \sqrt{\frac{8RT}{\pi M_w}} \quad (10)$$

In the presence of Knudsen flow

$$J \propto \frac{1}{\sqrt{M_w}} \quad (11)$$

and the ideal separation factor for gas pair can be calculated on the basis of the square root of the molecular weight of the two gas.

If the membrane pore are between the diameter of the smaller and the larger gas molecules, only the smallest of the two components can permeate, and the mechanism is molecular sieving.

Transport mechanism through dense membranes can be described by solution-diffusion mechanism. In the solution diffusion process, the gas dissolves in the membrane and then diffuse through it under a concentration gradient.

In the case of a linear relation (Henry's law) between the gas or vapour pressure and the concentration of the same species at the membrane interface, the concentration at the interface is given by:

$$C = S \cdot p \quad (12)$$

where  $S$  is the solubility (coefficient) of the gas or the vapour in the membrane,  $p$  is the partial pressure. If the diffusion coefficient is constant ( $D$ ), the permeability ( $P$ ), is given by the equation:

$$P = D \cdot S \quad (13)$$

If the solubility is known, for example by absorption measurements, this equation allows calculating the diffusion coefficient from permeability measurements.

While solubility is a thermodynamic parameter that gives the amount of penetrant dissolved in the membrane under equilibrium conditions, diffusivity is a kinetic parameter indicating ability of the penetrant to be transferred across the membrane.

The diffusion in dense polymeric membrane is strictly influenced by the polymer glass transition temperature ( $T_g$ ) and the degree of crystallinity.<sup>4</sup>

Transport through dense membranes is generally considered an activated process, and temperature has a consistent influence on the permeation rate. The dependence of permeability on temperature is usually described by an Arrhenius-type equation:

$$P = P_0 \exp\left(-\frac{E_a}{RT}\right) \quad (14)$$

where  $P_0$  is a constant,  $E_a$  is the activation energy,  $R$  the gas constant,  $T$  the temperature. Transmembrane flux  $J_i$  of  $i$ -th component is given by:

$$J_i = \frac{P_i}{\delta} \Delta p_i \quad (15)$$

where  $\delta$  is the membrane thickness.

If polymer/penetrant can not be considered as a non-interactive system, the dependence of  $P$ ,  $S$  and  $D$  on concentration has to be taken into account. Henry's law is applicable for small non-condensable gases; the Flory-Huggins thermodynamics offers adequate tools in case of larger easy condensable penetrants<sup>43</sup>.

## REFERENCES

- <sup>1</sup> X. S. Zhao, Xiao Ying Bao, Wanping Guo, Fang Yin Lee, *Mat. Tod.* 9 (2006) 32-39
- <sup>2</sup> J.-C. Charpentier, *Ind. Eng. Chem. Res.* 46 (2007) 3465-3485
- <sup>3</sup> Drioli, E.; Fontananova, E.; *Chem. Eng. Res. Des.* 82 (A12) (2004) 1557-1562.
- <sup>4</sup> I.F.J. Vankelecom, *Chem. Rev.* 102 (2002) 3779-3810
- <sup>5</sup> S. Miachon, J.-A. Dalmon, *Top. Catal.* 29 (2004) 59-65
- <sup>6</sup> V.M. Gryaznov, *Pet. Chem.* 35 (1995) 181-188
- <sup>7</sup> V. Gryaznov, *Catal. Tod.* 51 (1999) 391-395
- <sup>8</sup> R. Dittmeyer, K. Svajda, M. Reif, *Top. Catal.* 29 (2004) 3-27
- <sup>9</sup> X. Tan, Z. Pang, Z. Gub, S. Liu, *J. Membr. Sci.* 302 (2007) 109-114
- <sup>10</sup> H. Dong, Z. Shao, G. Xiong, J. Tong, S. Sheng, W. Yang, *Catal. Tod.* 67 (2001) 3-13
- <sup>11</sup> V.V. Kharton, J.C. Waerenborgh, D.P. Rojas, A.A. Yaremchenko, A.A. Valente, A.L. Shaula, M.V. Patrakeev, F.M.B. Marques, J. Rocha, *Catal. Lett.* 99 (2005) 249-255
- <sup>12</sup> T. Norby, *Solid State Ionics* 125(1999)1-11
- <sup>13</sup> E. Piera, C. Téllez, J. Coronas, M. Menéndez, J. Santamaria, *Catal. Tod.* 67 (2001) 127-138
- <sup>14</sup> L. van Dyk, S. Miachon, L. Lorenzen, M. Torres, K. Fiaty, J.-A. Dalmon, *Catal. Today* 82 (2003) 167-177
- <sup>15</sup> K. Tanaka, R. Yoshikawa, C. Ying, H. Kita, K. Okamoto, *Catal. Tod.* 67 (2001) 121-125
- <sup>16</sup> P. Bernardo, C. Algieri, G. Barbieri, E. Drioli, *Catal. Tod.* 118 (2006) 90-97.
- <sup>17</sup> M. Ulbricht, *Polymer* 47 (2006) 2217-2262
- <sup>18</sup> D.W. Van Krevelen *Properties of Polymers-* Elsevier Third edition 1990
- <sup>19</sup> I.F.J. Vankelecom, R.F. Parton, M.J.A. Casselman, J.B. Uytterhoeven, P.A. Jacobset, *J. Catal.* 163 (1996) 457-464
- <sup>20</sup> P.G.N. Mertens, M. Bulut, L.E.M. Gevers, I.F.J. Vankelecom, P.A. Jacobs, D.E. De Vos, *Catal. Lett.* 102(2005) 57-61
- <sup>21</sup> D. Nair, J.T. Scarpello, L.S. White, L.M. Freitas dos Santos, I.F.J. Vankelecom, A.G. Livingston, *Tetrahedron Lett.* 42 (2001) 8219-8222
- <sup>22</sup> R. Molinari, L. Palmisano, E. Drioli, M. Schiavello, *J. Membr. Sci.* 206 (2002) 399-415
- <sup>23</sup> T. Okuhara, *Water-Tolerant Solid Acid Catalysts*, *Chem. Rev.* 102 (2002) 3641-3666
- <sup>24</sup> M. T. Pope, *Heteropoly and Isopoly Oxometalates*, Springer-Verlag, New York, 1983.
- <sup>25</sup> I.V. Kozhevnikov, *J. Mol. Catal. A: Chem.* 262 (2007) 86-92
- <sup>26</sup> J.E. Castanheiro, A.M. Ramos, I. Fonseca, J. Vital, *Cat. Tod.* 82 (2003) 187-193
- <sup>27</sup> L. Guerreiro, J.E. Castanheiro, I.M. Fonseca R.M. Martin-Arand, A.M. Ramos, J. Vital, *Catal. Tod.* 118 (2006) 166-171
- <sup>28</sup> D. Fritscha, I. Randjelovica, F. Keil, *Catal. Tod.* 98 (2004) 295-308
- <sup>29</sup> E. Drioli, L. Giorno, *Biocatalytic Membrane Reactors: Application in Biotechnology and the Pharmaceutical Industry*, Taylor & Francis Publisher, Padstow, UK, 1999



- <sup>30</sup> L. Giorno, E. Drioli, Trends in Biotechnol., 18 (2000) 339-348
- <sup>31</sup> G. Capobianco, E. Drioli, G. Ragosta, J. Solid-phase biochemistry, 2, 315(1977).
- <sup>32</sup> E. Drioli, F. Bellucci, G. Ragosta, "Influence of electrolytes and non-electrolytes on ultrafiltration processes with dynamically formed gelled-enzyme composite membranes" in "Recent Advances in Separation Sci.", Ed. N.N. Li, Vol. IV., CRC Press, 1978, pp13-28.
- <sup>33</sup> K. Sakaki, L. Giorno, E. Drioli, J. Membr. Sci. 184 (2001) 27–38
- <sup>34</sup> E. Drioli, E. Curcio, E. Fontananova, (2006), Mass Transfer Operation–Membrane Separations, in Chemical Engineering, [Eds. John Bridgwater, Martin Molzahn, Ryszard Pohorecki], in Encyclopedia of Life Support Systems (EOLSS), Developed under the Auspices of the UNESCO, Eolss Publishers, Oxford, UK, [<http://www.eolss.net>]
- <sup>35</sup> M. Brockmann, C.F. Seyfried, Wat Sci Technol 35(10) (1997) 173-181
- <sup>36</sup> J.K. Kim, I.-K. Yoo, Y.M. Lee, Process Biochem. 38 (2002) 279-285
- <sup>37</sup> C. Vigiano, La Chimica e l'Industria 5 (2007) 90- 94
- <sup>38</sup> H. Strathmann, L. Giorno, E. Drioli, An introduction to membrane science and technology, Publisher CNR Roma, ISBN 88-8080-063-9
- <sup>39</sup> D.W. Van Krevelen, Properties of polymers, third ed., Elsevier Science, Amsterdam, 1990.
- <sup>40</sup> A.F.M. Barton, Handbook of Polymer-Liquid Interaction Parameters and Solubility Parameters, CRC Press, Boca Raton, Florida; 1990.
- <sup>41</sup> E. Reverchon, S. Cardea., J. Membr. Sci. 240 (2004) 187.
- <sup>42</sup> E. Fontananova, J.C. Jansen, A. Cristiano, E. Curcio and E. Drioli, Desalination 192 (2006) 190–197
- <sup>43</sup> P. Schaetzel, Z. Bendjama, C. Vauclair, Q.T. Nguyen, J. Membr. Sci. 191 (2001) 95-102.

## **Chapter 2:**

# **Integration of molecular separation and energy conversion in a fuel cell (FC)**

## 2.1 Basic aspect of fuel cells technology

Proton exchange membranes have today many important applications including molecular separation in electrodialysis, chemical conversion in acid catalysis and energy conversion in the so called fuel cells.<sup>1</sup>

Fuel cells are electrochemical devices for chemical energy conversion, characterized by an high efficiency and a low environmental impact because of their potential to reduce the use of fossil fuels in combustion engines.

Unlike the classical battery, FCs do not store the energy within the chemicals internally, but they use a continuous supply of fuel and oxidant from an external storage tank. Moreover, while the electrodes within a battery react and change as a battery is charged or discharged, in a fuel cell the electrodes are catalytic.

The primary components of a fuel cells are: the anode, the cathode and the ion conducting electrolyte (Fig. 1).

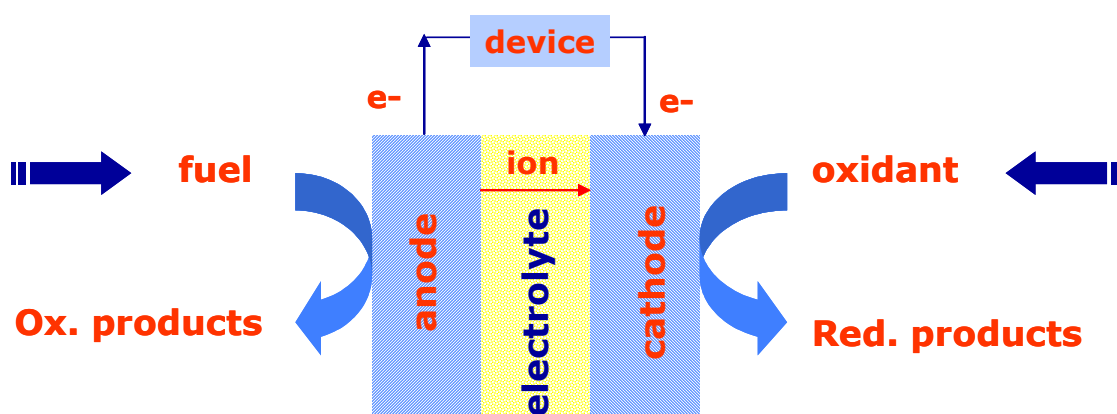


**Figure 1.** Scheme of a fuel cell

There are different types of fuel cells characterized by various operative temperatures, fuels, electrolytes and power density (Tab. 1).<sup>2</sup>

**Table 1.** Different types of fuel cells

Type	Temperature (°C)	Fuel	Electrolyte	Mobile ion	Power density (W/kg)
<b>PEMFC:</b> polymer electrolyte membrane fuel cell	50 - 110	H <sub>2</sub> CH <sub>3</sub> OH	Ion exchange membrane	(H <sub>2</sub> O) <sub>n</sub> H <sup>+</sup>	400-1000
<b>AFC:</b> alkali fuel cell	100 - 250	H <sub>2</sub>	Aqueous KOH	OH <sup>-</sup>	90-240
<b>PAFC:</b> Phosphoric acid fuel cell	150 - 250	H <sub>2</sub>	H <sub>3</sub> PO <sub>4</sub>	H <sup>+</sup>	90
<b>MCFC:</b> Molten carbonate fuel cell	500 - 700	Hydrocarbons CO	(Na,K) <sub>2</sub> CO <sub>3</sub>	CO <sub>3</sub> <sup>2-</sup>	40
<b>SOFC:</b> Solid oxide fuel cell	700 - 1000	Hydrocarbons CO	(Zr,Y)O <sub>2-d</sub>	O <sub>2</sub> <sup>-</sup>	100

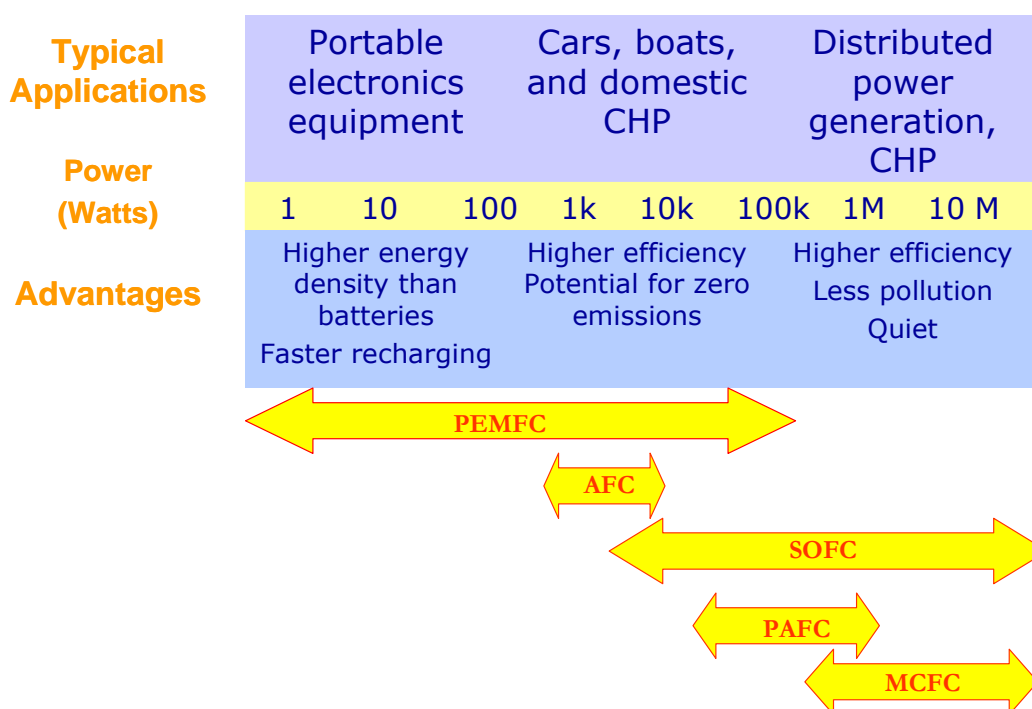


**Figure 2.** Typical range of application and power of FCs (adapted from 3)

The low operating temperature and the high power density of the Polymer Electrolyte Membrane Fuel Cells (PEMFCs) make them ideal for mobile applications (such as energy sources for vehicles) and small applications (such as cell phones and laptop computers) (Tab. 1 and Fig. 2).<sup>3</sup>

In a PEMFC the electrolyte is a proton exchange membrane (PEM) which allows the transport of the protons from the anode, where they are produced in the oxidation of the fuel, typically H<sub>2</sub> (H<sub>2</sub>-PEMFC) or methanol (DM-PEMFC), to the cathode where the protons react with O<sub>2</sub> to produce water. The flow of ionic charge through the PEM is balanced by the flow of electronic charge through the outside circuit producing an electrical power. The only secondary products in the overall reaction are water, heat (eventually recoverable) and CO<sub>2</sub>, if the fuel contains carbon (methanol, ethanol, etc.) (Tab. 2).

**Table 2.** Reactions occurring in an hydrogen (H<sub>2</sub>-PEMFC) and a direct methanol polymer electrolyte fuel cell (DM-PEMFC)

	<b>H<sub>2</sub>-PEMFC</b>	<b>DM-PEMFC</b>
<b>ANODE:</b>	$\text{H}_2 \rightarrow 2 \text{H}^+ + 2 \text{e}^-$	$\text{CH}_3\text{OH} + \text{H}_2\text{O} \rightarrow \text{CO}_2 + 6\text{H}^+ + 6\text{e}^-$
<b>CATHODE:</b>	$1/2 \text{O}_2 + 2 \text{H}^+ + 2 \text{e}^- \rightarrow \text{H}_2\text{O}$	$3/2 \text{O}_2 + 6\text{H}^+ + 6\text{e}^- \rightarrow 3 \text{H}_2\text{O}$
<b>OVERALL:</b>	$1/2 \text{O}_2 + \text{H}_2 \rightarrow \text{H}_2\text{O}$	$\text{CH}_3\text{OH} + 3/2 \text{O}_2 \rightarrow \text{CO}_2 + 2 \text{H}_2\text{O}$

The reaction at the anode is exothermic, however it requires to overcome an activation energy barrier. Three strategies are used in fuel cell technology in order to improve the kinetic reaction: the use of catalysts (usually Pt or Pt/Ru for anode reaction in respectively H<sub>2</sub>- and DM-PEMFCs), raising the temperature and increasing the surface electrode (porous) area.

A typical PEMFC gives a voltage from 0.6 V to 0.7 V and to produce a useful voltage many cells are connected in series. Such a design is called a fuel cell stack (Fig. 3).

Bipolar plates, generally made of graphite, interconnect the cathode of one cell with the anode of the next cell conducting electricity, feeding oxygen to the cathode and fuel to the anode and channelling away waste water and heat from the reaction (Fig. 3, C).

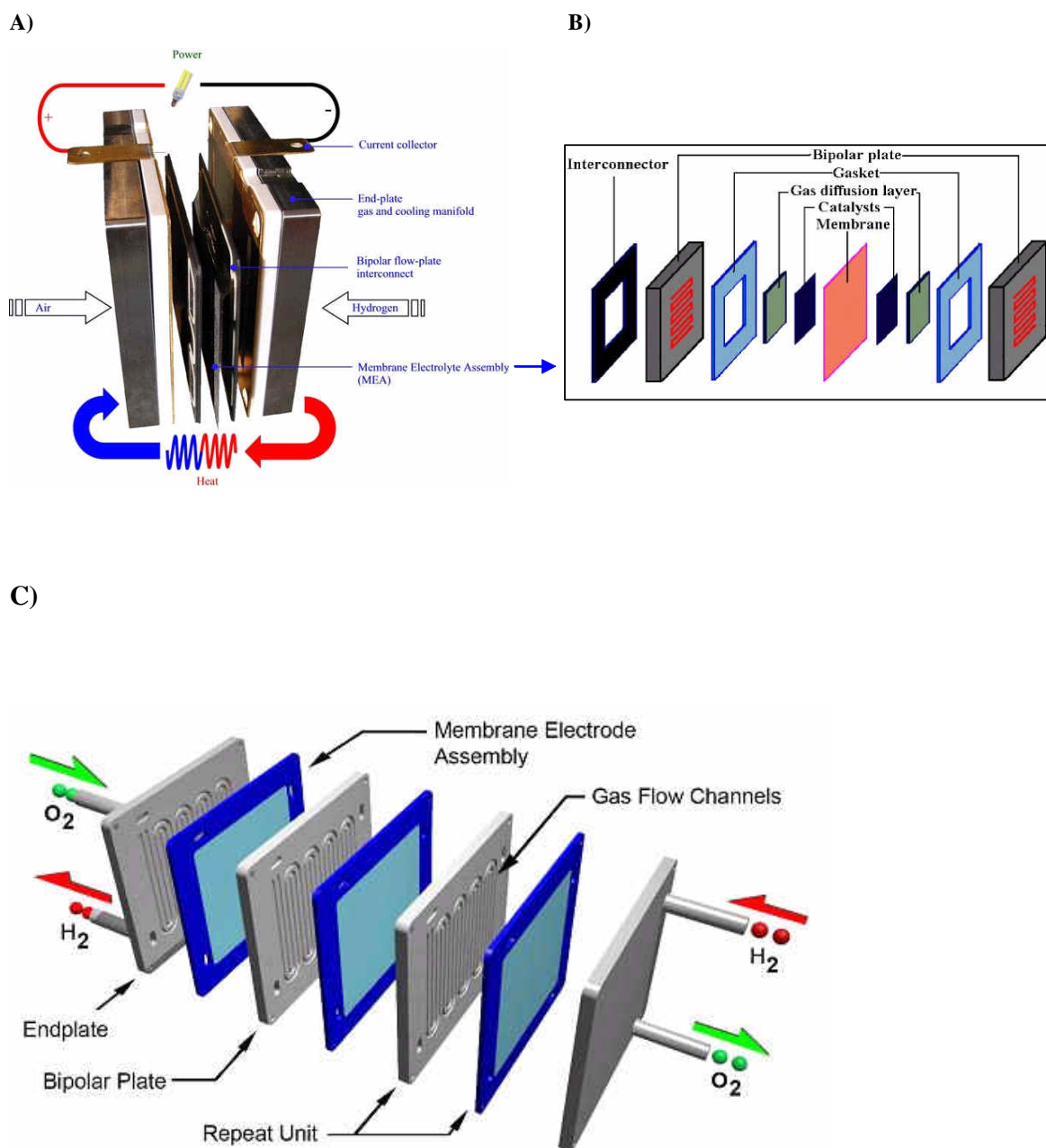


**Figure 3.** Scheme of an H<sub>2</sub>/Air-PEMFC (A), MEA components (B) and a H<sub>2</sub>/O<sub>2</sub>-PEMFC stack (A from <http://www.ird.dk>; B from <http://www.kemi.dtu.dk> and D adapted from <http://www.futureenergies.com> )

Fuel cell technology has many advantages: high energy efficiency, zero- or near-zero emissions, very low noise emissions, reliability and simplicity, modularity and easy up- and down scaling.<sup>3</sup>

PEMFCs have recently passed the demonstration phases and have reached a partial commercialization stage.<sup>4</sup> However there are many challenges remaining that need to be overcome. The main limitations are the high investment cost and the fuel production and fuel storage.<sup>3</sup>

Concerning the first point, the large scale application of this technology imposes addition efforts for the development of new materials with improved properties and reduced cost for the fuel cell components.

In particular the cost of the proton exchange membranes (PEM) is a significant part of the cost of the PEMFCs and the design and the development of new PEM is a crucial aspect.

## 2.2 Thermodynamics fundamentals

For a reversible reaction

$$\Delta G = \Delta H - T\Delta S \quad (1)$$

where:

$\Delta G$  is the Gibbs free energy available to do external work

$\Delta H$  is the variation of the enthalpy, or the energy released by the reaction

$T$  is the absolute temperature

$\Delta S$  is the variation of entropy

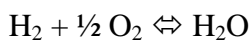
$T\Delta S$  is the heat associated with the organization/disorganization of the material.<sup>5</sup>

For a fuel cell  $\Delta G$  is the electrical work (charge x voltage [J]) done for moving electrons in the external circuit:

$$\Delta G = -nFE \quad (2)$$

where  $n$  is the number of electrons transferred per mole of reactants,  $F$  is the Faraday constant (96485 C),  $E$  is the voltage or electromotive force of the cell reaction.

Considering the reaction of an H<sub>2</sub>/O<sub>2</sub> PEMFC:



the open circuit voltage ( $E_{ocv}$ ) became:

$$E_{ocv} = -\frac{\Delta \tilde{G}_f}{nF} \quad (3)$$

$\Delta \tilde{G}_f$  is the molar (indicated with the symbol  $\sim$ ) Gibbs free energy of water formation:

$$\Delta \tilde{G}_f = (\tilde{G}_f)_{H_2O} - (\tilde{G}_f)_{H_2} - \frac{1}{2}(\tilde{G}_f)_{O_2} \quad (4)$$

$\Delta \tilde{G}_f$  depends from temperature and the state (liquid or gas) of the water, for example at 80°C is -228.2 kJ/mol for liquid water and -226.1 kJ/mol for gas water.

As a consequence:  $E_{ocv}=1.18$  V in the first case and  $E_{ocv}=1.17$  V in the second.

If the system is reversible (no losses) the electrical work is equal to  $\Delta\tilde{G}_f$  . However in a real system generally  $E_{real}$  is minor than  $E_{OCV}$  theoretical because of irreversible voltage losses or polarization phenomena (overvoltages):

- activation losses related to the kinetics of the electrochemical redox reactions taking place at the electrode/electrolyte interface;
- ohmic losses are due to the resistance of individual cell components (electrolyte, electrodes, current collectors, etc.) and to the resistance due to contact problems;
- concentration losses caused by the mass transport limitations of the active species during the cell operation.

These losses (Fig. 4) depend upon the detailed construction of the fuel cell and operative conditions<sup>3</sup> (temperature, current density, reactants).

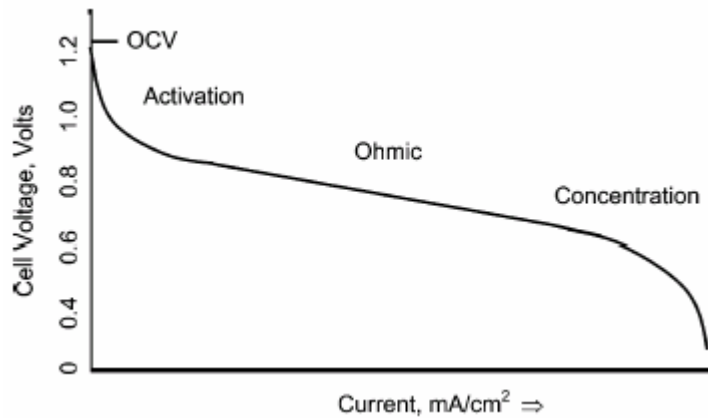


**Figure 4.** Typical voltage-current curve of a fuel cell (from ref.3 )

Fuel cells are generally characterized by high efficiency in comparison with traditional energy conversion systems (Fig. 5 and Ta. 3).

Because fuel cells don't include the conversion of thermal to mechanical energy, they are not subject to the Carnot efficiency limit typical of an heat engine (e.g. steam and gas turbine)<sup>6</sup>:

$$1 - \frac{T_2}{T_1} \quad (5)$$

where:

$T_1$  is the maximum temperature of the heat engine and  $T_2$  the temperature at which the heated fluid is released.



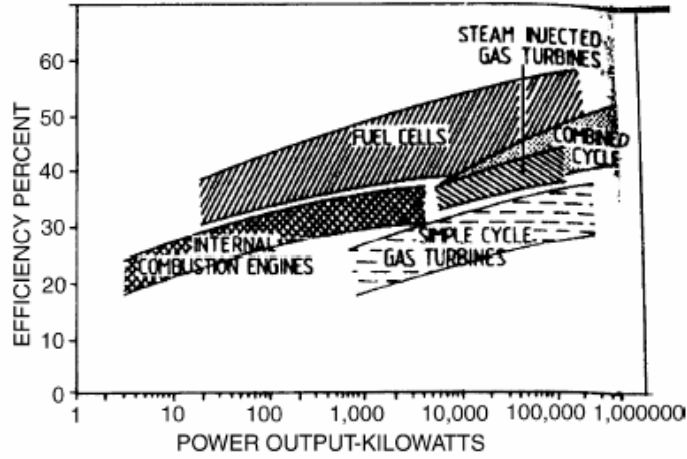


**Figure 5.** Efficiency obtained with various energy conversion systems included fuel cell (from ref. 7 )

**Table 3.** Typical ranges of energy efficiencies obtained using fuel cell and heat engine systems in electric power plant and transportation (data from ref. 8)

Application	Energy efficiency	
	Heat Engine	Fuel Cell
Electric power plant	30-37% <sup>a</sup>	70-80% <sup>b</sup>
Transportation	20-35% <sup>c</sup>	40-50% <sup>d</sup>

<sup>a</sup>combustion engine; <sup>b</sup>SOFC including heat recovery  
<sup>c</sup>internal combustion engine; <sup>d</sup> PEMFC or SOFC

The maximum energy efficiency of a fuel cell is generally defined as the ratio between the electrical energy produced per mole of fuel and the variation of enthalpy for the fuel combustion (heat that can be released):

$$\text{Eff.}_{\max} = \frac{\Delta \tilde{G}_f}{\Delta \tilde{H}_f} = -\frac{nFE_{\text{ocv}}}{\Delta \tilde{H}_f} \quad (6)$$

For the water formation from hydrogen there are two possible values of variation of enthalpy depending on the physical state of the product.

Considering the water in the vapour phase we have the “lower heating value” (LHV):

$$\Delta \tilde{H}_f = -241.83 \text{ kJ/mol}$$

considering the water in the liquid phase we have the “higher heating value” (HHV):

$$\Delta \tilde{H}_f = -285.84 \text{ kJ/mol}$$

The difference between the HHV and the LHV is the molar enthalpy of water vaporization 44.01 kJ/mol.

The maximum efficiency for a fuel cell depends on the temperature because  $\Delta\tilde{G}_r$  depends on this parameter, moreover is necessary to specify if the value is calculated using the HHV or the LHV (Tab. 4).

Because of the voltage losses, the real energy efficiency of a fuel cell is lower than the calculated maximum efficiency.

Although the calculation of the maximum efficiency suggests that lower temperature can allow better performance in a H<sub>2</sub>-PEMFC (Tab. 4), the voltage losses are generally minor at higher temperatures and better efficiencies can be generally obtained operating at higher temperature.<sup>3</sup>

**Table 4.** Calculated maximum energy efficiency for an H<sub>2</sub>/O<sub>2</sub>-PEMFC ( $\Delta\tilde{G}_r$  data from ref. 3)

Form of water product	Temperature (°)	$\Delta\tilde{G}_r$ (kJ/mol)	Maximum Efficiency
Liquid	80	-228.2	94.4%(LHV) 79.8%(HHV)
Gas	80	-226.1	93.5%(LHV) 79.1%(HHV)
Gas	100	-225.3	93.2%(LHV) 78.8%(HHV)
Gas	200	-220.4	91.1%(LHV) 77.1%(HHV)

### 2.3 Proton exchange membranes for PEMFC applications

In a PEMFC the electrolyte used to selectively separate the anode from the cathode is a proton exchange membrane (PEM). The desirable characteristics of a PEM are not only high proton conductivity, but also low permeability to gases (in particular H<sub>2</sub> and O<sub>2</sub>), low permeability to methanol and water, absence of electronic conductivity, chemical and mechanical stability under the operative condition over long time.

#### 2.3.1 Nafion and other polymers used in PEMFCs

Currently, the most commonly used PEMs for applications in PEMFC are made of ion-exchange perfluoropolymers such as Nafion (Du Pont), Aciplex (Asahi Chemical), Flemion (Asahi Glass) and Gore-Select (Gore and Associates).<sup>9</sup> The previous polymers are also called

long-side-chain (LSC) perfluoro-ionomers in order to distinguish them from the so called short-side-chain (SSC) perfluoro-ionomers initially proposed in the 1980s by the Dow company (under the trade name Dow Ionomer) and more recently by the Solvay Solexis (under the trade name Hyflon Ion).<sup>10</sup> These SSC ionomers are characterized by shorter pendent group carrying the ionic functionality, higher crystallinity and higher glass transition (Tg) than LSC ionomers at given equivalent weight.<sup>11</sup>

In particular, among the various perfluoro ionomers developed, Nafion membranes (Fig. 6) still today dominate the PEMFC market because of its high proton conductivity and high chemical, thermal and mechanical stability.

Nafion has been developed in the 1960s by Du Pont and employed in a GE fuel cell designed for NASA spacecraft mission. Nafion has been found also successfully application in chloro-alkali industry and acid catalysis.

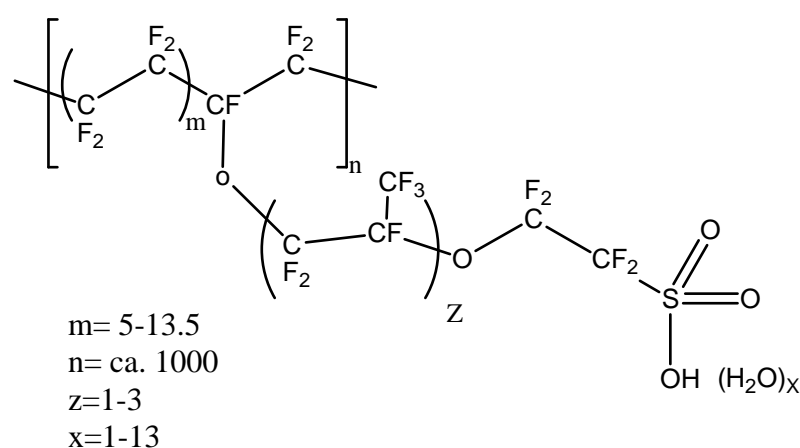


**Figure 6.** Chemical formula of the Nafion

However, Nafion has high costs (600-1200 US\$/m<sup>2</sup>)<sup>12</sup> which limits its practical applications. Moreover Nafion membranes have an elevated water and methanol permeability which reduces the process performance in FCs.

In particular the methanol crossover during operations in a direct methanol fuel cell (DM-PEMFC) can lead to a significant decreases of the overall performance in three main ways: poisoning of the cathode catalyst, fuel efficiency reduction and electrode potential reduction due to methanol oxidation at the cathode.<sup>13</sup>

Also excessive hydraulic permeability of the membrane can have severe consequence on the fuel cell performances including membrane dehydration, with successive loss of conductivity, and cathode flooding, with consequent restrict oxygen transport through the porous gas

diffusion electrode (Fig. 7)<sup>14</sup>.

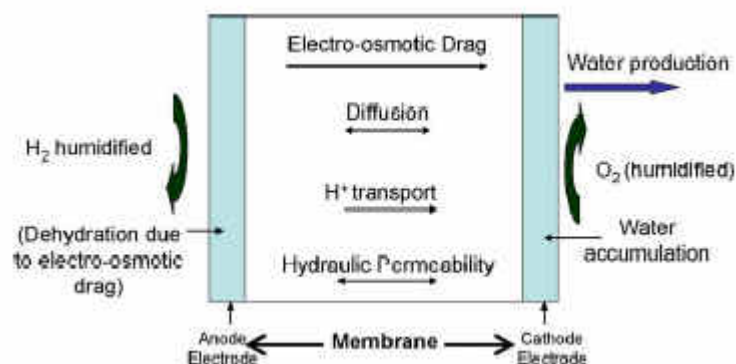


**Figure 7.** Water transport in an H<sub>2</sub>-PEMFC (from ref. 14): the electro-osmotic drags consists in the transport of the water molecules with the protons from the anode to the cathode; in the same time the gradient of water content across the membrane may result in water back diffusion from the cathode (where water is produced) to the anode. Moreover if a difference in transmembrane pressure is applied ( $P_{\text{cathode}} > P_{\text{anode}}$ ) this can further force water transport.

A further disadvantage of the Nafion<sup>®</sup> membranes is the loss of conductivity if operated for a long period of time above 80 °C because of dehumidification problems.<sup>13,15</sup> On the other hand, the use of relatively high temperature (> 80°C) is fundamental in order to improve the reaction kinetic and reduce the poisoning by CO of the Pt based catalysts used in the PEMFC's (CO covers the catalyst preventing the H<sub>2</sub> reaction and the CO content in the fuel should be < 10 ppm). The effect is very temperature-dependent and can be partially suppressed at elevated temperature.<sup>16</sup>

In the last decade, the development of new ion-exchange membranes with improved properties for PEMFCs applications has received much attention.

Not only perfluoropolymers but also partially fluorinated, non-fluorinated hydrocarbon, non fluorinated aromatic and acid base blend membranes have been proposed (Tab. 5).<sup>7</sup>

Several new industrial partnerships also reflect the great effort to develop new membranes<sup>17</sup>:

- Dais-Analytic, Odessa, Fla., is teaming with Dow Plastics, Midland, Mich., to commercialize a lower-cost membrane based on Dow's Index ethylene-styrene interpolymer (ESI).
- Celanese Ventures GmbH, Frankfurt, Germany, is developing a polybenzimidazole (PBI)-based membrane for fuel cells that operate at relatively high (150 C) temperatures.

- Cell maker Ballard is working with the British parent of Victrex USA, Greenville, S.C., to produce two new membrane alternatives. One is the Ballard's BAM ionomer, a partially fluorinated membrane with hydrocarbon pendant groups, which cost less than Nafion. Even less expensive is a sulfonated variant of Victrex PEEK, a high-temperature resin. One is based on sulfonated polyaryletherketone (a variant of PEEK) supplied by Victrex.

**Table 5.** Properties of the main families of membranes used in PEMFCs (from ref. 7)

Category	Structure	Physical Properties	Performance in fuel cell
Perfluorinated membranes	<ul style="list-style-type: none"> <li>▪ Fluorinated backbone like PTFE</li> <li>▪ Fluorocarbon side chain</li> <li>▪ Ionic clusters consisting of sulfonic acid ions attached to the side chains</li> </ul>	<ul style="list-style-type: none"> <li>▪ Strong and stable in both oxidative and reductive environments</li> </ul>	<ul style="list-style-type: none"> <li>- Membrane is durable upto 60,000 h</li> <li>- Proton conductivities in well humidified membranes are 0.2 S/cm at PEMFC operating temperatures</li> <li>- Cell resistance of 0.05 <math>\Omega\text{cm}^2</math> for 100 <math>\mu\text{m}</math> thick membrane with voltage loss of only 50mV at 1 A/cm<sup>2</sup> is achievable</li> </ul>
Partially fluorinated membranes	<ul style="list-style-type: none"> <li>▪ Fluorocarbon base</li> <li>▪ Hydrocarbon or aromatic side chain grafted onto the backbone, which can be modified</li> </ul>	<ul style="list-style-type: none"> <li>▪ Relatively strong in comparison to perfluorinated systems, but degrade fast</li> </ul>	<ul style="list-style-type: none"> <li>- Less durable than perfluorinated ones</li> <li>- Low performance</li> <li>- On suitable modification, yield membranes with comparable proton conductivities</li> </ul>
Non-fluorinated hydrocarbon membranes	<ul style="list-style-type: none"> <li>▪ Hydrocarbon base, typically modified with polar groups</li> </ul>	<ul style="list-style-type: none"> <li>▪ Good mechanical strength</li> <li>▪ Poor chemical and thermal stability</li> </ul>	<ul style="list-style-type: none"> <li>- Poor conductors of protons</li> <li>- Exhibit low durability on account of swelling obtained by incorporation of polar groups into the polymer matrix</li> </ul>
Non-fluorinated aromatic membranes	<ul style="list-style-type: none"> <li>▪ Aromatic base, typically modified with polar/sulfonic acid groups</li> </ul>	<ul style="list-style-type: none"> <li>▪ Good mechanical strengths</li> <li>▪ Chemically and thermally stable even at elevated temperatures</li> </ul>	<ul style="list-style-type: none"> <li>- Good water absorption</li> <li>- Relatively high proton conductivity is attainable-</li> </ul>
Acid-base blend membranes	<ul style="list-style-type: none"> <li>▪ Incorporation of acid components, into an alkaline polymer base</li> </ul>	<ul style="list-style-type: none"> <li>▪ Stable in oxidizing, reducing and acidic environments</li> <li>▪ High thermal stability</li> </ul>	<ul style="list-style-type: none"> <li>- Good dimensional stability</li> <li>- Exhibit proton conductivity comparable to Nafion</li> <li>- Durability of the membranes is still to be proven</li> </ul>

Considering the high cost of the fluoropolymers, a huge number of polymer families membranes based on nonfluorinated ionomers such as of poly(butadiene styrene) block copolymer, polystyrene, polyimides, poly(arylether sulfones), poly(arylether ketones), polyphosphazenes, polybenzimidazole, etc., have been used as starting material to prepare PEM (Tab. 6).<sup>33, 18, 19, 20</sup>

The majority of these polymers are sulfonated in order to realize membranes with ion exchange capacity. In addition, blend or cross-linked polymers are used to introduce or improve the membranes in terms of proton conductivity.<sup>21, 22</sup>

Although the presence of the fluorinated backbone induces an higher acidity of the sulfonic group in the perfluoro membranes such as Nafion and, in general, an higher proton conductivity in comparison with non-fluorinated membranes<sup>9</sup>, the last polymers have lower cost.<sup>7</sup>

Moreover, in many works, organic-inorganic (hybrid) proton exchange membranes have been prepared in order to improve the membrane performance (proton conductivity, water and methanol permeability, thermal stability, etc.).

SiO<sub>2</sub>, TiO<sub>2</sub>, ZrO<sub>2</sub>, zirconium phosphate have been introduced in SPEK and SPEEK membranes obtaining a reduction of the water and methanol flux in pervaporation experiments.<sup>23,24</sup> However in these hybrid membranes also the proton conductivity is reduced in comparison with polymeric membranes.<sup>23, 24</sup>

Composite proton exchange membranes have been prepared from H<sub>3</sub>PO<sub>4</sub>-doped silica gel and a styrene-ethylene-butylene-styrene (SEBS) block copolymer showing 10<sup>-5</sup> Scm<sup>-1</sup> proton conductivity at 25°C in a dry N<sub>2</sub> atmosphere.<sup>25</sup>

The synthesis of SiO<sub>2</sub>/polyethylene oxides (PEO), SiO<sub>2</sub>/polypropylene oxide (PEO), SiO<sub>2</sub>/polytetramethylene oxide (PTMO)) composite membranes stable up to 250°C has been also carried-out by sol-gel method.<sup>26</sup>

Interesting blends between SPEKK and a hybrid polyphenylsulfone with –SiPh(OH)<sub>2</sub> groups covalently linked to the polymer chain (SiPPSU) have been used to prepared membranes with good conductivity at 120°C.<sup>27</sup>

Recast Nafion membranes filled with in situ grown zirconium phosphate, have showed enhanced stability of proton conductivity at temperature higher than 100°C and high relative humidity.<sup>28</sup> This result has been ascribed to the enhanced membrane stiffness.<sup>28</sup>

However particular interesting results have been obtained using heteropolyacids (HPA) additives incorporated in PEMs.

The most commonly used HPAs are characterized by Keggin structure (see also chapter I) interconnected by an high number of hydrogen-bonded water molecules or dioxonium ions (Fig. 8).<sup>29</sup>

These HPAs compounds are characterized by superionic proton conductivity, high thermal and chemical stability.<sup>29</sup>

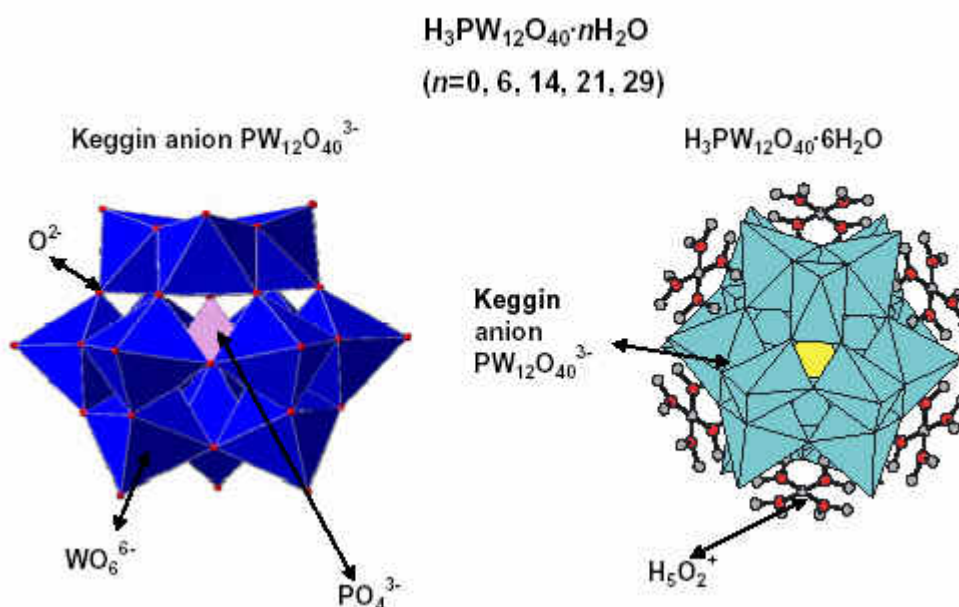


**Figure 8.** Representation of the Keggin type heteropolyacid  $H_3PW_{12}O_{40}$  and its hexahydrate (from ref. 29)

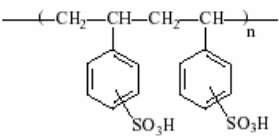
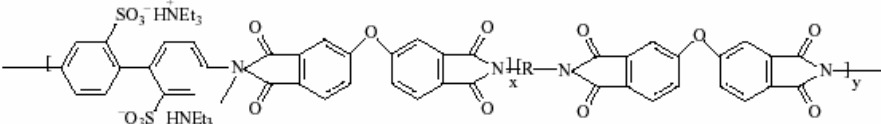
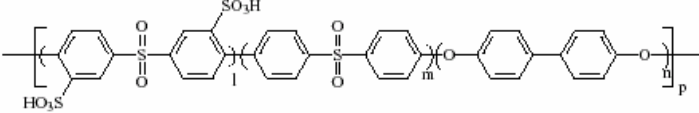
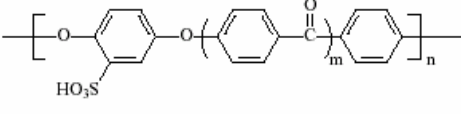
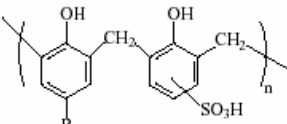
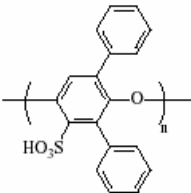
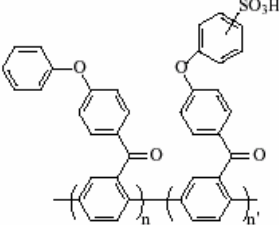
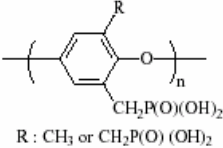
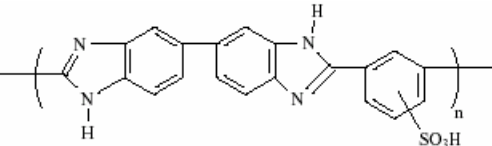
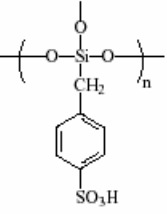
Composite membranes with higher  $T_g$  and the high temperature stability of the proton conductivity, have been obtained by incorporation of 60wt% of three different HPA ( $H_3PW_{12}O_{40}$ ,  $H_3PMo_{12}O_{40}$ ,  $Na_2HPW_{12}O_{40}$ ) in SPEEK membranes with 70, 74 and 80% degree of sulfonation.<sup>46</sup>

Hybrid membranes prepared from sulfonated PEK, heteropolyacids and an inorganic network of  $ZrO_2$  or  $RSiO_{3/2}$  have been also prepared obtaining an higher proton conductivity of the membranes.<sup>30</sup>

The HPAs have been also used to stabilize the proton conductivity of the Nafion membranes at elevated temperature and low relative humidity.

For example,  $H_3PW_{12}O_{40}$ , also exchanged with larger cations such as  $Cs^+$ ,  $NH_4^+$ ,  $Rb^+$  and  $Tl^+$ , has been heterogenized in Nafion membranes observing better proton conductivity.<sup>31,32</sup>

**Table 6.** Some examples of non fluorinated ion-exchange polymers used for PEMFC applications(from ref. 33)

Polymers	Structure
Sulfonated poly-styrenes	
Sulfonated polyimides	
Sulfonated poly(aryl ether sulfones)	
Sulfonated poly(aryl ether ketones) SPEEK	
Sulfonated phenol formol resins	
Sulfonated poly(phenylene oxide)	
Sulfonated poly(p-phenoxy-benzoyl-1,4-phenylene)	
Phosphonic poly(phenylene oxide)	 R : CH <sub>3</sub> or CH <sub>2</sub> P(O)(OH) <sub>2</sub>
Sulfonated poly(benzimidazole)	
Sulfonated silicates	
Polyphosphazenes	



Different variants of sulfonated polyarylenetherketones (Fig. 9) have been proposed in literature as possible alternatives to Nafion: polyetherketone (PEK)<sup>38</sup>, poly(etheretherketone) (PEEK)<sup>15, 34, 35, 36</sup>, poly(etherketoneketone) (PEKK)<sup>37</sup>, poly(ether ether ketone ketone) (PEEKK)<sup>9</sup>, etc (Fig. 9).

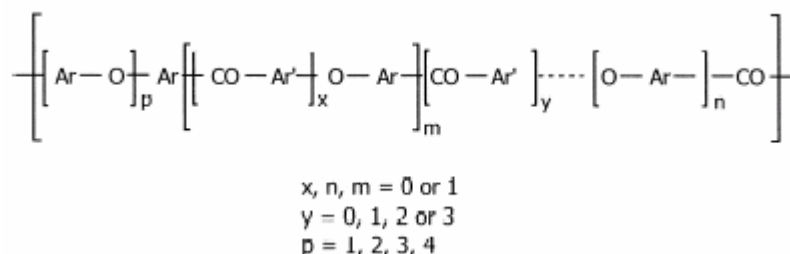


**Figure 9.** General formula of the polyarylenetherketones (from ref. 38)

The oxidation stability is expected to increase with increasing content of ketone segments, and with the decrease in ether segments.<sup>38</sup>

Sulfonation of polyarylenetherketones is usually carried out in concentrated sulfuric acid and the extent of sulfonation is controlled by the reaction time and temperature.<sup>38</sup> The membranes prepared using these polymers are characterized by a good chemical, thermal and mechanical stability.

Another interesting aspect of the sulfonated non-fluorinated aromatic membranes is the generally lower water and methanol permeability compared to Nafion membranes. The different behaviour can be explained by differences in the microstructures of these systems.<sup>9</sup>

In the perfluorosulfonic polymer extremely hydrophobic perfluorinated regions are combined with highly hydrophilic sulfonic groups. In the presence of water the hydrophilic portions of the polymer aggregate forming hydrophilic domains. The Nafion membranes present three phases in their structure: the perfluorinated hydrocarbon backbone, the side-chains with fixed sulfonic end groups and the water (or water/methanol) swelled hydrophilic channels (Fig. 10).

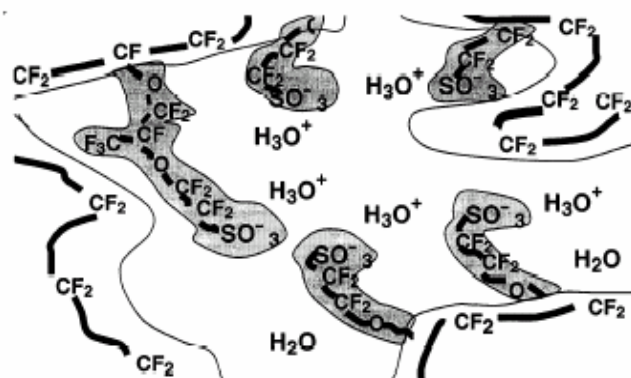


**Figure 10.** Sketch of the structure in Nafion membranes highlighting the three phases present: the perfluorinated hydrocarbon backbone, the side-chains with fixed sulfonic end groups and the water (or water/methanol) swelled hydrophilic channels (from ref. 39)

In the cluster network model<sup>40</sup>, used to rationalize the transport mechanism in Nafion membranes, hydrophilic pockets of about 4 nm in diameter formed by sulfonic acid groups and absorbed water are interconnected by a network of short and narrow channels of approximately 1 nm in diameter, and separated from the hydrophobic region formed by the fluorinated backbone of the polymer (Fig. 11).

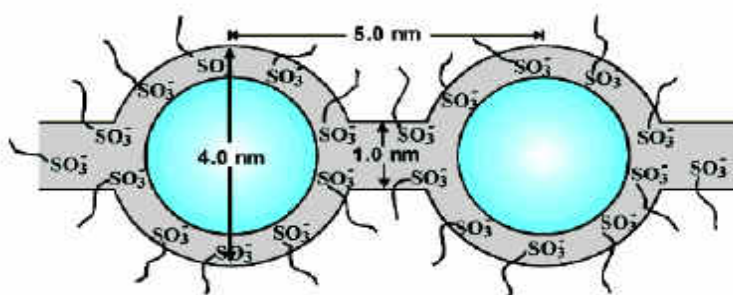


**Figure 11.** Cluster-network model for the hydrated Nafion (from ref. 40)

The proton, water and methanol transport occurs through these hydrophilic regions. The hydrophobic domains are responsible of the morphological stability of the system.

Of course the microstructure of the Nafion and, in general, of all type of polymeric ion-exchange membranes, depends on the level of hydration (Fig. 12).

For example the mean dimension of the hydrophilic pockets in the Nafion with equivalent weight(EW) 1200 shrink from 4 to 2.44 nm when the relative humidity is changed from 100 to 34%.<sup>41</sup> As a consequence, also the transport properties typically vary from the dry to the wet state.

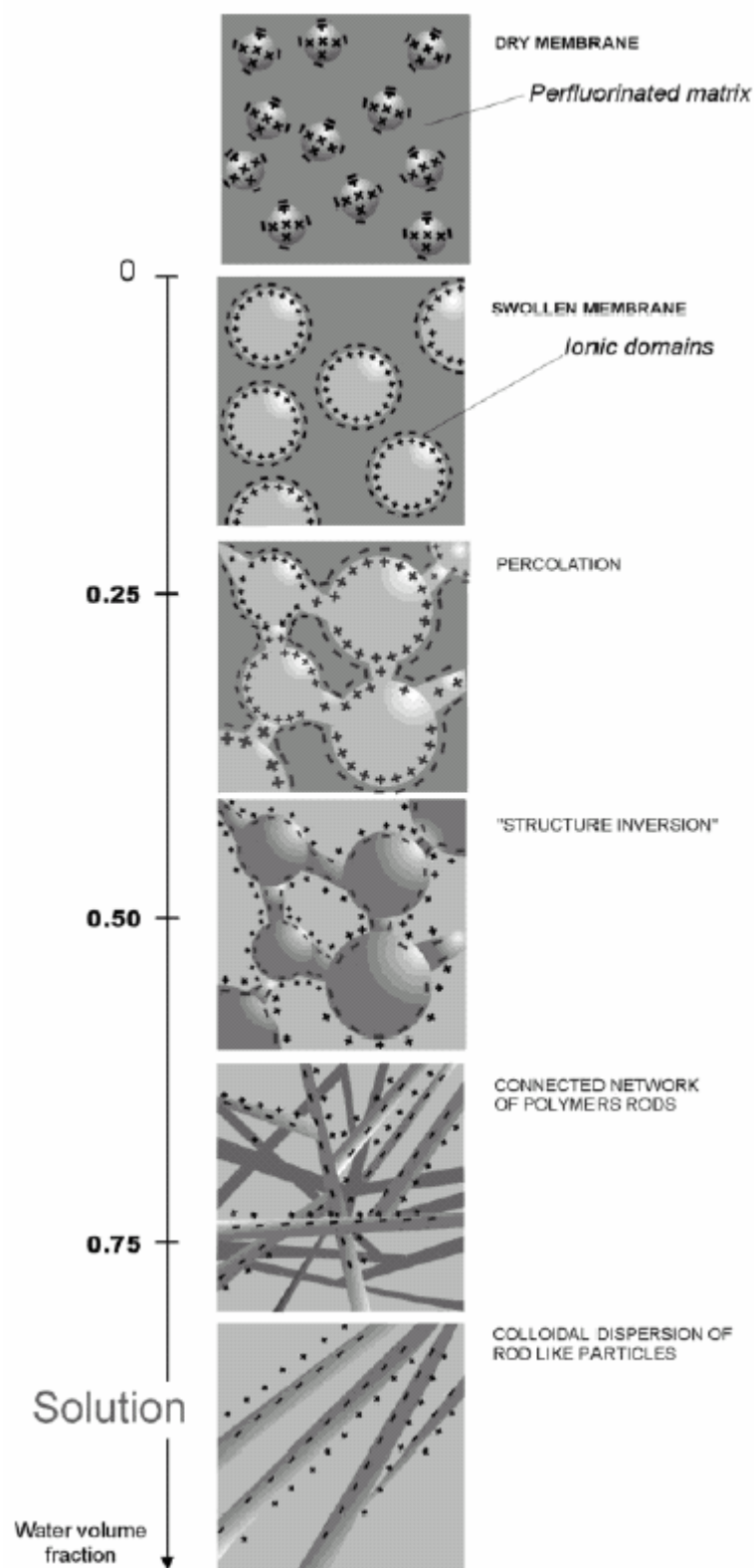


**Figure 12.** Conceptual model describing the morphological reorganization of the ionic domains in Nafion as the dry membrane is swollen with water to the state of complete dissolution (from ref. 40)

### 2.3.2 Sulfonated PEEK and sulfonated PEEK-WC membranes

In the sulfonated polyarylenetherketone membranes the hydrophilic channels are narrower compared to Nafion, less separated from the hydrophobic regions and more branched because the polymer backbone is less hydrophobic and the sulfonic groups less acid than those of the Nafion (Fig. 13).<sup>9,42</sup>. Numerous authors confirmed these different microstructures by Small Angle X-ray Scattering (SAXS) experiments carried out on Nafion and various sulfonated polyarylenetherketone.<sup>9, 39, 43</sup>

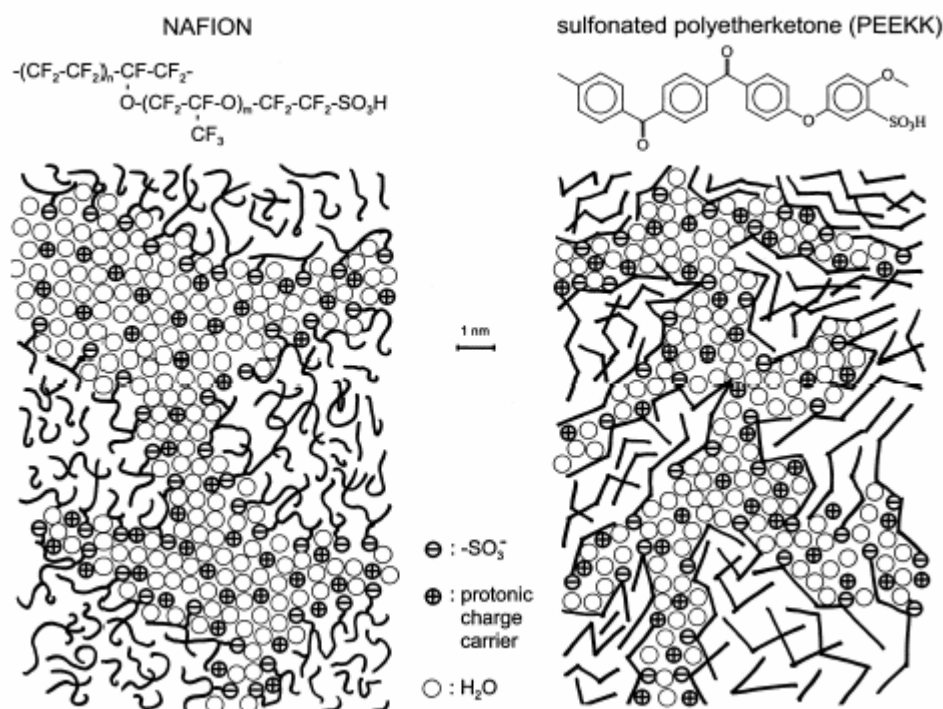


**Figure 13.** Comparison of the microstructure of the hydrated Nafion and a sulfonated PEEKK (from ref. 9)

As a consequence, the water and methanol diffusion coefficient of this family of polymers are typically lower compared to Nafion(Fig.14)<sup>9,44 45</sup>,

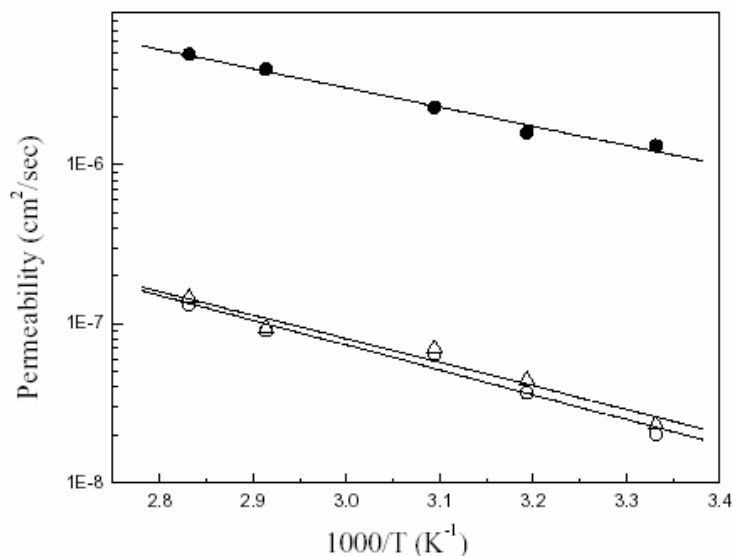


**Figure 14.** Arrhenius plots of the methanol permeability for (●) Nafion<sup>®</sup> 115 membrane, (Δ) SPEEK membrane with sulfonation level 0.47, (○) SPEEK membrane with sulfonation level 0.39, measured using a diaphragm diffusion cell (from ref. 45)

Among the different polyarylenetherketones investigated as possible alternative to the expensive perfluorosulfonic membranes, very interesting systems are the sulfonated polyetheretherketones (SPEEK) membranes.<sup>15,34,35,36,45,46, 47,48</sup>

The polyetheretherketone (PEEK, Fig. 15) polymer generally used in many literature works and in a wide range of industrial applications is a semicrystalline thermoplastic polymer known as Victrex<sup>®</sup> PEEK<sup>49</sup>.

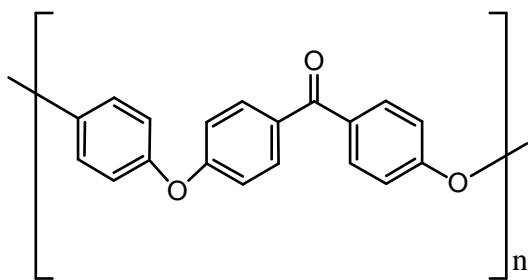


**Figure 15.** Chemical structure of the PEEK polymer

PEEK is insoluble in organic solvents and cannot be used for the preparation of membranes by phase inversion technique.<sup>50</sup>

Unlike native PEEK, the sulfonated derivative of the Victrex<sup>®</sup> PEEK, widely investigated in literature as possible alternative to Nafion<sup>®</sup>, is amorphous and soluble in many organic solvents. However the low solubility of the starting material generally complicates the

sulfonation process usually carried out using concentrated sulphuric acid at room temperature for long reaction times. The sulfonation reaction is initially a heterogeneous process and as a consequence it yields different fractions of polymer with various sulfonation levels.<sup>46</sup>

Unlike classical PEEK, a modified PEEK indicated as PEEK-WC or poly(oxa-p-phenylene-3,3-phthalido-p-phenylene-oxa-p-phenylene-oxy-p-phenylene) (Fig. 16), is amorphous and soluble in many organic solvents with medium polarity, whereas it is not soluble in water, methanol and ethanol (Tab. 7).

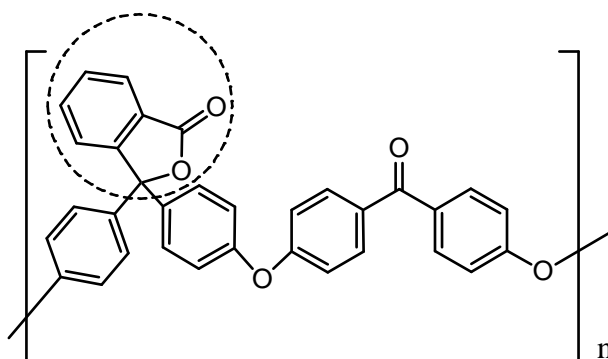


**Figure 16.** Chemical formula of the PEEK-WC polymer with indicated the so called Cardo group

PEEK-WC has a lactonic group, called Cardo group (WC in the polymer name is for With Cardo), along the polymer chain (Fig. 16) which break the crystalline character of the traditional PEEK. As consequence, PEEK-WC is amorphous and it is suitable for the preparation of membranes by phase inversion techniques.<sup>51</sup>

**Table 7.** Some examples of solvents and non-solvents for the PEEK-WC polymer

<b>Soluble</b>	<b>Non soluble</b>
Chloroform	Water
Dichloromethane	Methanol
Dimethylsulfoxide	Ethanol
Tetrahydrofuran	Acetonitrile
dimethylacetamide	Cyclohexane
dimethylformamide	Cyclohexanol
1-methyl-2-pyrrolidinone	1,4-Dioxane
Cyclohexanone	Toluene

Moreover PEEK-WC has a high glass transition temperature ( $T_g = 235^\circ\text{C}$ , vs.  $143^\circ\text{C}$  of the

Victrix<sup>®</sup> PEEK) and very good chemical, thermal and mechanical stability (Tab. 8).<sup>52</sup>

**Table 8.** Some properties of the PEEK-WC polymer

Properties	Value
Glass transition temperature T <sub>g</sub> (from DSC)	235(°C)
5% weight loss temperature (from TGA)	512(°C)
Molar mass of the structural unit	496.5(g/mol)
Molecular weight <sup>a</sup>	223.9 kg/mol
Density (25°C) <sup>b</sup>	1.33 (g/cm <sup>3</sup> )
Molar volume of the structural unit <sup>b</sup>	373 (cm <sup>3</sup> /mol)
Maximum using temperature <sup>b</sup>	200 (°C)
Tensile strength <sup>b</sup>	1000 (kg/cm <sup>2</sup> )
Resistance at low temperature <sup>b</sup>	77 (K)
Impact strength <sup>b</sup>	60 (kg/cm <sup>2</sup> )
Mean interchain spacing (WAXD) <sup>b</sup>	4.62 (Å)

<sup>a</sup> from ref. 53,

<sup>b</sup> from ref. 54)

The membranes prepared using this polymer are characterized by excellent transport properties and selectivity for gas and liquids.<sup>55,56</sup> Moreover, PEEK-WC based membranes can be modified by the introduction of specific chemical groups on the polymer chain.

The reaction with chlorosulfonic acid at room temperature introduces a sulfonic group on the aromatic ring obtaining a polymer (SPEEK-WC) with ion exchange capacity, without polymer degradation (Fig. 17).<sup>57</sup>

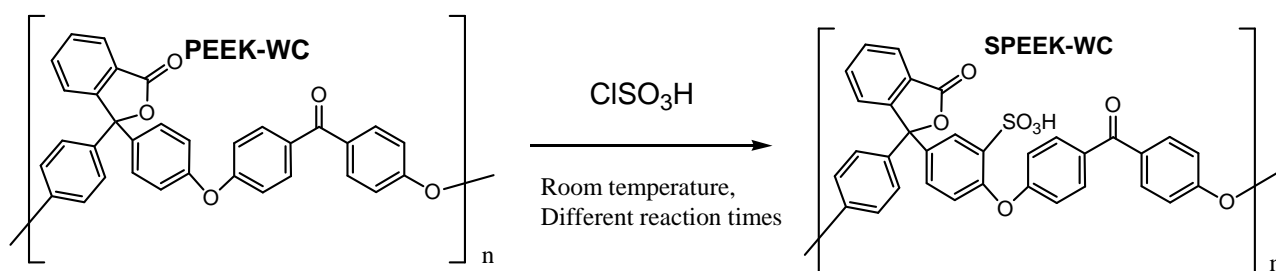


**Figure 17.** Sulfonation reaction of the PEEK-WC

Acting on the reaction times it is possible to modulate the degree of sulfonation (DS).<sup>57</sup>

The reaction is carried out in homogenous phase and in shorter reaction times compared to those of the Victrex PEEK. For example the reaction of Victrex PEEK with concentrated sulphuric acid at room temperature for 192 hours give a polymer with DS =0.85,<sup>46</sup> for PEEK-WC the same DS can be obtained by reaction with chlorosulfonic acid at room temperature in 4 hours.<sup>58</sup>

SPEEK-WC with different degree of sulfonation have been already used for the preparation of PEMs.<sup>58</sup>

The properties of the membranes depends on sulfonation level.

Composite membranes have been also prepared dispersing amorphous zirconium sulfophenylphosphonate (Zr(SPP)), as gel form, in a SPEEK-WC matix.<sup>59</sup>

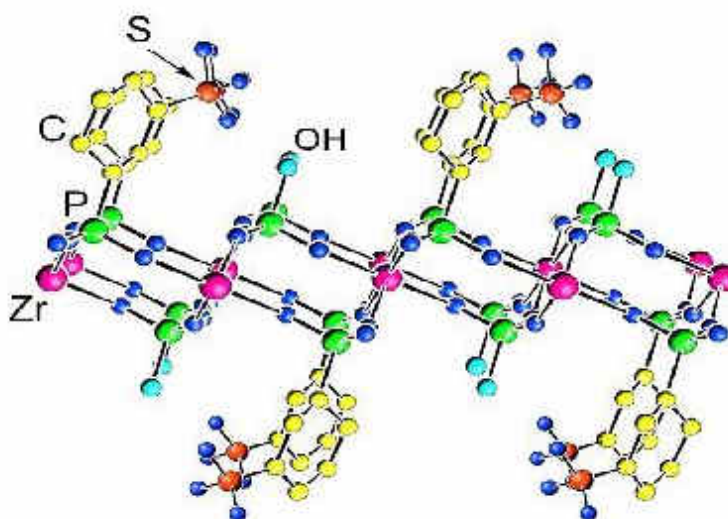


**Figure 15.** Structure of the amorphous zirconium phosphate sulfophenylphosphonate (ZrSPP =  $Zr(HPO_4)_{1.0} (C_6H_4SO_3H)_{1.0} \cdot nH_2O$ ) used to prepare composite SPEEK-WC membranes (from ref. 59)

The membranes obtained were dense and characterized by a good distribution of the inorganic filler.

At low DS value (0.2) the presence of Zr(SPP) improves ion conductivity, at higher DS level (0.57 and 1.04) the polymeric membranes showed an higher conductivity compared to composite membranes but is still lower in comparison with Nafion membranes.<sup>59</sup>

All the composite Zr(SPP)/SPEEK-WC membranes have a lower swelling degree in water and methanol, compared to polymeric ones at the same DS, in the whole range of temperature investigated (25-90 °C); as consequence composite membranes are characterized by an higher stability in the operative conditions of a PEMFC (Fig. 19).<sup>59</sup>



One of the aim of the present has been the development of new SPEEK-WC membranes with improved proton conductivity.

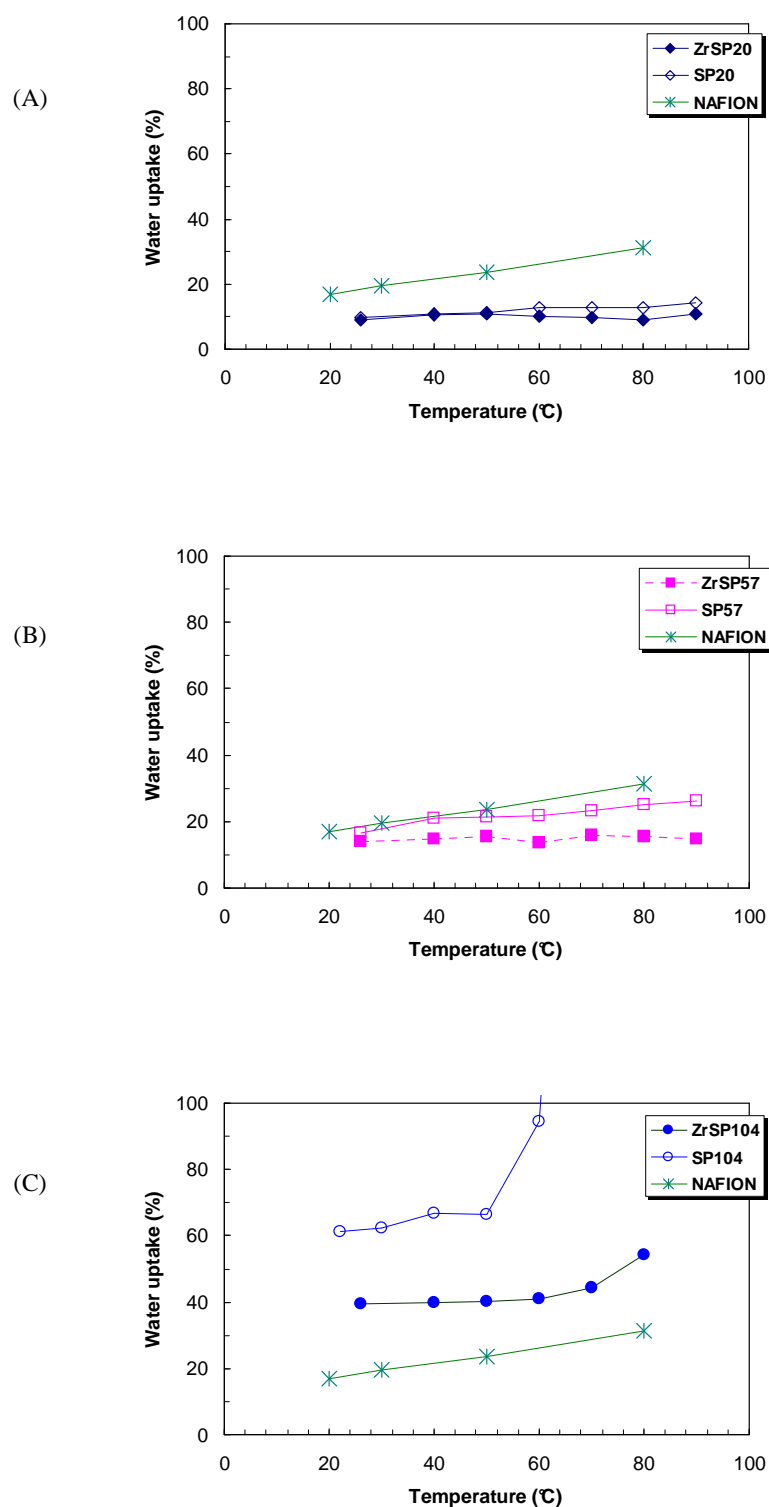


**Figure 19.** Swelling in water as a function of temperature for polymeric (symbol SP followed by DS) and composite membranes (symbol ZrSP followed by DS) at different degree of sulfonation ((A) DS=0.2; (B) DS=0.57; (C) DS=1.04). The water uptake of a commercial Nafion 117 membrane has been reported as a reference (data from ref. 59)

### 2.3.3 Mechanisms of proton transport in PEMs

To understand the proton mechanism in PEMs, it is necessary to keep in mind that protons cannot exist in the bare state (except in particular situation such as plasmas and synchrotron rings),<sup>60</sup> but they strongly interact with electronic density of the environment. The proton localization within the valence electron density of electronegative species (e.g. nitrogen, oxygen) and self-organization due to solvent interactions play a key role in the proton diffusivity.

In hydrated solid proton conductors the transport can be occur by a vehicle or by a Grotthus type mechanism.<sup>61,62</sup>

In the first one the protons are linked to a vehicle, in the specific case water (e.g. as  $\text{H}_3\text{O}^+$  and  $\text{H}_5\text{O}_2^+$  ions), and they diffuse together under a gradient of electrochemical potential.

In the Grotthus mechanism the vehicle molecules are stationary and the transport involve the structural intermolecular reorganization of hydrogen bonds with the concomitant reorientation of the vehicle molecules (protons hopping) as illustrated schematically in the following scheme and in figure 17.

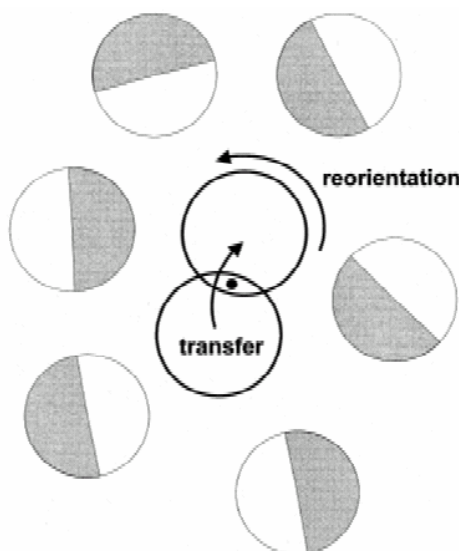


**Figure 17.** Schematic description of the two step occurring in proton transfer (from ref. 62)

At low water content the rate of bond breaking and forming is significantly reduced. Moreover the interaction of the water molecules with the acid functional groups of the polymer polarizes the protons near the anionic sites. This distribution and, as a consequence,

the inhomogeneous electrostatic potential distribution, depends on the chemical interaction of the protons with the anions (influenced by the pKa values), the local dielectric constant of the water and the spatial separation of the acid groups. The decreasing of the acidity, the decreasing of the dielectric constant and the increasing of the separation distance between the polar groups, favour the restriction of proton transport through the hydrophilic domains and reduces the transport coefficient on macroscopic scale<sup>62</sup> (Fig. 21).

The decrease of the water self-diffusion coefficient ( $D_{H_2O}$ ) and the proton conduction diffusion coefficient ( $D_{\sigma}$ ) with decreasing water volume fraction appear more pronounced for the sulfonated polyetherketone than for Nafion (Fig. 21).

In particular with decreasing water content,  $D_{\sigma}$  approaches  $D_{H_2O}$  in Nafion and drops below  $D_{H_2O}$  for the aromatic membranes as a consequence of the suppression of intermolecular proton transfer and the increase of the association of the protonic charge carries with the anionic counter ions (Fig. 21).<sup>62</sup>

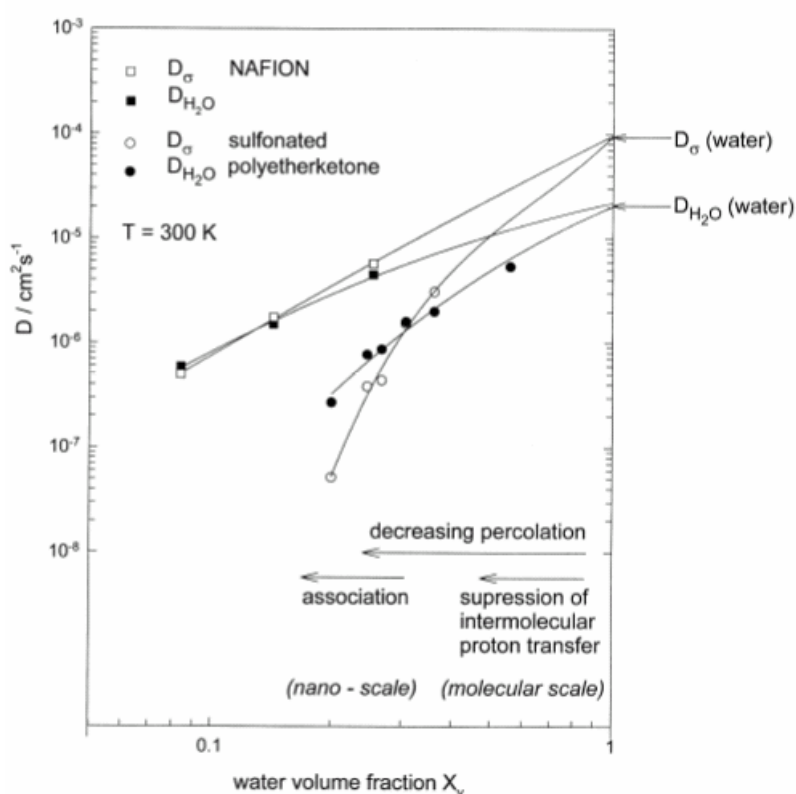


**Figure 21.** Proton conduction diffusion coefficient ( $D_{\sigma}$ ) and water molecular diffusion coefficient ( $D_{H_2O}$ ) for Nafion and a sulfonated polyetherketone (from ref. 62)

In numerous examples, it has been reported that the HPAs can reduce the resistance to the protons in PEMs.<sup>65</sup>

The reduction of the inorganic additive particle sizes and its good dispersion inside the polymeric matrix, is fundamental to have a positive effect on the proton conductivity because increases the surface to volume ratio of the additives and permit a more efficient proton hopping.<sup>63</sup>

HPAs typically exist in hydrated phase with the degree of hydration varying from 6 to 30 molecules of water, depending on the temperature and the relative humidity (for example 6 molecules of water are present in the  $H_3PW_{12}O_{40}$  structure up to 175-230°C).<sup>29</sup>

In a Keggin type HPAs, hydrogen bonds exist between each acid proton and two water molecules, hydrogen bonds are also present between water molecules and the terminal oxygen atoms of the HPAs and , finally, hydrogen bonds involving water molecules can exist between different Keggin units.<sup>64</sup>

If the HPAs sizes are in the order of a few nanometers and uniformly distributed in the proton exchange membrane, the water hydration molecules or dioxonium ions of the additive can be used to better interconnect the ionic cluster of the polymeric matrix providing a better pathway for proton hopping.<sup>65</sup>

For these reasons three commercial available Keggin type HPAs have been used in this work to functionalize polymeric membranes made of SPEEK-WC.

## REFERENCES

- 
- <sup>1</sup> H. Strathmann. Ion-exchange membrane separation processes. Membrane Science and Technology Series, Elsevier (2004)
  - <sup>2</sup> Strathmann H., Giorno L., Drioli E., An introduction to membrane science and technology, Publisher CNR, Roma, 2006.
  - <sup>3</sup> J. Larminie, D. Andrews, Fuel Cell Systems Explained; John Wiley & Sons, Ltd.: Chichester (2000).
  - <sup>4</sup> J.H. Wee, Renewable Sustainable Energy Review 11 (2007) 1720-1738
  - <sup>5</sup> M. Winter, R.J. Brodd, Chem. Rev. 104 (2004) 4245-4269
  - <sup>6</sup> L. Noam, Energy Conversion and Management 38 (1997) 941-955
  - <sup>7</sup> B. Smitha, S. Sridhar, A. Khan, J. Membrane Sci. 259 (2005) 10-26
  - <sup>8</sup> C. Song, Catal. Tod. 77 (2002) 17-49
  - <sup>9</sup> K. D Kreuer. J. Membrane Sci. 185 (2001) 29-39
  - <sup>10</sup> V. Arcella, C. Troglia, A. Ghielmi, Ind. Eng. Chem. Res. 44 (2005) 7645-7651
  - <sup>11</sup> A. Ghielmi P. Vaccarone, C. Troglia, V. Arcella, J. Power Sources 145 (2005) 108-115
  - <sup>12</sup> V. Neburchilov, J. Martin, H. Wang, J. Zhang, J. Power Sources 169 (2007) 221
  - <sup>13</sup> P.L. Antonucci, A.S. Aricò, P. Creti, E. Ramunni, V. Antonucci, Solid State Ionics 125 (1999) 431-437.
  - <sup>14</sup> J. Zhang, Z. Xie, J. Zhang, Y. Tang, C. Song, T. Navessin, Z. Shi, D. Song, H. Wang, a, D.P. Wilkinson, Z.-S. Liu, S. Holdcroft, J. Power Sources 169 (2007) 221–238
  - <sup>15</sup> S.D. Mikhailenko, K. Wang, S. Kaliaguine, P. Xing, G.P. Robertson, M.D. Guiver, Proton conducting membranes based on cross-linked sulfonated poly(ether ether ketone) (SPEEK), J. Membrane Sci. 233 (2004) 93–99
  - <sup>16</sup> Q. Li, R. He, J.-A. Gao, J.O. Jensen, N. J. Bjerrum, J. Electrochem. Soc., 150 (2003) A1599-A1605
  - <sup>17</sup> R. Leaversuch, New Specialty Polymers Improve Fuel-Cell Economics (<http://www.ptonline.com/articles/200201cu3.html>)
  - <sup>18</sup> J. A. Kerres, Development of ionomer membranes for fuel cells, J. Membr. Sci. 185 (2001) 3
  - <sup>19</sup> P. Staiti, F. Lufrano, A.S. Aricò, E. Passalacqua, V. Antonucci, J. Membr. Sci. 188 (2001) 71–78
  - <sup>20</sup> M. A. Hickner, H. Ghassemi, Y. S. Kim, B.R. Einsla, J.E. McGrath, Chem. Rev. 2004, 104, 4587-4612
  - <sup>21</sup> C. Manea, M. Mulder, Characterization of polymer blends of polyethersulfone/sulfonated polysulfone and polyethersulfone/sulfonated polyetherketone for direct methanol fuel cell applications, J. Membr. Sci. 206 (2002) 443
  - <sup>22</sup> P. Krishnan, J.-S.Park, C.-S. Chang-Soo, Eur. Polym. J. 43 (2007) 4019-4027
  - <sup>23</sup> S.P. Nunes, B. Ruffmann, E. Rikowski, S. Vetter, K. Richau, J. Membr. Sci. 203 (2002) 215-225
  - <sup>24</sup> V.S. Silva, B. Ruffmann, V.B. Silva, A. Mendes, L.M. Madeira, S. Nunes, J. Membr. Sci. 284 (2006) 137-144

- 
- <sup>25</sup> K. Hirata, A. Matsuda, T. Hirata, M. Tatsumisago, T. Minami, *J. Sol-Gel Sci. Technol.* 17 (2000) 61-69
- <sup>26</sup> I. Honma, S. Nomura, H. Nakajima, *J. Membr. Sci.* 185 (2001) 83-94
- <sup>27</sup> M.L. Di Vona, A. D'Epifanio, D. Marani, M. Trombetta, E. Traversa, S. Licoccia, *J. Membr. Sci.* 279 (2006) 186-191
- <sup>28</sup> G. Alberti, M. Casciola, D. Capitani, A. Donnadio, R. Narducci, M. Pica, M. Sganappa, *Electrochim. Acta* 52 (2007) 8125-8132
- <sup>29</sup> U.B. Mioč, M.R. Todorović, M. Davidović, Ph. Colomban, I. Holclajtner-Antunović, *Solid State Ionics* 176 (2005) 3005-3017
- <sup>30</sup> M.L. Ponce, L. Prado, B. Ruffmann, K. Richau, R. Mohr, S.P. Nunes, *J. Membr. Sci.* 217 (2003) 5-15
- <sup>31</sup> V. Ramani, H.R. Kunz, J.M. Fenton, *J. Power Sources* 152 (2005) 182-188
- <sup>32</sup> V. Ramani, H.R. Kunz, J.M. Fenton, *Electrochim. Acta* 50 (2005) 1181-1187
- <sup>33</sup> R. Souzy, B. Ameduri, *Prog. Polym. Sci.* 30 (2005) 644-687
- <sup>34</sup> M.L. Di Vona, Z. Ahmed, S. Bellitto, A. Lenci, E. Traversa, S. Licoccia, *J. Membr. Sci.* 296 (2007) 156-161
- <sup>35</sup> V.S. Silva, B. Ruffmann, S. Vetter, M. Boaventura, A.M. Mendesb, L.M. Madeira, S.P. Nunes, *Electrochim. Acta* 51 (2006) 3699-3706
- <sup>36</sup> G. Alberti, M. Casciola, L. Massinelli, B. Bauer, *J. Membr. Science* 185 (2001) 73-81
- <sup>37</sup> S. Vetter, B. Ruffmann, I. Buder, S.P. Nunes, Proton conductive membranes of sulfonated poly(ether ketone ketone), *J. Membr. Sci.* 260 (2005) 181
- <sup>38</sup> D.J. Jones, J. Roziere, *J. Membr. Sci.* 185 (2001) 41-58
- <sup>39</sup> H.-G. Haubold, Th. Vad, H. Jungbluth, P. Hiller, *Electrochim. Acta* 46 (2001) 1559-1563
- <sup>40</sup> K.A. Mauritz, R.B. Moore, *Chem. Rev.* 104 (2004) 4535-4585
- <sup>41</sup> W.Y. Hsu, T.D. Gierke, *Macromolecules* 15 (1982) 101.
- <sup>42</sup> S. Xue, G. Yin, Methanol permeability in sulfonated poly(ethrethrketone) membranes: A comparison with Nafion membranes, *Europ. Pol. J.* 42 (2006) 776-785.
- <sup>43</sup> S. Xue, G. Yin, Methanol permeability in sulfonated poly(ethrethrketone) membranes: A comparison with Nafion membranes, *European Polymer Journal* 42 (2006) 776-785.
- <sup>44</sup> B. Yang, A. Manthiram, *J. Power Sources* 153 (2006) 29-35
- <sup>45</sup> L. Li, J. Zhang, Y. Wang, *J. Membrane Sci.* 226 (2003) 159-167.
- <sup>46</sup> S.M.J. Zaidi, S.D. Mikhailenko, G.P. Robertson, M.D. Guiver, S. Kaliaguine, *J. Membrane Sci.* 173 (2000) 17-34.
- <sup>47</sup> S.D. Mikhailenko, K. Wang, S. Kaliaguine, P. Xing, G.P. Robertson, M.D. Guiver, *J. Membr. Sci.* 233 (2004) 93-99
- <sup>48</sup> S. Xue, G. Yin, *Europ. Pol. J.* 42 (2006) 776-785
- <sup>49</sup> [http://www.victrex.com/en/peek\\_poly/properties.php](http://www.victrex.com/en/peek_poly/properties.php)

- <sup>50</sup> H.N. Beck, *J. Appl. Polym. Sci.*, 45 (1992) 36-40
- <sup>51</sup> E. Fontananova, A. Basile, A. Cassano and E. Drioli, *J. Inclusion Phenom. Macrocyclic Chem.* 47 (2003) 33-37.
- <sup>52</sup> E. Drioli, H.-C. Zhang, *Chimicaoggi* 11 (1989) 59.
- <sup>53</sup> J.C. Jansen, M. Macchione, C. Oliviero, R. Mendichi, G.A. Ranieri, E. Drioli, *Polymer* 46 (2005) 11366–11379
- <sup>54</sup> E. Drioli, H.-C. Zhang, *Chimicaoggi* 11 (1989) 59.
- <sup>55</sup> F. Tasselli, J.C. Jansen, E. Drioli, *J. Appl. Polym. Sci.*, 91 (2004), 841-853.
- <sup>56</sup> J.C. Jansen, M. Macchione, E. Drioli, *J. Membrane Sci.* 255 (2005) 167–180
- <sup>57</sup> F. Trotta, E. Drioli, G. Moraglio, E. Baima Poma, *J. Appl. Polym. Sci.*, 70 (1998) 477-482
- <sup>58</sup> E. Drioli, A. Regina, M. Casciola, A. Oliveti, F. Trotta, T. Massari, *J. Membrane Sci.*, 228 (2004) 139-148.
- <sup>59</sup> A. Regina, E. Fontananova, E. Drioli, M. Casciola, M. Sganappa, F. Trotta, *J. Power Sources* 160 (2006) 139–147
- <sup>60</sup> P. Colomban (Ed.), *Chemistry of Solid State Materials. 2. Proton Conductors-Solids, Membranes and Gels-Materials and Devices*, Cambridge University Press, Cambridge, UK, 1992.
- <sup>61</sup> K.-D. Kreuer, *Chem. Mater.* 8 (1996) 610-641
- <sup>62</sup> K.-D. Kreuer, *Solid State Ionics* 136-137 (2000) 149-160
- <sup>63</sup> V.Ramani, H.R. Kunz, J.M. Fenton, *J. Membr. Sci.* 266 (2005) 110-114
- <sup>64</sup> J.B. Moffat, *Polyhedron* 5 (1986) 261
- <sup>65</sup> V.Ramani, H.R. Kunz, J.M. Fenton, *J. Membr. Sci.* 232 (2004)31-44

# **Chapter 3:**

## **Development of advanced functional polymeric membranes**



### 3.1 Heterogenization of polyoxometallates in polymeric membrane for oxidation reactions with a low environmental impact

Photocatalytic oxidations represents a key strategy towards the development of new sustainable methods for chemical transformations.<sup>1,2</sup> The combined use of photoactivation techniques and dioxygen might guarantee a minimal environmental impact, depending on the photocatalyst performance which ideally should: undergo photoexcitation employing sunlight at room temperature, promote fast and selective processes; activate dioxygen to form reactive oxygenated species; be stable, and easily recyclable for multi-turnover processes.<sup>3</sup>

These processes are of interest not only for the selective oxidations in photo-assisted synthetic procedures but also for the environmental remediation.

In wastewater most traditional processes simply transfer the pollutants from one medium to another (liquid-liquid extraction<sup>4,5</sup>, absorption onto activated carbon<sup>6,7</sup>, air stripping<sup>8</sup>) or generate waste that require further treatment and disposal (biological oxidation<sup>9</sup> and classical chemical treatment such as addition of chlorine or potassium permanganate<sup>10,11,12</sup>). On the contrary, advanced oxidation processes (AOP), are very promising methods for wastewater treatment<sup>13,14</sup>. These methods, mainly based on the photoinduced generation of hydroxyl radicals, can lead to complete mineralization of organic pollutants.

Polyoxometallates or polyoxoanions (POMs), early transition metals (V, Nb, Ta, Mo, W, etc.)-oxygen cluster anions, are a large class of inorganic compounds with interesting properties as catalysts for oxidation reactions in fine chemical synthesis and degradation of organic pollutants, by thermal or photochemical activation.<sup>15,16,17</sup>

Moreover POMs in the acid form, generally called heteropolyacids (HPAs), have superacid properties because the large size of the heteropolyanions<sup>18</sup> and they have been widely used not only as acid catalysts<sup>19</sup>, but also in order to improve the properties of polymeric proton exchange membranes<sup>20</sup>.

There is an high variety of POMs complexes differentiated in terms of chemical composition, structure and counterion (Fig. 1).

In particular, W-containing POMs have a well documented ability to promote photooxygenation of various substrates under mild reaction conditions (oxygen atmospheric pressure, room temperature), both in organic solvents and in water.

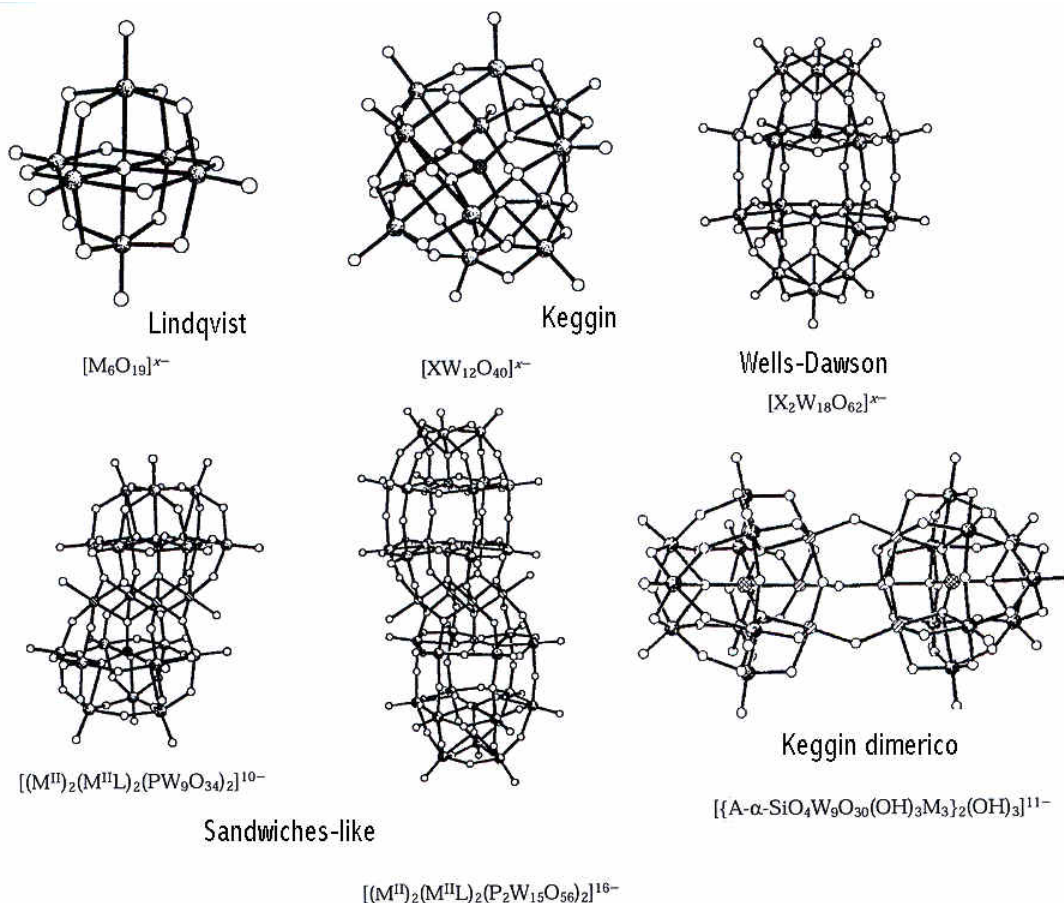


**Figure. 1** Some representative structural families of POMs (From ref. 21)

The proposed mechanism for POM based photocatalysis involves the absorption of light by the complex ground state forming a charge-transfer excited state (POM\*) with strong oxidizing properties (Fig. 2).<sup>21</sup> This is the primary photoreactant, which is able to undergo multi-electron reduction without structural rearrangement, leading to the well-known “blue” reduced form (heteropolyblue). In the presence of aliphatic hydrocarbons, the oxidative step occurs mainly through hydrogen atom abstraction (RH), generating in solution a reactive radical intermediate (substrate activation). Therefore, in the catalytic cycle, dioxygen plays a multifaceted role: by intercepting the organic radicals giving rise to an autooxidation chain, and providing to the re-oxidation of the POM<sub>(red)</sub> thus closing the cycle and generating reduced oxygenating species (dioxygen activation). Furthermore, in aqueous solution, the photooxidation performance can be strongly enhanced by the production of highly reactive hydroxyl radicals OH• formed through the direct reaction of water with the excited POM (solvent activation). The existence of three operating activation mechanisms for the catalytic functionalization of unreactive C-H bonds, is rather unique and deserves a special attention.

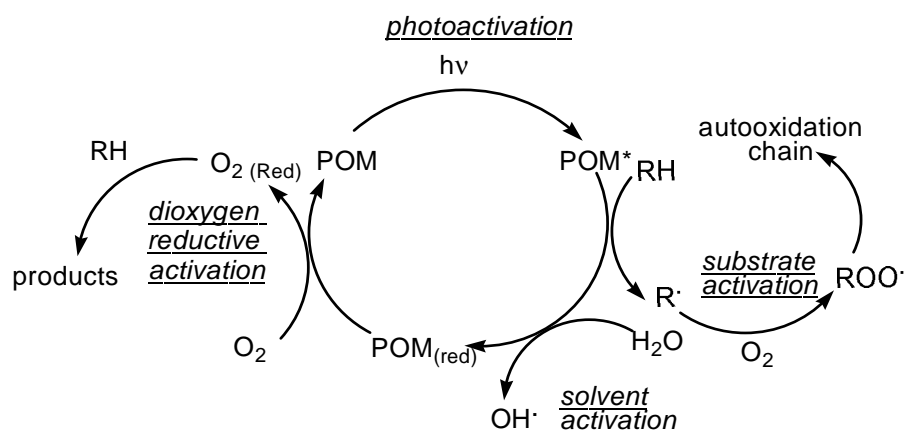


**Figure 2.** Composite activation mechanism in the photocatalytic oxidation cycle by polyoxometalates in water (from ref. 22)

Among POMs, decatungstate ( $W_{10}O_{32}^{4-}$ ) exhibits especially interesting properties for the photocatalytic detoxification of wastewater since its absorption spectrum ( $\lambda_{\max} = 324$  nm) partially overlaps the UV solar emission spectrum opening the potential route for an environmentally benign solar-photoassisted application.<sup>23</sup>

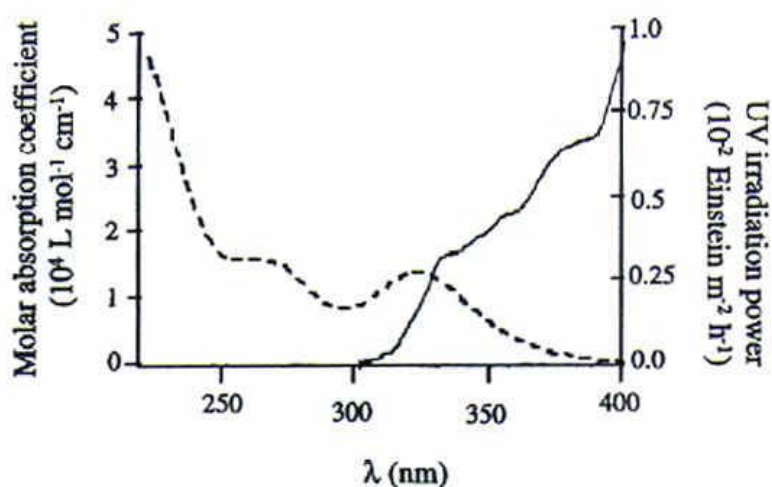


**Figure 3.** Decatungstate absorption spectrum (----) and solar emission spectrum (—) (From ref. 23)

However, decatungstate has also some relevant limitations: it is characterized by low quantum yields, small surface area, poor selectivity and limited stability at pH higher than 2.5.<sup>15</sup>

As reported in the Chapter 1, membrane technology could offer interesting possibilities in order to overcome these limitations and improve the advantages of catalysis mediated by POMs<sup>22</sup> by: the multi-turnover recycling associated to heterogeneous supports, the selectivity

tuning as a function of the substrate affinity towards the heterogeneous membrane, the effect of the polymeric micro-environment on catalyst stability and activity.

In this respect, the design of alternative heterogeneous photooxygenation systems able to employ visible light, oxygen, mild temperatures and solvent with a low environmental impact (water or neat reaction), has been investigated in of this thesis.

We have studied the heterogenization of the decatungstate (W10) in polymeric membranes.

The successfully heterogenization of the W10 has been guaranteed by a proper choice of both the catalyst and the polymeric material.

Because we are interested to photo-oxidation reactions of organic substrates, principally in aqueous phase, we have used hydrophobic polymeric materials for membrane preparations: the partially fluorinated polyvinylidene fluoride (PVDF) and the perfluorinated polymer Hyflon AD<sup>®</sup>. Both polymer are transparent in the region of interest of the catalyst, characterized by a high chemical, thermal and UV stability. Moreover the use of a fluorinated media to carry out oxidation reactions is particularly useful because the well known high solubility of oxygen in fluorinated environment.

In order to improve the catalyst/polymer interaction and to avoid catalyst leaching out from the membrane, we have employed lipophilic (not hydro soluble) derivatives of the decatungstate: the tetrabutylammonium salt ((n-C<sub>4</sub>H<sub>9</sub>N)<sub>4</sub>W<sub>10</sub>O<sub>32</sub> indicated as TBAW10) and the fluorine-tagged decatungstate, ([CF<sub>3</sub>(CF<sub>2</sub>)<sub>7</sub>(CH<sub>2</sub>)<sub>3</sub>]<sub>3</sub>CH<sub>3</sub>N)<sub>4</sub>W<sub>10</sub>O<sub>32</sub>. indicated as (R<sub>f</sub>N)<sub>4</sub>W10). The first one has been heterogenized in PVDF membranes and used for the aerobic photo-oxidation of phenol in water.<sup>24,25,26</sup> This reaction has been chosen because phenol and its derivatives constituted one of the main organic pollutants to be removed from wastewater, and the development of new effective and environmental benign methods for phenols degradation is an important research area.<sup>27, 28, 29</sup>

The second one has been heterogenized in perfluorinated Hyflon membranes and used in the solvent-free oxygenation of benzylic hydrocarbons<sup>30,25</sup>.

### **3.1.1 Preparation and characterization of PVDF membranes containing decatungstate**

#### *Choice of the polymeric material for catalyst heterogenization*

The stability of the catalytic system under reaction conditions and the firm fixation of the catalyst are key issue in catalyst heterogenization.

In a previous work<sup>22</sup> it has been demonstrated that PVDF is an appropriate material to prepare membranes stable under aerobic photo-oxidation conditions. Moreover, PVDF polymeric matrix can also interact with lipophilic salt of decatungstate by Van der Waals interactions.

The instauration of electron donor–electron acceptor interactions between the catalyst and fluorinated polymer is also possible between the C-F  $\sigma^*$  orbitals acting as electrons acceptor and oxygen lone pairs of W10 acting as electrons donor<sup>31</sup>.

PVDF is of particular interest in photocatalytic applications because of its optical transparency; moreover the fluorinated environment can promote oxidation reactions by specific interaction with oxygen<sup>32,33</sup>. Furthermore, the hydrophobic properties of this polymer can positively influence the approach near the catalytic sites of the phenol dissolved in water. This behaviour can be anticipated by the calculation of the *affinity parameters* ( $\Delta\delta$ )<sup>34, 35</sup> indicating the affinity between two systems in condensed phase.

The affinity parameters PVDF/phenol and PVDF/water were calculated using the following equation:

$$\Delta\delta t = [(\delta_{dp}-\delta_{ds})^2 + (\delta_{pp}-\delta_{ps})^2 + (\delta_{hp}-\delta_{hs})^2]^{1/2} \quad (1)$$

were the second symbol  $p$  is for polymer and  $s$  for water or phenol solubility parameters components;  $\delta d$ ,  $\delta p$  and  $\delta h$ , respectively for non-polar, polar interactions and hydrogen bonds ).<sup>34, 35</sup>

PVDF has a bigger affinity for phenol respect to water, as evident from the calculation of the affinity parameters ( $\Delta\delta$ ) PVDF/water and PVDF/phenol that result respectively 31,6 and 8,6  $J^{1/2}/cm^{3/2}$  (for a good affinity between two condensed systems,  $\Delta\delta$  must to be small<sup>34, 35</sup>). As consequence, phenol can be selectively absorbed from the aqueous phase into the polymeric matrix.

### Experimental

The sodium salt of the decatungstate  $Na_4W_{10}O_{32}$  and the lipophilic salt TBAW10, were prepared and supplied by Prof. Gianfranco Scorrano's group (University of Padua) following a literature procedures.<sup>36, 22</sup>

PVDF homopolymer was provided by Elf Atochem under the trade name Kinar 460. Phenol and N,N-dimethylacetamide (DMA) were used as received from Sigma-Aldrich, without further purification. Distilled water was obtained from a Purelab apparatus.

The cross-section and surface morphology of the membranes were examined by a Quanta 200 F FEI Philips scanning electron microscopy (SEM) using secondary electrons detector (SE) or back scattered electrons (BSE). Cross-sections were prepared by fracturing the membrane in

liquid nitrogen. EDX microanalyses were performed with a EDAX-Phoenix instrument (detector Super Ultra Thin Window, Si/Li crystal analyser).

Fourier transform infrared (FT-IR) analysis, also with an attenuated total reflectance method (ATR), were performed using a Perkin Elmer Spectrum One.

UV–Vis spectra were recorded with a Perkin Elmer LAMBDA 650 spectrophotometer operating with a 150 mm integrating sphere; UV-Vis transmittance spectra were performed by a Shimadzu 1610 spectrophotometer.

The micrometric film applicator used for casting solution was supplied by Elcometer.

The membranes thickness was determined by a digital micrometer Carl Mahr D7300 Esslingen a.N. Results reported are the mean of ten measurements of different regions of each membrane.

Contact angles were measured by a CAM 200 contact angle meter (KSV Instruments LTD, Helsinki, Finland). The measurements were performed by depositing the test liquid from the above using an motor driven microsyringe on the membrane surfaces. Results are the mean of five measurements of different regions of the membrane surfaces.

The experimental equipment used to measure gas permeance for pure gases, was manufactured by GKSS Forschung (Germany).

Dr. John Jansen (Institute on Membrane Technology, ITM-CNR) is gratefully acknowledged for his collaboration in gas permeation experiments.

The procedure is based on a pressure increase measurement on the fixed volume permeate side of the membrane cell, which is completely evacuated before the start of the measure. Permeation studies were carried out at 25°C and feed gas pressure of 1 bar.

The permeability is calculated from the pressure increase of the fixed permeate volume.

If the feed pressure is constant the steady-state permeance,  $P$ , defined as the gas volume ( $\text{m}^3_{\text{STP}}$ ) which penetrates a certain membrane area ( $\text{m}^2$ ) per unit time (h) at a given pressure difference (bar), can be calculated from the permeate pressure increase according to the following equation:

$$P = \frac{V_P \cdot V_m}{R \cdot T \cdot A \cdot t} \cdot \ln \left( \frac{p_F - p_0}{p_F - p_{P(t)}} \right) \quad \text{in} \quad \frac{\text{m}^3_{\text{STP}}}{\text{m}^2 \cdot \text{h} \cdot \text{bar}} \quad (2)$$

in which  $V_P$  is the permeate volume [ $\text{m}^3$ ],  $V_m$  is the molar volume of a gas at standard temperature and pressure [ $22.41 \cdot 10^{-3} \text{ m}^3_{\text{STP}}/\text{mol}$  at 0°C and 1 atm],  $R$  is the universal gas constant [ $8.314 \cdot 10^{-5} \text{ m}^3 \text{bar}/(\text{mol} \cdot \text{K})$ ],  $T$  is the absolute temperature [K],  $A$  is the exposed

membrane area [ $\text{m}^2$ ],  $t$  is the measurement time [s],  $p_F$  is the feed pressure and  $p_0$  and  $p_{P(t)}$  are the permeate pressure at  $t=0$  and at  $t=t$ , respectively.<sup>37</sup>

The pure gas selectivity,  $\alpha_{A/B}$ , is a measure of the potential separation characteristics of the membrane material. It is defined as the ratio of the permeability coefficients of pure gases A and B:

$$\alpha_{A/B} = P_A/P_B = (D_A/D_B) (S_A/S_B) \quad (3)$$

Crossflow water filtration experiments were carried out at  $30 \pm 1^\circ\text{C}$  using a ultrafiltration laboratory equipment constituted by a flat membrane cell, fed with distilled water at different transmembrane pressure (TMP).

A Perkin–Elmer Pyris Diamond DSC was used for studying the melting and crystallization behaviour of the polymeric membranes. Melting temperature (mean peak) and enthalpy were measured at the second heating (heating and cooling rate  $15^\circ\text{C}/\text{min}$ ).

The degree of crystallinity of PVDF-based membranes was measured as the ratio between  $\Delta H_m$  and  $\Delta H_0$ , where  $\Delta H_0$  is the melting enthalpy of totally crystalline PVDF ( $104,50 \text{ J/g}$ ).<sup>38</sup>

The membrane mean pores diameter was determined by a capillary flow porometer CFP 1500, Porous Materials Inc. Ithaca, NY.

Membrane porosity was obtained by a gravimetric method, measuring the weight of water contained in the membrane pores. The porosity,  $\varepsilon$ , was calculated by the following equation:

$$\varepsilon = \frac{(w_2 - w_1)/D_w}{((w_2 - w_1)/D_w) + (w_1/D_p)} \quad (4)$$

where  $w_1$  is the weight of the dry membrane,  $w_2$  the weight of the wet membrane,  $D_w$  the water density and  $D_p$  is the polymer density ( $1,76 \text{ g/cm}^3$  for PVDF).

The photocatalytic experiments were carried out with the membrane reactor described in figure 4.

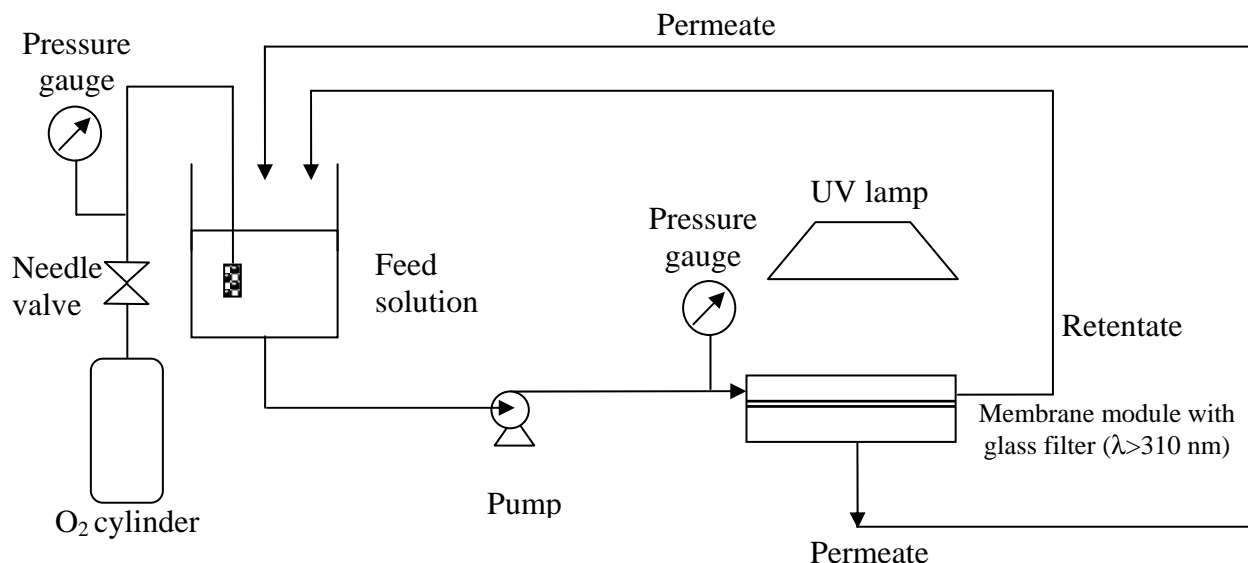


**Figure 4.** Schematization of the membrane photoreactor used for the catalytic tests

The membrane module equipped with a quartz window on the upper surface has an active surface area of  $4.5 \text{ cm}^2$ . In the catalytic tests an aqueous phenol solution ( $0.002 \text{ mol/L}$ ;  $\text{pH}=6$ ; volume  $150 \text{ mL}$ ), was fed to the membrane with a tangential flow rate of  $65 \text{ mL/min}$ . The feed solution was hosted in a thermostatic bath held at  $30 \pm 1^\circ\text{C}$  under magnetic stirring. Oxygen was bubbled into the phenol solution at a pressure of  $0.3 \text{ bar}$ , which was necessary to achieve saturation and promote photodegradation reaction. The oxygen concentration in the phenol solution was  $25 \text{ ppm}$  (oximeter Hanna Instruments 964400). A glass filter ( $310 \text{ nm}$  cut-off) was positioned on the quartz window of the membrane module in order to prevent phenol auto-photolysis. Irradiation was performed with a  $500 \text{ W}$  quartz UV mercury vapour lamp (Helios Italquartz). In all experiments the membranes were irradiated on the upper surface. The lamp was placed upper the reactor and the distance between its bulb and the surface of the liquid was  $15 \text{ cm}$ ; the measured light intensity (radiometer UVX-36, by Helios Italquartz) at this distance was  $3 \text{ mW/cm}^2$ . Homogeneous catalytic reactions were carried out using an aqueous solution of  $\text{Na}_4\text{W}_{10}\text{O}_{32}$  ( $4.23 \cdot 10^{-4} \text{ mol/L}$ ).

The reactions were monitored by HPLC determination of the phenol at different time. Analyses were performed on a HPLC Agilent 110 series. The column was a PhenomenexC18  $250 \times 4.6 \text{ mm}$ ,  $4 \mu\text{m}$ . The mobile phase was acetonitrile/water  $65/35$  (v/v). Total organic carbon (TOC) analyses were performed on a TOC-C csn Shimadzu.

All the catalytic test were performed in duplicate to assess the reproducibility of the determinations.



At the end of the photocatalytic tests, the membranes were washed with water and then dried before their reuse in successive catalytic runs.

### Membranes preparation

Asymmetric porous membrane in flat configuration have been prepared by phase inversion technique induced by a non-solvent.<sup>39</sup> Homogenous solutions have been prepared by dissolving the polymer in DMA by magnetic stirring at room temperature, then the appropriate amount of catalyst (14.3, 25.0 or 33.3 wt% respect the final membrane mass) was added and the solutions were left under stirring for additional 24 h. For comparison we also prepared in the same conditions a membrane of PVDF without the catalyst indicated in the following text as PVDF reference (Table 1).

**Table 1.** Composition of the casting solutions used to prepare polymeric and catalytic membranes. The composition of all solution is expressed by considering the weight percentage (wt%).

Membrane code	Composition of the casting solution (wt %)		Catalyst loading respect to membrane mass (wt %)
PVDF (reference)	PVDF	15.0	0
	DMA	85.0	
PVDF-W10 (14.3 wt%)	PVDF	15.0	14.3
	DMA	82.5	
	TBA <sub>4</sub> W <sub>10</sub> O <sub>32</sub>	2.5	
PVDF-W10 (25.0 wt%)	PVDF	15.0	25.0
	DMA	80.0	
	TBA <sub>4</sub> W <sub>10</sub> O <sub>32</sub>	5.0	
PVDF-W10 (33.3 wt%)	PVDF	15.0	33.3
	DMA	77.5	
	TBA <sub>4</sub> W <sub>10</sub> O <sub>32</sub>	7.5	

The solutions were cast on a glass plate by a micrometric film applicator adjusting the blade gap at 250  $\mu\text{m}$ . The cast film was immersed for 2 h in a coagulation bath containing distilled water (a non solvent for the PVDF but miscible with DMA) at  $20\pm 2^\circ\text{C}$ . After few seconds the formation of a white condensed film, detached form the glass support, was observed. This film, i.e. the membrane, was removed from the coagulation bath and immersed in a fresh water bath for additional 24hours to remove residual traces of solvent, the membranes were dried at room temperature for 24 hours and finally in a vacuum oven at  $60^\circ\text{C}$  for additional 24 hours.

At the end of the photocatalytic tests, the membranes were washed with water and then dried before their reuse in successive catalytic runs.

### Membranes preparation

Asymmetric porous membrane in flat configuration have been prepared by phase inversion technique induced by a non-solvent.<sup>39</sup> Homogenous solutions have been prepared by dissolving the polymer in DMA by magnetic stirring at room temperature, then the appropriate amount of catalyst (14.3, 25.0 or 33.3 wt% respect the final membrane mass) was added and the solutions were left under stirring for additional 24 h. For comparison we also prepared in the same conditions a membrane of PVDF without the catalyst indicated in the following text as PVDF reference (Table 1).

**Table 1.** Composition of the casting solutions used to prepare polymeric and catalytic membranes. The composition of all solution is expressed by considering the weight percentage (wt%).

Membrane code	Composition of the casting solution (wt %)		Catalyst loading respect to membrane mass (wt %)
PVDF (reference)	PVDF	15.0	0
	DMA	85.0	
PVDF-W10 (14.3 wt%)	PVDF	15.0	14.3
	DMA	82.5	
	TBA <sub>4</sub> W <sub>10</sub> O <sub>32</sub>	2.5	
PVDF-W10 (25.0 wt%)	PVDF	15.0	25.0
	DMA	80.0	
	TBA <sub>4</sub> W <sub>10</sub> O <sub>32</sub>	5.0	
PVDF-W10 (33.3 wt%)	PVDF	15.0	33.3
	DMA	77.5	
	TBA <sub>4</sub> W <sub>10</sub> O <sub>32</sub>	7.5	

The solutions were cast on a glass plate by a micrometric film applicator adjusting the blade gap at 250  $\mu\text{m}$ . The cast film was immersed for 2 h in a coagulation bath containing distilled water (a non solvent for the PVDF but miscible with DMA) at  $20\pm 2^\circ\text{C}$ . After few seconds the formation of a white condensed film, detached from the glass support, was observed. This film, i.e. the membrane, was removed from the coagulation bath and immersed in a fresh water bath for additional 24 hours to remove residual traces of solvent, the membranes were dried at room temperature for 24 hours and finally in a vacuum oven at  $60^\circ\text{C}$  for additional 24 hours.

At the end of the photocatalytic tests, the membranes were washed with water and then dried before their reuse in successive catalytic runs.

### Membranes preparation

Asymmetric porous membrane in flat configuration have been prepared by phase inversion technique induced by a non-solvent.<sup>39</sup> Homogenous solutions have been prepared by dissolving the polymer in DMA by magnetic stirring at room temperature, then the appropriate amount of catalyst (14.3, 25.0 or 33.3 wt% respect the final membrane mass) was added and the solutions were left under stirring for additional 24 h. For comparison we also prepared in the same conditions a membrane of PVDF without the catalyst indicated in the following text as PVDF reference (Table 1).

**Table 1.** Composition of the casting solutions used to prepare polymeric and catalytic membranes. The composition of all solution is expressed by considering the weight percentage (wt%).

Membrane code	Composition of the casting solution (wt %)		Catalyst loading respect to membrane mass (wt %)
PVDF (reference)	PVDF	15.0	0
	DMA	85.0	
PVDF-W10 (14.3 wt%)	PVDF	15.0	14.3
	DMA	82.5	
	TBA <sub>4</sub> W <sub>10</sub> O <sub>32</sub>	2.5	
PVDF-W10 (25.0 wt%)	PVDF	15.0	25.0
	DMA	80.0	
	TBA <sub>4</sub> W <sub>10</sub> O <sub>32</sub>	5.0	
PVDF-W10 (33.3 wt%)	PVDF	15.0	33.3
	DMA	77.5	
	TBA <sub>4</sub> W <sub>10</sub> O <sub>32</sub>	7.5	

The solutions were cast on a glass plate by a micrometric film applicator adjusting the blade gap at 250  $\mu\text{m}$ . The cast film was immersed for 2 h in a coagulation bath containing distilled water (a non solvent for the PVDF but miscible with DMA) at  $20\pm 2^\circ\text{C}$ . After few seconds the formation of a white condensed film, detached from the glass support, was observed. This film, i.e. the membrane, was removed from the coagulation bath and immersed in a fresh water bath for additional 24 hours to remove residual traces of solvent, the membranes were dried at room temperature for 24 hours and finally in a vacuum oven at  $60^\circ\text{C}$  for additional 24 hours.

At the end of the photocatalytic tests, the membranes were washed with water and then dried before their reuse in successive catalytic runs.

### Membranes preparation

Asymmetric porous membrane in flat configuration have been prepared by phase inversion technique induced by a non-solvent.<sup>39</sup> Homogenous solutions have been prepared by dissolving the polymer in DMA by magnetic stirring at room temperature, then the appropriate amount of catalyst (14.3, 25.0 or 33.3 wt% respect the final membrane mass) was added and the solutions were left under stirring for additional 24 h. For comparison we also prepared in the same conditions a membrane of PVDF without the catalyst indicated in the following text as PVDF reference (Table 1).

**Table 1.** Composition of the casting solutions used to prepare polymeric and catalytic membranes. The composition of all solution is expressed by considering the weight percentage (wt%).

Membrane code	Composition of the casting solution (wt %)		Catalyst loading respect to membrane mass (wt %)
PVDF (reference)	PVDF	15.0	0
	DMA	85.0	
PVDF-W10 (14.3 wt%)	PVDF	15.0	14.3
	DMA	82.5	
	TBA <sub>4</sub> W <sub>10</sub> O <sub>32</sub>	2.5	
PVDF-W10 (25.0 wt%)	PVDF	15.0	25.0
	DMA	80.0	
	TBA <sub>4</sub> W <sub>10</sub> O <sub>32</sub>	5.0	
PVDF-W10 (33.3 wt%)	PVDF	15.0	33.3
	DMA	77.5	
	TBA <sub>4</sub> W <sub>10</sub> O <sub>32</sub>	7.5	

The solutions were cast on a glass plate by a micrometric film applicator adjusting the blade gap at 250  $\mu\text{m}$ . The cast film was immersed for 2 h in a coagulation bath containing distilled water (a non solvent for the PVDF but miscible with DMA) at  $20\pm 2^\circ\text{C}$ . After few seconds the formation of a white condensed film, detached from the glass support, was observed. This film, i.e. the membrane, was removed from the coagulation bath and immersed in a fresh water bath for additional 24 hours to remove residual traces of solvent, the membranes were dried at room temperature for 24 hours and finally in a vacuum oven at  $60^\circ\text{C}$  for additional 24 hours.

At the end of the photocatalytic tests, the membranes were washed with water and then dried before their reuse in successive catalytic runs.

### Membranes preparation

Asymmetric porous membrane in flat configuration have been prepared by phase inversion technique induced by a non-solvent.<sup>39</sup> Homogenous solutions have been prepared by dissolving the polymer in DMA by magnetic stirring at room temperature, then the appropriate amount of catalyst (14.3, 25.0 or 33.3 wt% respect the final membrane mass) was added and the solutions were left under stirring for additional 24 h. For comparison we also prepared in the same conditions a membrane of PVDF without the catalyst indicated in the following text as PVDF reference (Table 1).

**Table 1.** Composition of the casting solutions used to prepare polymeric and catalytic membranes. The composition of all solution is expressed by considering the weight percentage (wt%).

Membrane code	Composition of the casting solution (wt %)		Catalyst loading respect to membrane mass (wt %)
PVDF (reference)	PVDF	15.0	0
	DMA	85.0	
PVDF-W10 (14.3 wt%)	PVDF	15.0	14.3
	DMA	82.5	
	TBA <sub>4</sub> W <sub>10</sub> O <sub>32</sub>	2.5	
PVDF-W10 (25.0 wt%)	PVDF	15.0	25.0
	DMA	80.0	
	TBA <sub>4</sub> W <sub>10</sub> O <sub>32</sub>	5.0	
PVDF-W10 (33.3 wt%)	PVDF	15.0	33.3
	DMA	77.5	
	TBA <sub>4</sub> W <sub>10</sub> O <sub>32</sub>	7.5	

The solutions were cast on a glass plate by a micrometric film applicator adjusting the blade gap at 250  $\mu\text{m}$ . The cast film was immersed for 2 h in a coagulation bath containing distilled water (a non solvent for the PVDF but miscible with DMA) at  $20\pm 2^\circ\text{C}$ . After few seconds the formation of a white condensed film, detached from the glass support, was observed. This film, i.e. the membrane, was removed from the coagulation bath and immersed in a fresh water bath for additional 24 hours to remove residual traces of solvent, the membranes were dried at room temperature for 24 hours and finally in a vacuum oven at  $60^\circ\text{C}$  for additional 24 hours.

Membranes characterization

The membranes morphology was investigated by scanning electron microscopy. The PVDF-based membranes are porous and asymmetric. The PVDF reference membrane exhibits asymmetrical morphology characterized by a thin skin layer, finger-like macrovoids, interconnected cellular pores and nodular morphology particularly evident on the bottom surface and on the inner walls of the macrovoids (Fig. 5).

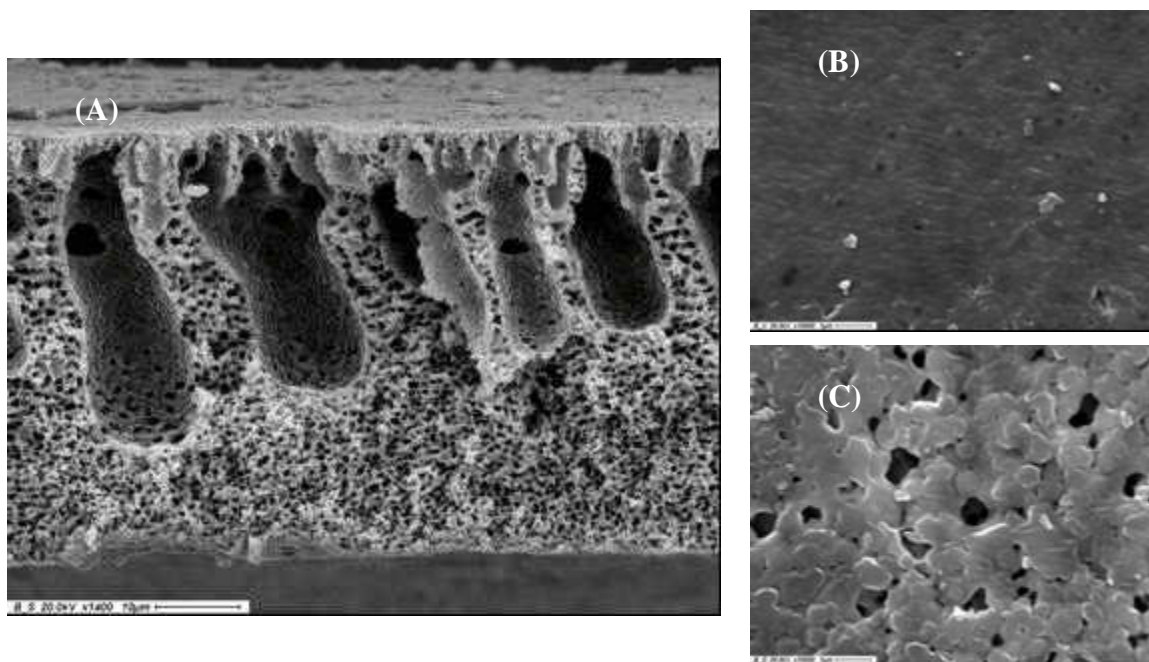


**Figure 5.** SEM image of the PVDF reference membrane: cross section (A), up surface (B) and down surface (C).

When the catalyst is present in the casting solution the macrovoids in the cross-section became more accentuated (Figs. 6 and 7).

In the phase inversion process induced by a non-solvent, a homogeneous polymeric solution is initially demixed in to two liquid phases because of the exchange of the solvent and non-solvent. The phase with the higher polymer concentration will form the solid membrane, the phase with lower polymer concentration will form the membrane pores. During the process, the exchange of solvent and non-solvent in the demixed phases continues to cause an increase of the polymer concentration in the concentrated phase surrounding the pores. The polymer molecules may rearrange their structure until the solidification (vitrification or crystallization) of the concentrated phase occurs.<sup>40</sup> The presence of the catalyst in the casting solution induces the enhancement of phase separation rate that takes place instantaneously after immersion of the cast solution in the harsh water bath. The catalyst works as non-solvents for the polymer, reducing the thermodynamic miscibility of the casting solution (thermodynamic effect), and inducing the enhancement of liquid-liquid demixing.

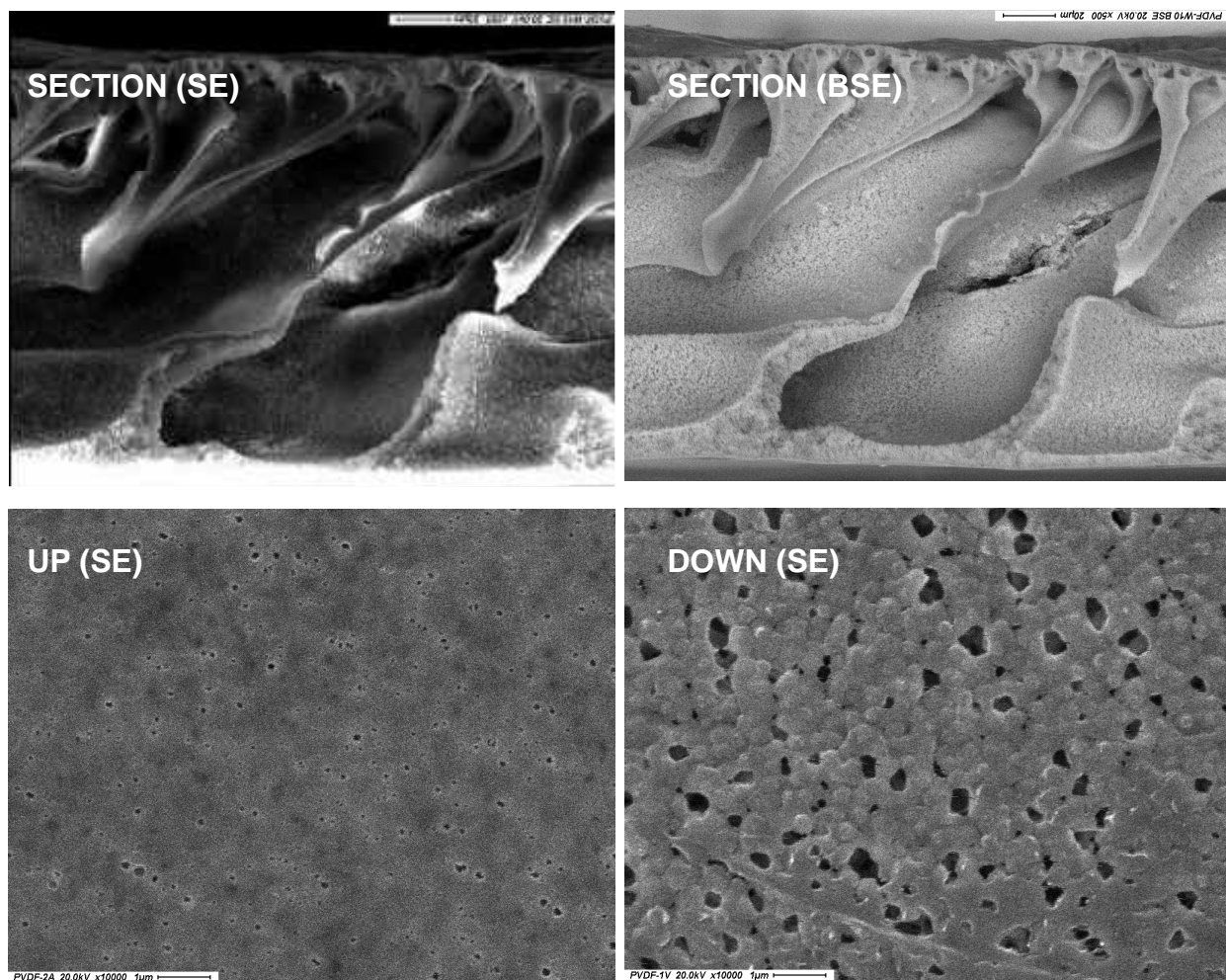


**Figure 6.** SEM images of the PVDF-W10 (25.0 wt%) membrane (in secondary electrons mode (SE) or back-scattered electron mode (BSE))

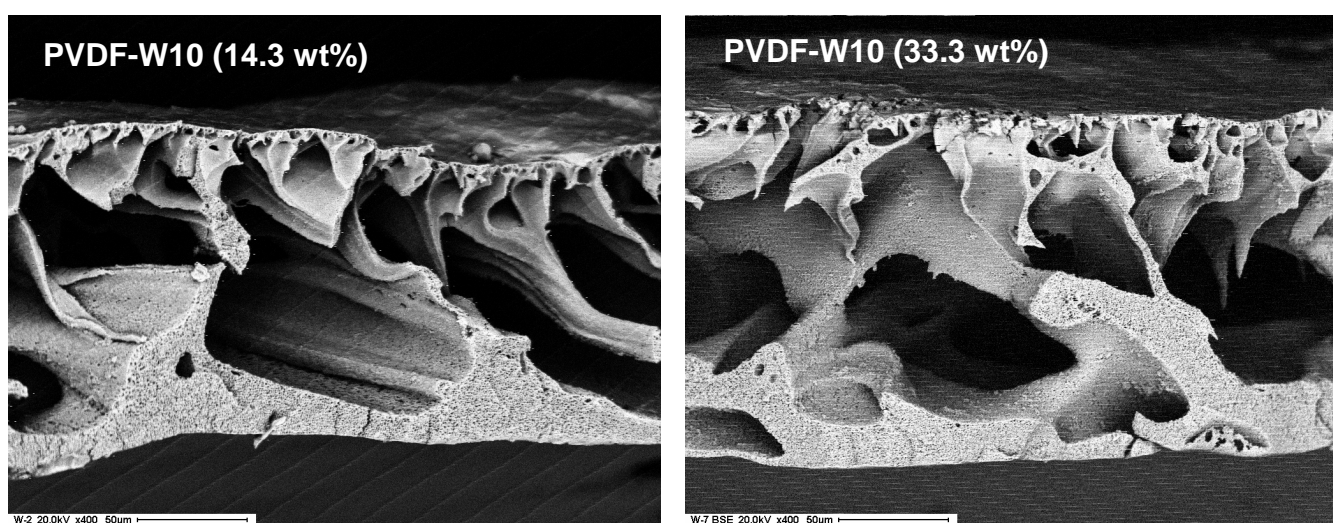


**Figure 7.** SEM images of the cross section (BSE mode) of the PVDF-W10 (14.3 wt%) and PVDF-W10 (33.3 wt%)

Micrographs in back scattered electrons mode (BSE) and linear RX maps on the cross sections, have been used to investigate the catalyst distribution within the membranes.

Linear RX maps carried out on the PVDF-W10 (25 wt%) (596 analyses carried out from the up to the down side) qualitatively show a good distribution of the W and O atoms (from the catalyst) in the polymeric matrix (Figs. 8).

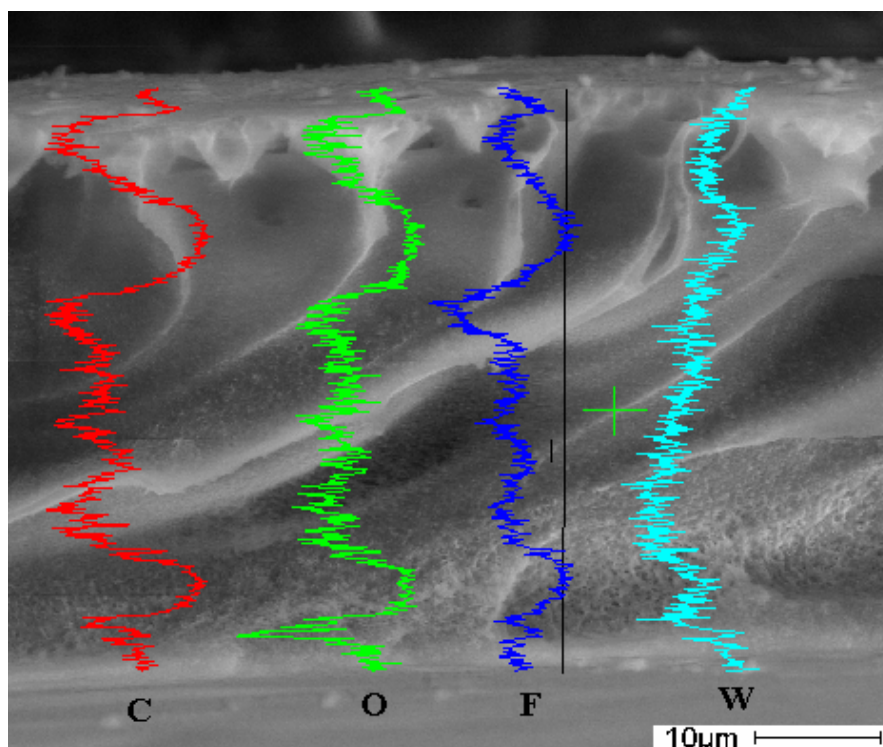
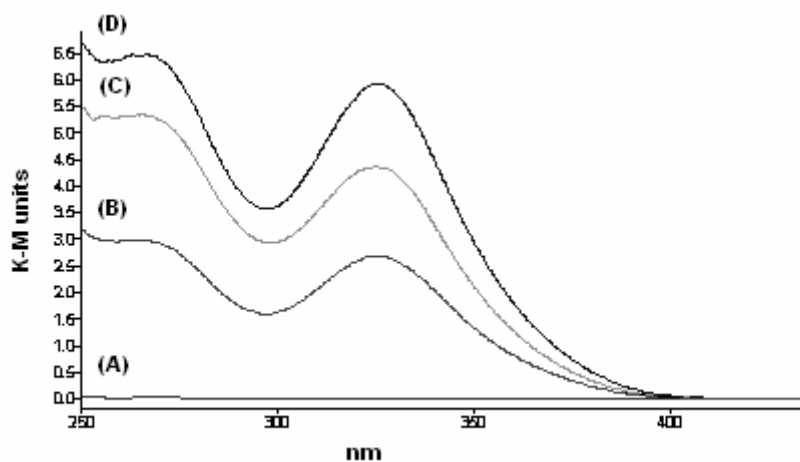


**Figure 8.** SEM image of the cross section of the PVDF-W10 (25.0 wt%) membrane with superimposed EDX analyses for W, F, O and C atoms.

Also the BSE images highlight a good distribution of the catalyst because the white points, indicating the presence of heavy elements (in this case W), are present in the whole section (Figs. 6, 7).

One of the crucial aspect during catalyst heterogenization is the maintaining of its structure. Solid state characterization technique were used to investigate the decatungstate structure in membrane. Both DR-UV and FT-IR analyses confirmed that the catalyst did not suffer any modification during the membrane preparation process. The presence of the charge transfer band at 324 nm, typical of the decatungstate, was evident in the DR-UV spectra of the catalytic membranes surface (Fig. 9). The intensity of the CT band increase with the increase of the catalyst loading. The DR-UV-Vis spectra carried out on the PVDF reference membrane confirmed that the polymer does not absorb in the region of interest of the catalyst (Fig. 9).





I

**Figure 9.** UV-Vis spectra in diffuse reflectance of the PVDF reference membrane (A) and the catalytic membranes at different catalyst loading (14.3 % (B); 25.0 % (C) and 33.3 % (D)) carried out on the up surface

Also FT-IR analyses confirmed that the catalyst structure is preserved within the polymeric membrane. The infrared spectra of the catalytic membranes show the characteristic bands of  $W_{10}O_{32}^{4-}$  units as well as those typical of the employed alkylammonium cation (Figs. 10,11 and Tab. 2).<sup>41</sup>

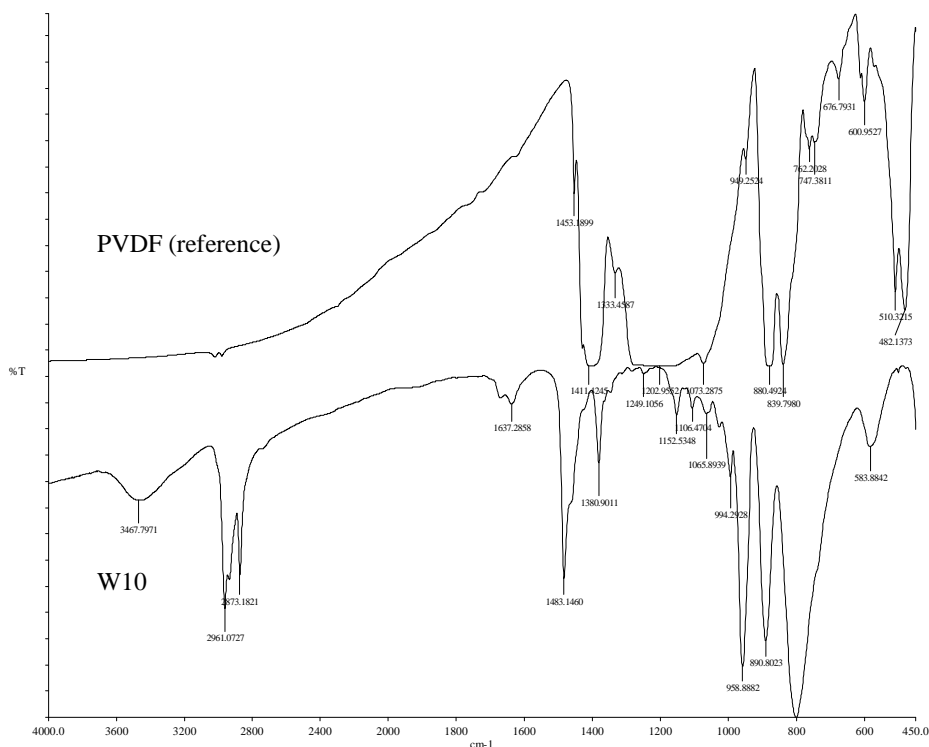
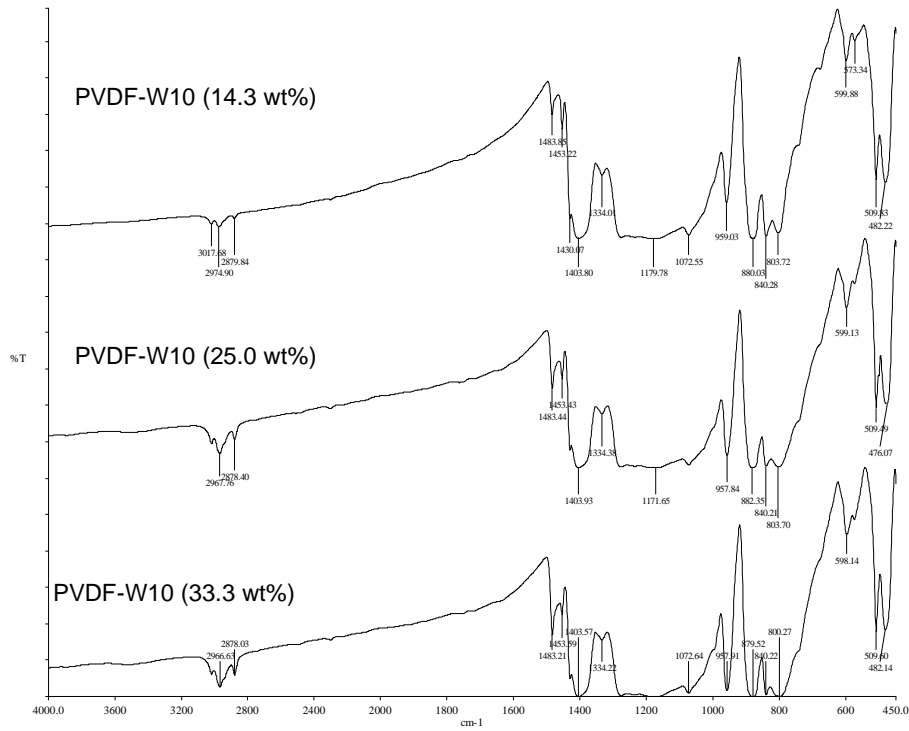


**Figure 10.** FT-IR spectra of the PVDF reference membrane and the  $(n\text{-C}_4\text{H}_9\text{N})_4\text{W}_{10}\text{O}_{32}$  in KBr.

**Table 2.** Characteristic bands of the decatungstate (TBAW<sub>10</sub>) and the PVDF polymer identified in the FT-IR spectra

<b>Characteristic bands of TBAW<sub>10</sub></b>	
<b>Wavenumber (<math>\text{cm}^{-1}</math>)</b>	<b>Group Vibration</b>
595	W-O <sub>c</sub> -W
803	W-O <sub>b</sub> -W
895	W-O <sub>b</sub> -W
958	W=O
2870	CH <sub>2</sub> (TBA group)
<b>Characteristic bands of PVDF polymer</b>	
<b>Wavenumber (<math>\text{cm}^{-1}</math>)</b>	<b>Crystalline phase</b>
510	$\beta$
763	$\alpha$
840	$\beta$
976	$\alpha$
1179	$\beta$
1233	$\gamma$
1275	$\beta$

(A)



(B)

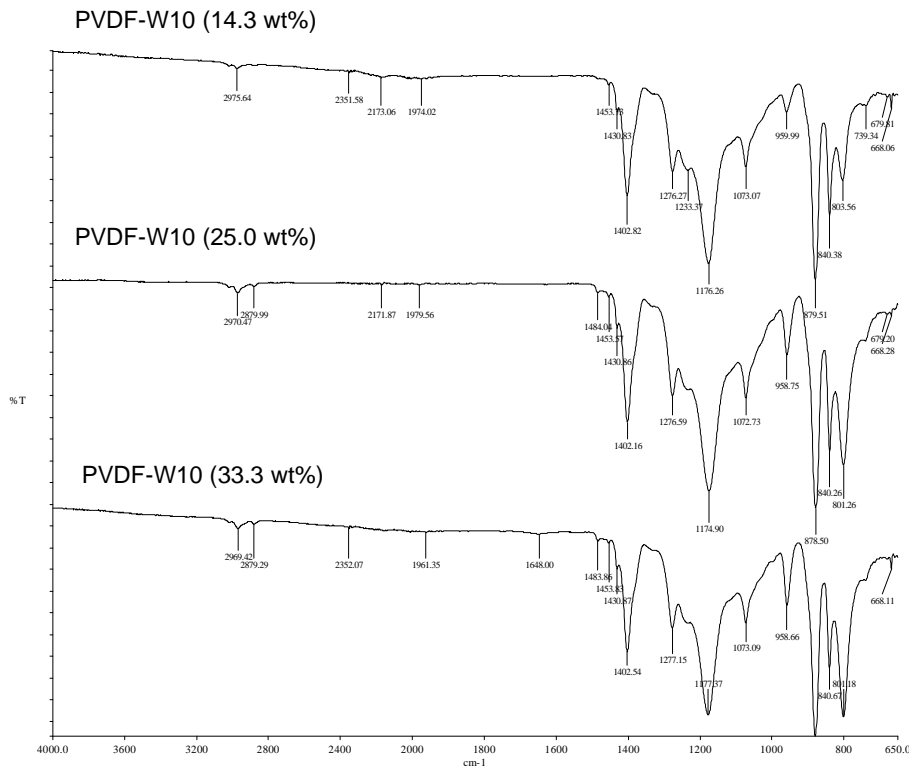


**Figure 11.** FT-IR spectra of the catalytic membranes in transmittance (A) and in ATR mode on the up surface (B) of the PVDF-W10 catalytic membranes

Increasing the amount of catalyst in the casting solution, increase the catalyst loading in the membrane as can be observed comparing the absorbance at  $958\text{ cm}^{-1}$  (catalyst W=O stretching) and the absorption band at  $840\text{ cm}^{-1}$  (polymer  $\text{CH}_2$  rocking and  $\text{CF}_2$  asymmetric stretching) characteristic of the PVDF in the  $\beta$  form (Fig. 12).

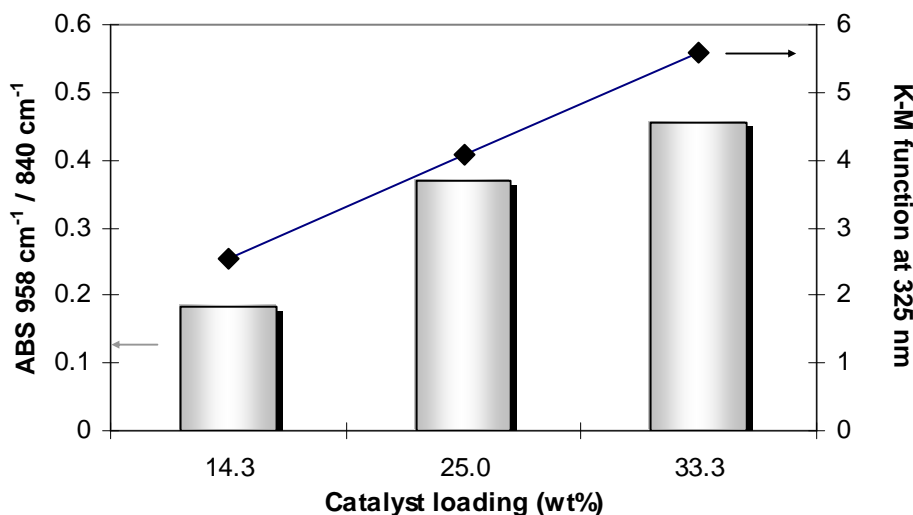


**Figure 12.** Comparison between ratio of absorption at  $958\text{ cm}^{-1}$  (catalyst W=O stretching) and  $840\text{ cm}^{-1}$  (polymer  $\text{CH}_2$  rocking and  $\text{CF}_2$  asymmetric stretching) with the values of the Kubelka-Munk (K-M) transformation of the DR-UV spectrum of the PVDF catalytic membranes at  $324\text{ nm}$ . All the data (ATR-FT-IR and DR-UV) correspond to the upper surface of the membranes.

The firm fixation of the catalyst in membrane was confirmed in a leaching test carried out by immersion of a sample of PVDF-W10 (25.0 wt%) membrane in a solution of NaCl (3 mol/L in water) at  $100^\circ\text{C}$  for 24 hours. The catalyst leaching out in water, or the exchange of the salt, can be excluded by analyses of the UV-Vis spectrum of the immersion solution and comparison of the FT-IR and DR-UV spectra of the membrane before and after the test.

FT-IR spectra were also used in order to investigate the content of the three main crystalline forms of PVDF:  $\alpha$  (or form II; unit cell containing trans-Gauche sequences; kinetically favorite),  $\beta$  (or form I; presents polymer chains with an all trans structure; thermodynamically favoured) and  $\gamma$  (or form III; sequences of three trans bonds separated by a Gauche bond).<sup>42</sup> Other crystalline forms of PVDF different than  $\alpha$ ,  $\beta$  and  $\gamma$  are also possible (Fig. 13).<sup>43</sup> Depending on the membrane preparation conditions PVDF can present one or more of the different crystalline structure.

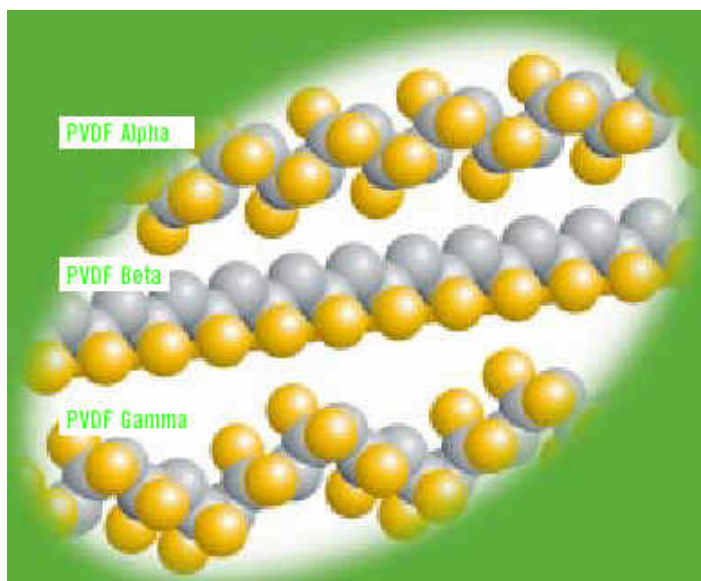


**Figure 13.** Conformation of the three main crystalline form of PVDF (F atoms are represented in orange; from [www.elf-atochem.com](http://www.elf-atochem.com))

The characteristic bands of the  $\alpha$ ,  $\beta$  and  $\gamma$  phase of the PVDF are present in the FT-IR spectra of the PVDF membrane (Tab. 2 ). By using the FT-IR in ATR mode it was possible to study the different crystalline forms present on the upper and bottom membrane surface. The bands at 1275, 1179 and 840  $\text{cm}^{-1}$ , characteristic of the  $\beta$  phase, were observed in both the upper and bottom surface of the PVDF reference membrane and all the PVDF-W10 catalytic membranes (Fig. 14)

The typical bands of the  $\alpha$  form of the polymer at 976 and 762  $\text{cm}^{-1}$ , were present only in the spectrum of upper surface of the PVDF reference (Fig. 14). A strong band at 1233  $\text{cm}^{-1}$ , indicative of the  $\gamma$  form of the polymer, can be observed in the spectrum of the bottom surface of both polymeric and catalytic membranes; only a weak signal in this region, is present in the spectrum of the upper surface.

The presence of the catalyst in the casting solution modify the crystalline composition of the membranes. In the catalytic PVDF-W10 membranes the typical signals of the  $\alpha$  phase are not present (Fig. 11). The effect is more evident comparing the ATR-FT-IR spectra of the polymeric and catalytic membranes: in the first one the  $\alpha$  and  $\beta$  form are present, in the second one only the  $\beta$  form is present.

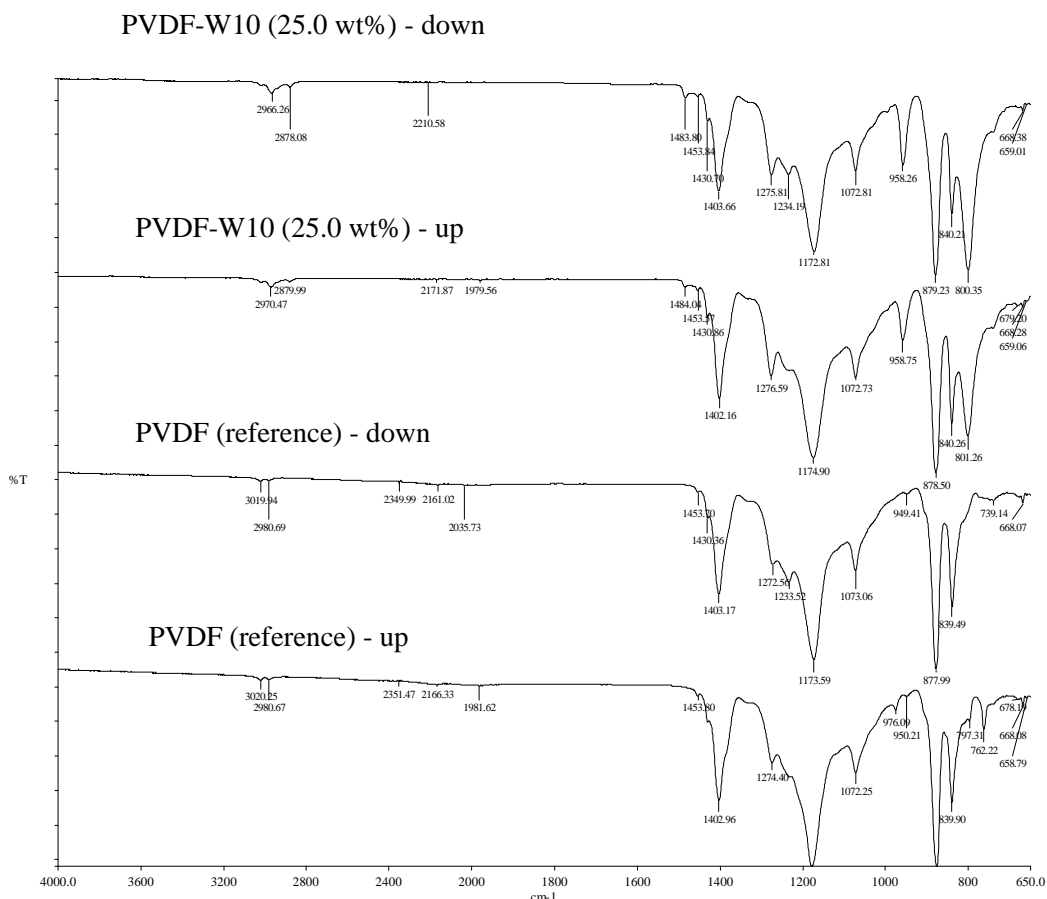


**Figure 14.** ATR-FT-IR analyses carried out on the up surface and down surface of the PVDF reference membrane and the catalytic PVDF-W10 (25.0 wt%) membrane

These results are very interesting to better understand the mechanisms that take place during the formation of the catalytic membranes (polymer catalyst interaction) and their correlation with the membrane morphology.

The formation of intermolecular interactions (hydrogen bonds and polar interactions) between the fluorine atom (with a partial negative charge) and the catalyst is supposed to occur in the PVDF-W10 system that favour a trans conformation of the CF<sub>2</sub> and CH<sub>2</sub> bonds in short segments of PVDF during crystallization (i.e.  $\beta$  or  $\gamma$  phase, Fig. 13).

The effect of the catalyst on the physicochemical and transport properties of the membranes was also investigated. For comparison the same characterization were carried out on the PVDF reference membrane and the catalytic membrane (Tab. 3).

**Table 3.** Some properties of the polymeric and catalytic membranes

MEMBRANE	Thickness ( $\mu\text{m}$ )	Pore diameter ( $\mu\text{m}$ )	Porosity (%)
PVDF (reference)	53	0.10	24
PVDF-W10 (14.3 wt%)	143	0.38	68
PVDF-W10 (25.0 wt%)	185	0.44	32
PVDF-W10 (33.3 wt%)	228	0.53	45

When the catalyst is present in the casting solution the mean pore diameter increases and the resistance to the mass transport is reduced. The water fluxes at different transmembrane pressure of the PVDF-based membranes are reported in figure 15.

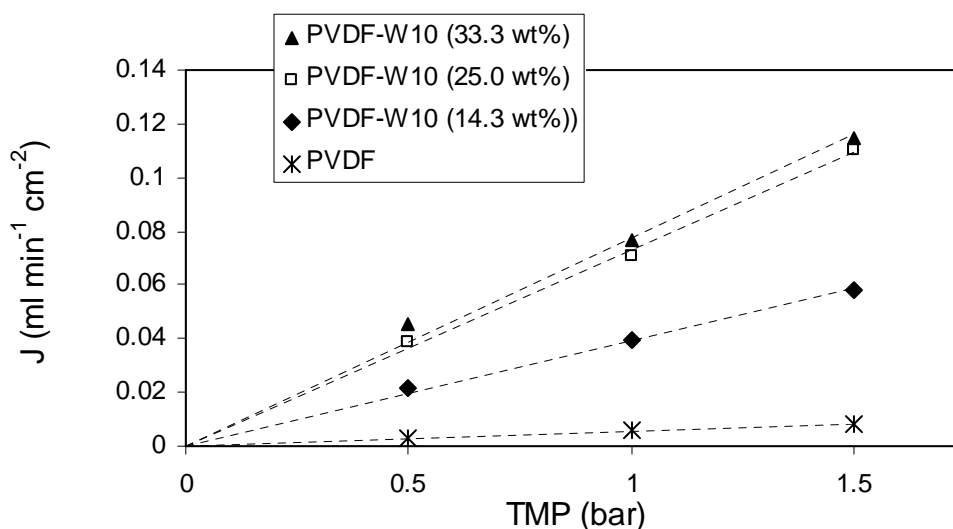


**Figure 15.** Water fluxes at  $30 \pm 1$  °C of the PVDF reference and PVDF catalytic membranes at different transmembrane pressure (TMP)

Increasing the catalyst loading in the membrane, increases the water flux. Moreover, catalytic PVDF-W10 membranes are characterized by an higher gas permeance than PVDF reference membrane, but similar selectivity (Fig. 16) in good agreement with Knudsen diffusion.<sup>44</sup>

As reported in the Chapter 1, in the presence of Knudsen flow the a gas molecule undergoes more collisions with the pore walls than with the other gas molecules ( $\lambda/r > 1$ ; where  $\lambda$  is the free path of the gas molecules and  $r$  is the pore radius) and the permeance trough the membrane is proportional to  $1/\sqrt{MM}$  (where  $MM$  is the molar mass of the gas)

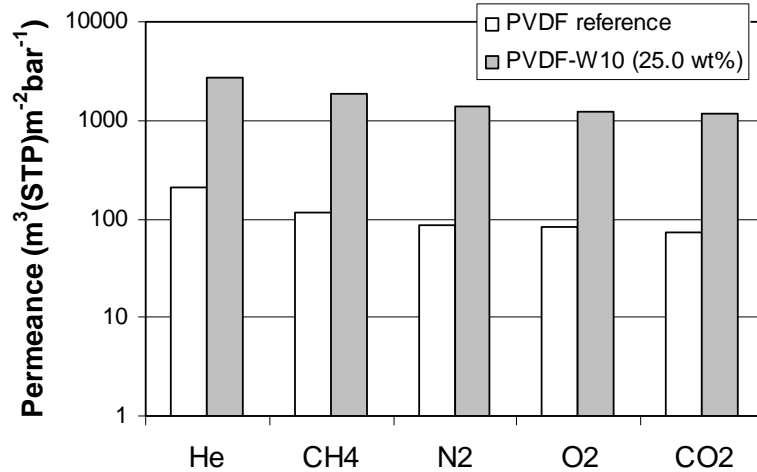
The ideal separation factor for gas pair calculated on the basis of the square root of the

molecular weight of the two gas:

$$S = \sqrt{MM_{N_2}} / \sqrt{MM_i} \quad (5)$$

is very similar to the experimental values (Fig. 16).

(A)



(B)

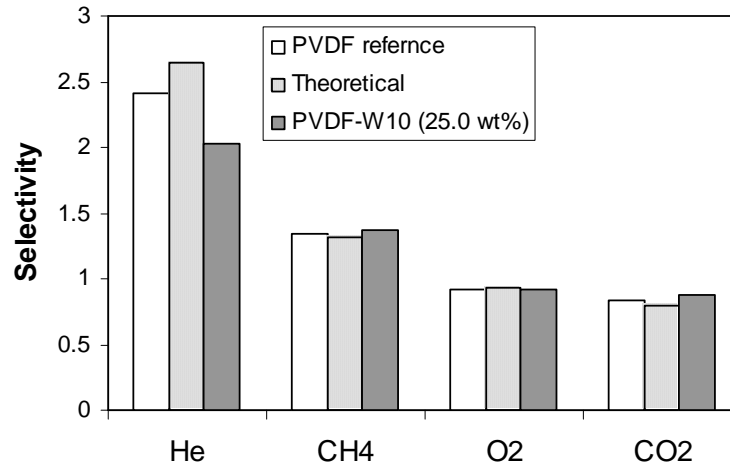


**Figure 16.** Gas permeance (A) and selectivity respect to N<sub>2</sub> (B) at 25°C ±1 of the PVDF reference and the PVDF-W10 (25.0 wt%) catalytic membrane. The Knudsen theoretical selectivity for gas pair (gas *i*-th and N<sub>2</sub>) were calculated on the basis of the square root of the molar mass of the two gas:  $\sqrt{MM_{N_2}} / \sqrt{MM_i}$ .

The membrane thickness of the catalytic membranes increase with the increasing of the catalyst loading because of the more rapid solidification process of the film (initial thickness of the film was 250 μm for all the membranes) (Tab. 3). Also the total porosity of the catalytic membranes was higher in comparison with the PVDF reference membrane, however the value



does not increase linearly with the catalyst loading because there is also a reduction of the total amount of solvent in the casting solution containing the catalyst (Tab. 1).

The thermal behaviour of the PVDF-based membranes was determined by DSC analyses.

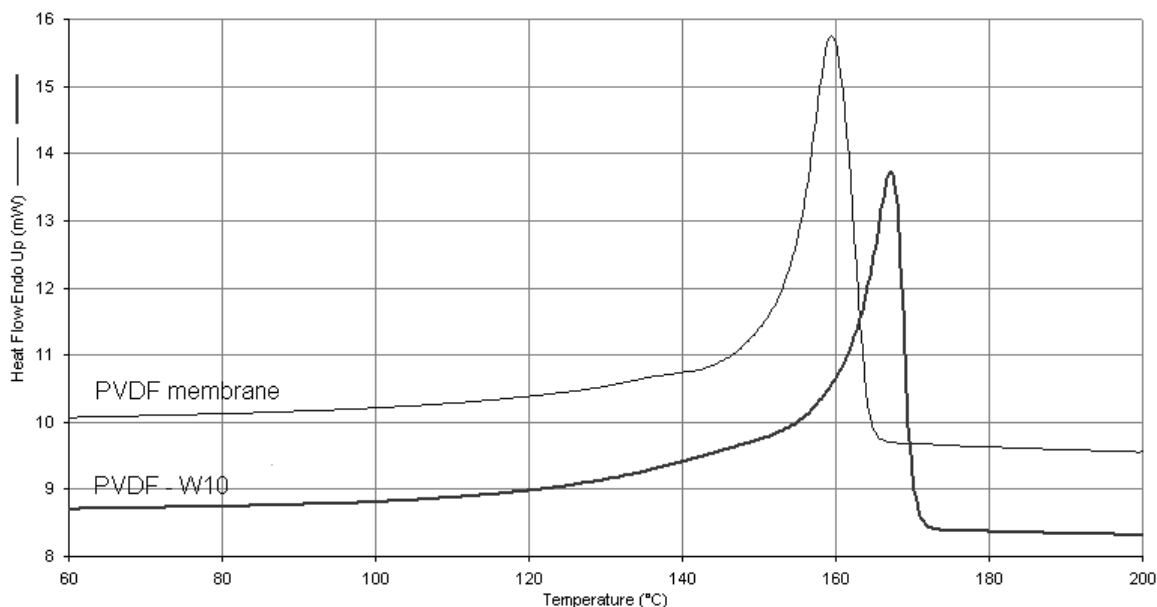


**Figure 17.** DSC thermogram of the PVDF reference membrane and the PVDF-W10 (25.0 wt%) catalytic membrane at the second heating (heating and cooling rate 15°C/min).

The presence of the catalyst in the casting solution increases the melting temperature ( $T_m$ ) and the crystallinity of the PVDF (Tab. 4 and Fig. 17). A maximum increase of the  $T_m$  was observed for the membrane containing 25.0 wt% of catalyst. These results indicate a good molecular interaction between the polymer and the catalyst that promoted the crystallization of the  $\beta$ -polymorph of the PVDF which has higher  $T_m$ .<sup>45</sup>

**Table 4.** Melting temperature ( $T_m$ , mean peak) and enthalpy ( $\Delta H_m$ ) measured at the second heating by differential scanning calorimetry (heating and cooling rate 15°C/min).

The degree of crystallinity of PVDF-based membranes was measured as the ratio between  $\Delta H_m$  (obtained dividing the  $\Delta H$  of the sample by the weight fraction of PVDF in the membrane) and  $\Delta H_0$ , where  $\Delta H_0$  is the melting enthalpy of totally crystalline PVDF (104,50 J/g)

<i>Membrane</i>	<i>T<sub>m</sub> (°C)</i>	<i>ΔH<sub>m</sub> (J/g)</i>	<i>Crystallinity (%)</i>
<b>PVDF</b>	159,41	44,62	42,70
<b>PVDF-W10 (14.3 %)</b>	165,56	48,14	46,10
<b>PVDF-W10 (25.0%)</b>	167,22	45,26	43,31
<b>PVDF-W10 (33.3%)</b>	166,07	48,26	46,18

We studied the hydrophobic properties of the PVDF membranes by water contact angle measurements (WCA). We observed an higher WCA on the down surface than on the up surface for both polymeric and catalytic membranes (Fig. 18).

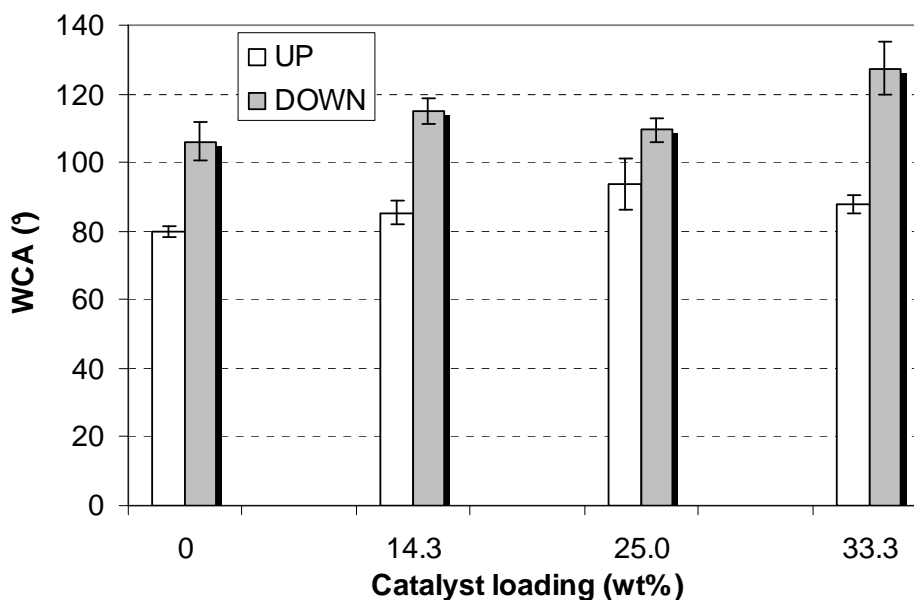


**Figure 18.** Water contact angle (WCA) on the surfaces (up and down) of the PVDF-based membranes at different catalyst loading.

This different wettability is due to differences in the surface morphology. SEM images of the upper and the bottom surface of the membranes, reveal significant differences between the two sides of the same membrane (Figs. 5 and 6). The down surface, in comparison with the up surface, is characterized by an higher roughness which increases the WCA value.<sup>46</sup> Similar behaviour was observed for the PVDF reference membrane and the catalytic PVDF-W10 membranes.

#### Catalytic tests

The photocatalytic membrane reactor used to test the performance of the catalytic membranes was equipped with a glass filter (310 nm cut-off) in order to prevent phenol auto-photolysis. The phenol has a maximum absorption at 270 nm wavelength, the decatungstate at 324 nm, as a consequence the use the filter avoids the phenol auto-photolysis without significantly influence the charge transfer band of the catalyst (Fig. 19).

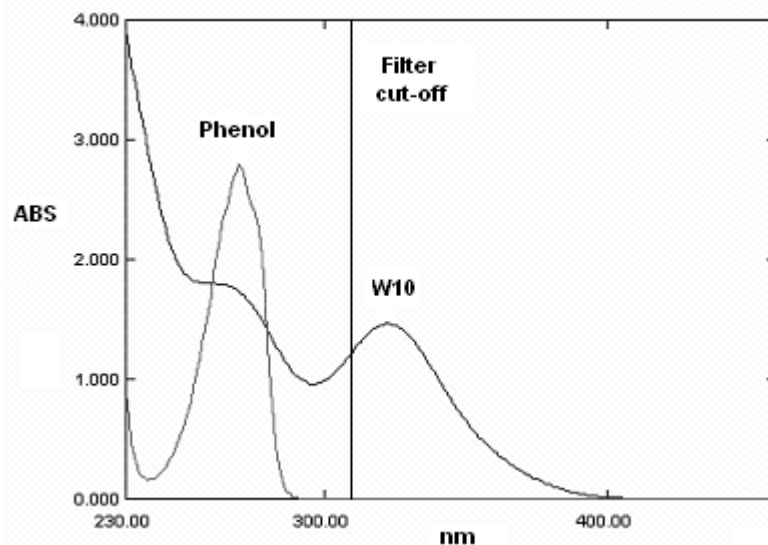


**Figure 19.** Uv-Vis spectra of a phenol solution (0.002 mol/L) and a solution of  $\text{Na}_4\text{W}_{10}\text{O}_{32}$  (0.00011 mol/L) with superimposed a line indicating the cut-off of the glass filter.

We investigated the effect of the catalyst loading in membrane and the transmembrane pressure on the phenol degradation. From the experimental tests a dependence of the phenol degradation rate from the catalyst loading in the membrane, was observed (Fig.20). Increasing the catalyst loading from 14.3 wt% to 25.0 wt%, we observed an increase of the phenol degradation. However, a further increase of the catalyst loading (33.3 wt%) reduces the reaction rate (Fig. 20).

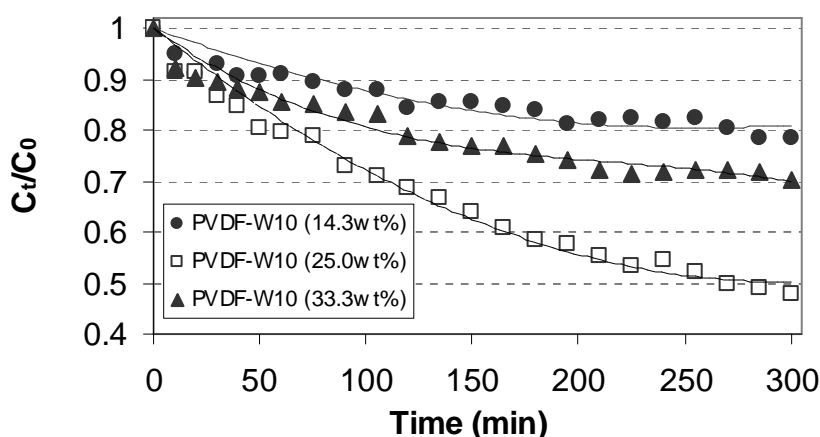


**Figure 20.** Photocatalytic degradation of phenol by PVDF-W10 membranes at different catalyst loading.  $C_t$  is the phenol concentration at the time  $t$  and  $C_0$  the initial concentration. Micromoles of catalyst in each membrane were respectively: 0.088, 1.73 and 2.83 for PVDF-10 (14.3 wt%), PVDF-10 (25.0 wt%) and PVDF-10 (33.3 wt%). Operative transmembrane pressure (TMP) was 1 bar.

The transmembrane pressure (TMP) is another critical parameter in catalytic membrane reactors because it influences the contact time substrate/catalyst calculated as:

$$\text{Contact time} = \frac{\text{Memb. Thickness}(cm)}{\text{Permeation velocity}(cm/min)} \quad (6)$$

We have carried out phenol degradation reaction with the PVDF-W10 (25.0 wt%) membrane at different TMP (Fig. 21).

The less efficient phenol degradation was observed at TMP=0 bar. In this condition there is not transmembrane flux and only the catalyst present on the membrane surface is active. Increasing the TMP we observed an higher percentage of phenol degradation and the better results were obtained at TMP=1 bar corresponding to a contact time 0.20 min (Fig.21).

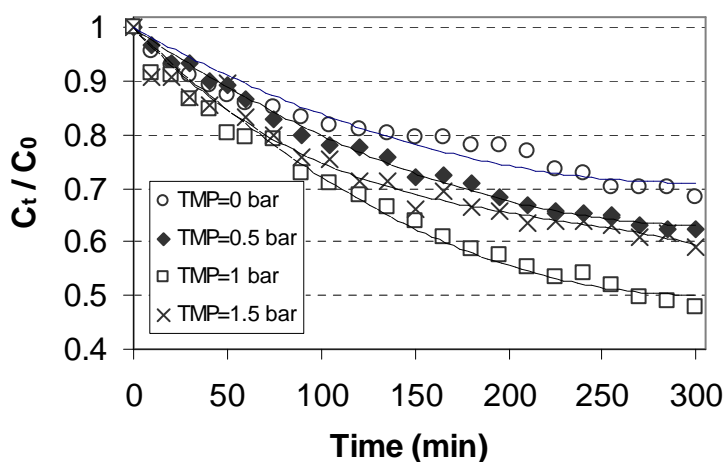


**Figure 21.** Photocatalytic degradation of phenol by PVDF-W10 (25.0 wt%) at different TMP.  $C_t$  is the phenol concentration at the time  $t$  and  $C_0$  the initial concentration.

We compared also the rates of phenol degradation catalysed by homogenous  $\text{Na}_4\text{W}_{10}\text{O}_{32}$  and heterogeneous PVDF-W10 (25.0 wt%). The amount of phenol degraded in the homogeneous and heterogeneous reaction was similar (Fig. 22 and Tab. 5). In both cases, after 6 hours of reaction about 50% of the phenol is converted. However in the case of the homogenous reaction several persistent intermediate were observed (benzoquinone, hydroquinone and catechol) in the HPLC chromatogram. The formation of different intermediate products not identified by HPLC analyses is also possible.<sup>15</sup>

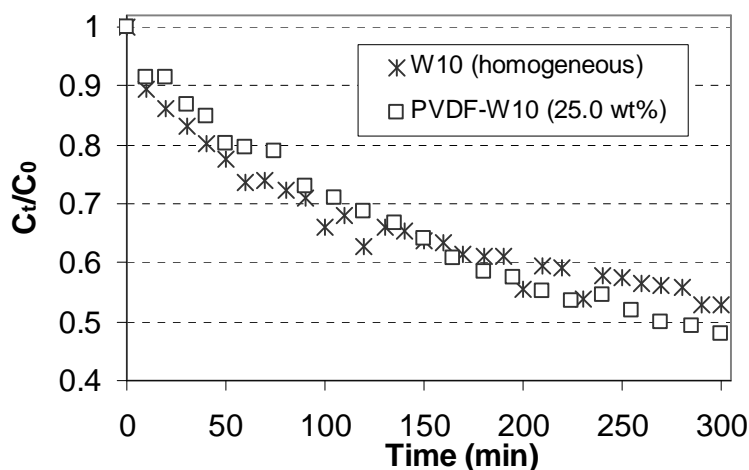


**Figure 22.** Phenol photodegradation catalysed by homogeneous  $\text{Na}_4\text{W}_{10}\text{O}_{32}$  and heterogeneous PVDF-W10 (25.0 wt%) (TMP=1 bar for the heterogeneous reaction).

On the contrary, during photodegradation performed by PVDF-W10 membrane these persistent intermediate products were not identified by HPLC analyses. Moreover with the catalytic membrane the phenol converted is almost completely mineralized to  $\text{CO}_2$  and  $\text{H}_2\text{O}$ , as confirmed by a similar (48.8 %) percentage of total organic carbon (TOC) loss (Tab. 5).

The high catalytic activity of the PVDF-W10 (25.0 wt%) membrane in comparison to the homogeneous catalyst can be ascribed to the selective absorption of the organic substrate from water on the hydrophobic PVDF polymer membrane that increases the effective phenol concentration around the catalytic sites.

Moreover, the polymeric hydrophobic environment protect the decatungstate from the conversion to an isomer which absorb only light under 280 nm.<sup>23</sup> This phenomenon, occurring in homogeneous solution at  $\text{pH} > 2.5$  (Fig. 23), was monitored also in our homogeneous catalytic test ( $\text{pH}=6$ ) by the reduction of the intensity of the CT band (324 nm) in the UV-Vis spectra of the homogeneous  $\text{Na}_4\text{W}_{10}\text{O}_{32}$ . As consequence the reduction of the homogeneous catalyst efficiency over long time ( $> 150$  min) was also observed.

Catalytic membranes can be recycled in successive catalytic runs with a loss of activity  $< 10$  % (Tab. 5).

The phenol degradation in the presence of the PVDF reference membrane used in the same experimental conditions of the catalytic membranes, was negligible.

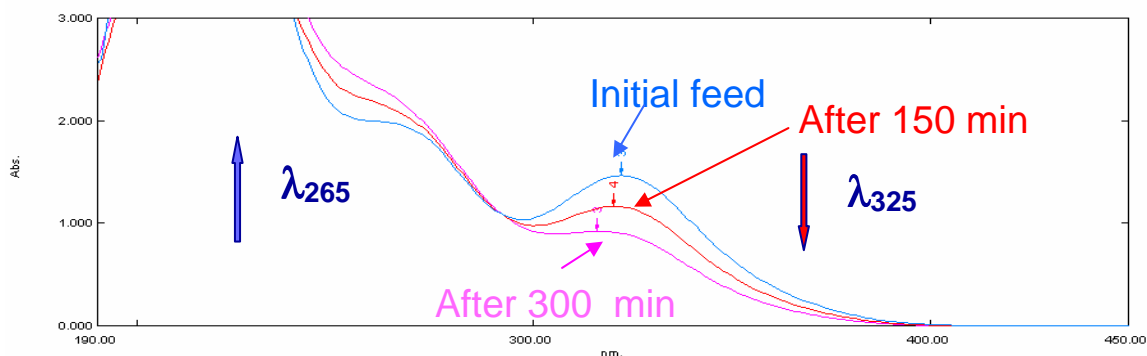


**Figure 23.** UV spectra of Na<sub>4</sub>W<sub>10</sub>O<sub>32</sub> in water (10<sup>-4</sup> mol/L; pH = 6) at different times

**Table 5.** Phenol degradation by HPLC analyses and phenol mineralization by TOC loss for the reaction catalysed by decatungstate in homogeneous phase and decatungstate heterogenized in membrane (PVDF-W10 (25.0 wt%); TMP=1 bar)

PHENOL DEGRADATION (%)			
TIME (min)	W10 (homogeneous)	PVDF-W10 (25.0 wt%) 1 <sup>st</sup> run	PVDF-W10 (25.0 wt%) 2 <sup>nd</sup> run
150	36.2	36.0	35.1
300	49.5	52.0	48.0
PHENOL MINERALIZATION (%)			
TIME (min)	W10 (homogeneous)	PVDF-W10 (25.0 wt%) 1 <sup>st</sup> run	PVDF-W10 (25.0 wt%) 2 <sup>nd</sup> run
150	24.7	35.9	34.7
300	34.0	48.8	46.1

### Conclusions-1/3

New heterogenous photocatalytic systems, operating in water with O<sub>2</sub>, have been prepared by entrapping a lipophilic salt of decatungstate (TBAW10) in polymeric membranes made of polyvinylidene fluoride (PVDF), by a non solvent induced phase inversion technique.

Solid state characterization techniques (FT-IR and DR-UV-Vis) confirmed that the catalyst structure is preserved in the polymeric membranes.

A variety of techniques including scanning electron microscopy (SEM), differential scanning calorimetry (DSC), water contact angle (WCA) measurements, liquid and gas permeation

tests, have been used to characterize the membranes. Chemical-physical and transport properties of the PVDF-based membranes were found to depend on the compositions of the casting solution. The presence of the catalyst in the casting solution induces the enhancement of the phase inversion process. As a consequence, increasing the catalyst loading, the membrane mean pore diameters increase and the resistance to the mass transport is reduced. The presence of the catalyst in the casting solution increases also the melting temperature ( $T_m$ ) and the crystallinity of the PVDF by promoting the crystallization of the  $\beta$ -polymorph of the PVDF, as confirmed also by FT-IR analyses and DSC analyses.

The effect of catalyst loading (CL) in membrane and TMP on phenol photodegradation rate were investigated and the maximum efficiency was reached with CL= 25.0 wt% and TMP=1 bar (contact time substrate/catalyst 0.20 min)

The rate of phenol degradation catalysed by decatungstate in homogeneous (NaW10 in water) and heterogeneous phase (TBAW10 in membrane) was similar; however when the catalyst is immobilised in the polymeric membranes an higher mineralization degree of the phenol was observed. Moreover, over longer times the catalyst embedding in the PVDF membrane results in an higher catalyst stability in comparison with homogeneous phase at pH near the neutrality.

The PVDF-W10 photocatalytic membranes are completely stable under UV irradiation (no catalyst leaching or membrane damage) and can be recycled in successive runs

### **3.1.2 Preparation and characterization of Hyflon membranes containing decatungstate**

#### **Catalyst design for tuning the affinity towards a perfluorinated polymeric environment**

Considering the positive results obtained with the heterogenization of the decatungstate in membrane made of the partially fluorinated polymer PVDF, in order to better understand and exploit the role of the polymeric matrix on catalyst activity, we have also carried out the heterogenization of the decatungstate in perfluorinated membranes.<sup>30</sup>

Perfluoropolymers offer several advantages when compared to other polymeric materials.<sup>48</sup> Besides their outstanding thermal and oxidative resistance, the peculiar nature of the C-F bond confers to these materials some unique physical-chemical properties<sup>47</sup>, in particular, dioxygen preferential solubility in fluorinated membranes.

We used an amorphous copolymer of the tetrafluoroethylene (TFE) and the 2,2,4-trifluoro, 5-trifluoromethoxy-1,3 dioxane (TTD) known as Hyflon AD (Fig. 24).

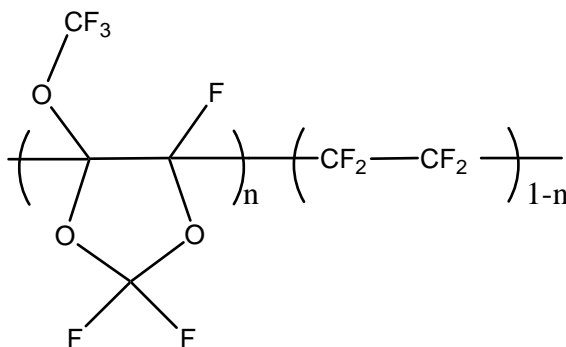


**Figure 24.** Chemical structure of the Hyflon AD ( $n = 0.85$  for Hyflon AD 80X and  $n = 0.6$  for the Hyflon AD 60X)

Hyflon is an hydrophobic perfluoropolymer, highly transparent to light from deep UV to near infrared, characterized by an high thermal decomposition temperature ( $>400^\circ\text{C}$ ) and an high glass transition temperature ( $T_g = 110^\circ\text{C}$  for the Hyflon AD60X and  $T_g = 135^\circ\text{C}$  for the l'Hyflon AD80X).<sup>48</sup>

Initially, we tried to heterogenize the fluoros-free TBAW10 in the hyflon membranes. However the low affinity between the catalyst and the polymeric matrix induced the formation of irregular catalyst aggregates not well dispersed in the polymeric matrix.

A proper choice of both the polymeric material and of the catalyst is fundamental to obtain functionalized material with good properties.

In order to have a good dispersion of the catalyst in the Hyflon membranes, a fluoros-tagged decatungstate,  $([\text{CF}_3(\text{CF}_2)_7(\text{CH}_2)_3]_3\text{CH}_3\text{N})_4\text{W}_{10}\text{O}_{32}$ . indicated as  $(\text{R}_f\text{N})_4\text{W}_{10}$  has been used (Fig. 25).<sup>30</sup>



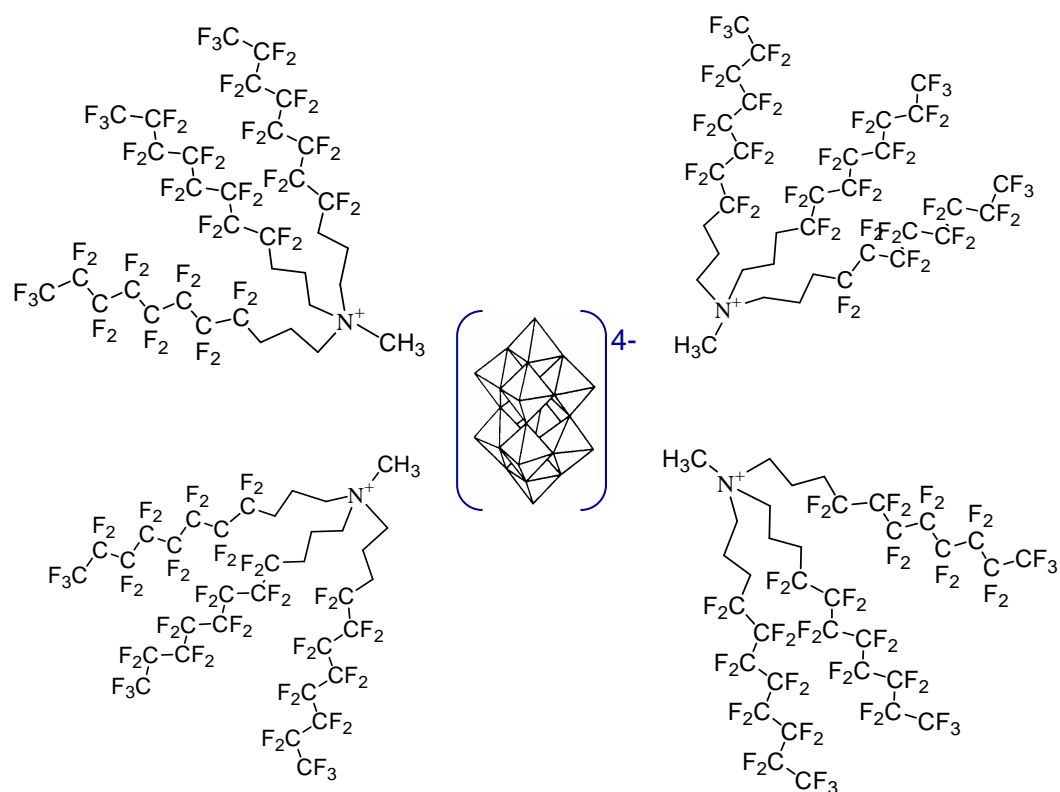


**Figure 25.** Structure of the  $(R_fN)_4W_{10}$  catalyst heterogenized in Hyflon membranes

### Experimental

The  $(R_fN)_4W_{10}$  has been synthesized by metathesis reaction between the sodium salt  $Na_4W_{10}O_{32}$ <sup>36</sup> and  $[CF_3(CF_2)_7CH_2CH_2CH_2]_3CH_3N^+ CH_3OSO_3^-$  and supplied by Prof. Scorrano's Group.<sup>30</sup>

Hyflon AD60x and Galden HT 55 were kindly supplied by Solvay Solexis.

Commercially available reagents and solvents were used as received without further purification.

Characterization of the membranes by FT-IR (also in ATR), UV-vis and SEM spectroscopies, WCA measurements, have been carried out as described in the previously section.

The gas solubility in the dense membranes, has been measured by the time lag method.<sup>49</sup> The time lag,  $\Theta$  was determined from the first pressure increase curve.<sup>37</sup>

. For a membrane with known thickness,  $l$ , the gas diffusion coefficient,  $D$ , could then be determined by the following equation:

$$\Theta = \frac{l^2}{6D} \quad (6)$$

Assuming simple Fickian diffusion and assuming transport according to the solution-diffusion model, the gas solubility of dense membrane,  $S$ , can be derived from the experimental diffusion coefficient and the steady-state permeability,  $P$ :

$$S = \frac{P}{D} \quad (7)$$

#### Membranes preparation

Flat sheet membranes were prepared by mixing a solution of Hyflon in Galden (2.4 wt%, *sol. 1*) with a solution of  $(R_fN)_4W_{10}O_{32}$  solution in hexafluoroisopropanol (6.8 wt%, *sol. 2*) in an appropriate ratio in order to have the desired loading of catalyst in membrane.

Galden is a good solvent for the Hyflon, but not for the  $(R_fN)_4W_{10}$ ; on the contrary hexafluoroisopropanol is a good solvent for the catalyst but not for the polymer. However we have found that when the ration between *sol. 1* : *sol. 2* is in the range 14.2 -7.9 (g:g) an homogeneous solution can be obtained.

Hy- $R_fN_4W_{10}$  membranes with catalyst loading up to 26% and different thickness 7-94  $\mu\text{m}$  have been prepared by phase inversion induced by solvent evaporation in an environment with temperature and relative humidity controlled.

The solutions were cast on a inert glass support removed after membrane formation (Hy- $R_fN_4W_{10}$ ), or on a Teflon/PP porous support (thickness 117  $\mu\text{m}$ , mean pore radius 0.22  $\mu\text{m}$ , supplied by GE Osmoics) in a climatic box with temperature and humidity controlled (-Hy-Tef.- $R_fN_4W_{10}$ ).

We prepared also a membrane by dispersing the TBAW10 in a solution of Hyflon in Galden and successive phase inversion induced by solvent evaporation (Hy-TBAW10).

#### Membranes characterization

Fundamental observations were obtained by SEM images analyses of the catalytic membranes. In the case of the Hy-TBAW10 membranes the formation of aggregates of catalyst, which tend to precipitate in the down side of the membrane are evident (Fig. 26).

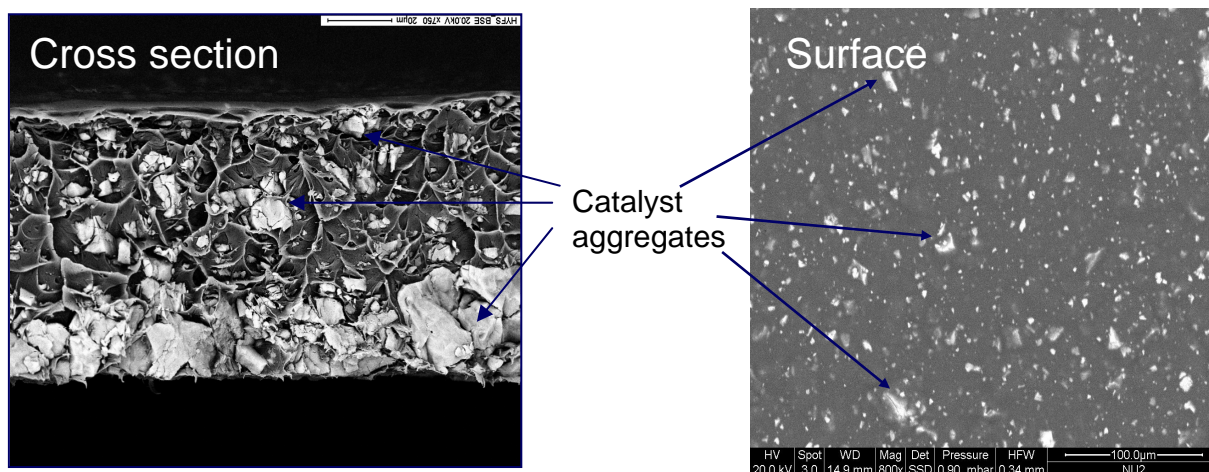


**Figure 26.** SEM images in BSE modality of the Hyflon membrane embedding the TBAW10 catalyst (20 wt% catalyst loading)

On the contrary, in the case of the fluorus-tagged decatungstate, SEM images of the membrane surface and cross-section highlight a highly dispersed, homogeneous distribution of the catalyst domains which appear as spherical particles with uniform size (Fig. 27).

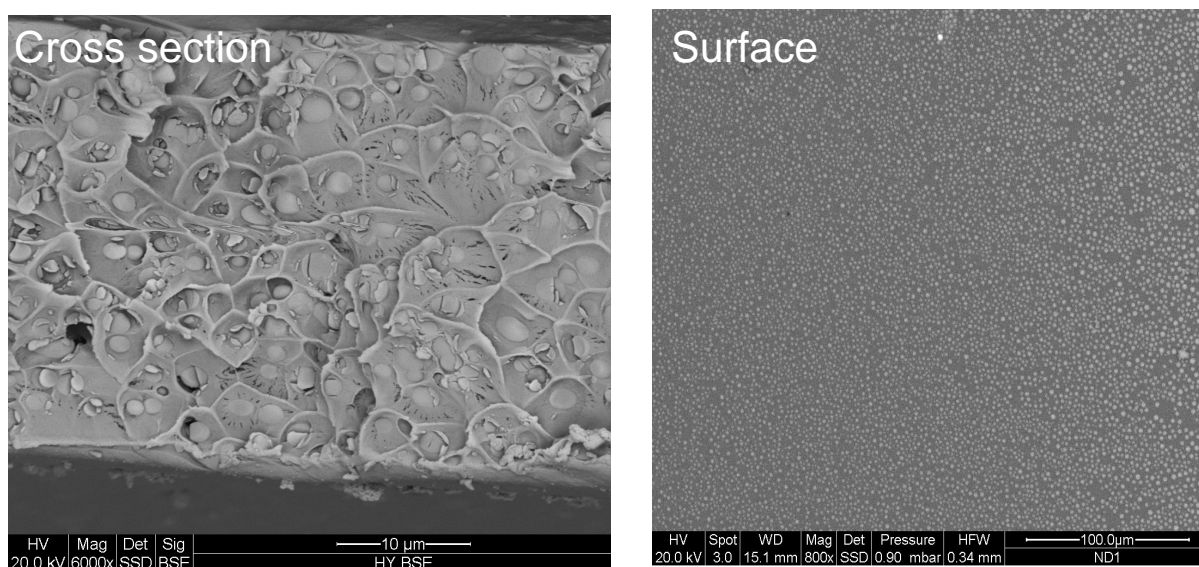


**Figure 27.** SEM images in BSE modality of the Hyflon membrane embedding the  $R_fN_4W_{10}$  catalyst (16.7 wt% catalyst loading)

The dimensions of these clusters can be modulated acting on the membrane preparation conditions. In particular, increasing the membrane formation time for example by an increase of the membrane thickness (increase of the cast solution initial thickness) the mean dimensions of the  $R_fN_4W_{10}$  clusters became larger because they have more time for aggregate before the solidification of the membrane (Fig. 28). Also the increase of the catalyst loading contribute to increase the mean dimension of the cluster.

Using various combination of catalyst concentration, membrane thickness and environmental conditions (temperature and humidity), catalytic membranes with cluster dimensions in the range from 0.1 to 4  $\mu\text{m}$  have been prepared.

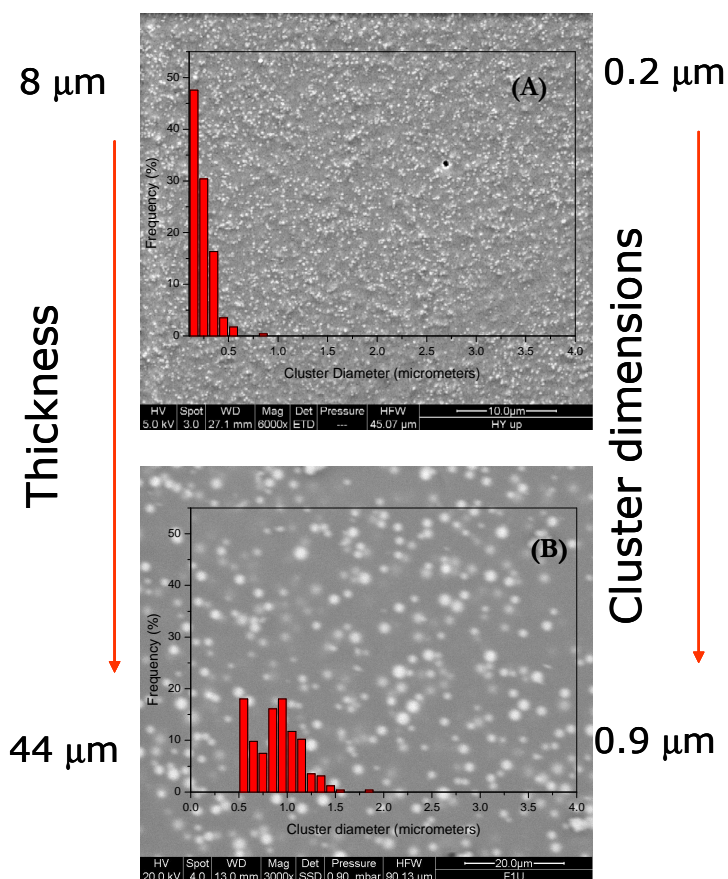


**Figure 28.** SEM images of the surfaces of the Hyflon- $\text{R}_f\text{N}_4\text{W}10$  membranes at same loading (16.7 wt%) but different membrane thickness ((A) 6000x; (B) 3000x) with superimposed the distribution of clusters diameter

The cationic amphiphiles  $\text{R}_f\text{N}^+$  groups induce the self-assembly of the surfactant-encapsulated clusters ( $\text{R}_f\text{N}^+$  groups capped on  $\text{W}_{10}\text{O}_{32}^{4-}$ ) which, during membrane formation process, give supramolecular assemblies of the catalyst, stabilized by the polymeric matrix

This self-assembly processes has been recently described also for the amphiphilic POM ( $\text{DODA}$ ) $_4\text{SiW}_{12}\text{O}_{40}$  ( $\text{DODA}$ = dimethyldioctadecylammonium) dispersed in organic solvents (Fig. 29).<sup>50, 51</sup>

At the best of our knowledge, we described for the first time this phenomenon in a membrane.

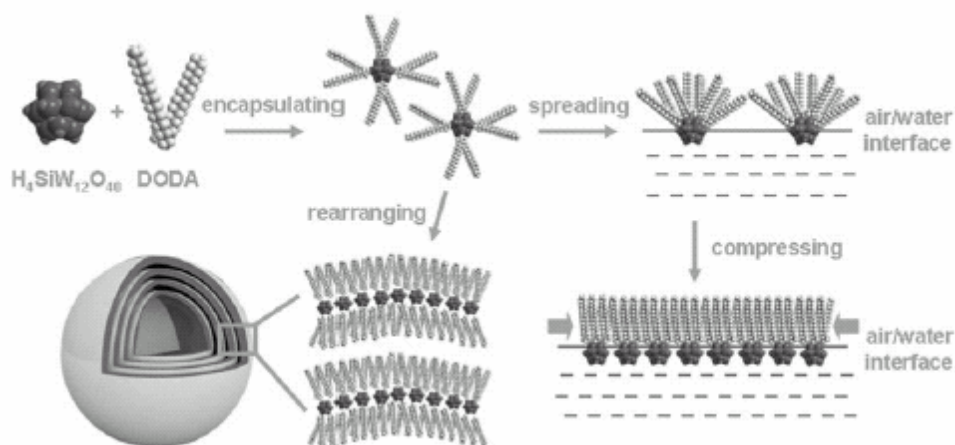


**Figure 29.** Self-assembly mechanism of the amphiphiles  $(\text{DODA})_4\text{SiW}_{12}\text{O}_{40}$  (DODA= dimethyldioctadecylammonium), in surfactant encapsulated complexes under different conditions (from ref. 50)

Moreover the coexistence of hydrophobic F-containing chains and hydrophilic ionic clusters in the Hyflon/ $(\text{R}_f\text{N})_4\text{W}_{10}\text{O}_{32}$  casting solution exposed to humidity, results in the formation of ordered porous membrane by the templating effect of the water molecules.

Water molecules can be absorbed on the liquid films surface, in correspondence of the catalyst hydrophilic domains, when the membrane is forming under elevated relative humidity. The successive removal of the water molecules, initially coordinated around the surfactant-encapsulated clusters, induces the formation of the membrane pores.

For example porous self supporting membrane with mean pore diameter of 0.2  $\mu\text{m}$  have been prepared by casting a solution of Hyflon- $\text{R}_f\text{N}_4\text{W}_{10}$ (25.0 wt%) at 25°C and 80%RH.

Also the gas permeation measurements confirm the porous structure of this membrane (Tab. 6).

**Table 6.** Permeance of pure gases of the Hyflon- $\text{R}_f\text{N}_4\text{W}_{10}$ -Hyflon (25.0 wt%) porous membrane at 1 bar and 25°C

Gas $i$	Molar weight	Permeance	Select. ( $P_i/P_{\text{N}_2}$ )
	( $\text{g mol}^{-1}$ )		
$\text{H}_2$	2	11088	2.29
He	4	7194	1.49
$\text{CH}_4$	16	6973	1.44
$\text{N}_2$	28	4832	1
$\text{O}_2$	32	4397	0.91
$\text{CO}_2$	44	4657	0.96

This result is very interesting considering the difficulty to find appropriate liquid in which the Galden is mixable but the Hyflon is not soluble, in order to prepare porous membranes by phase inversions technique induced by immersion-precipitation method.

The mechanical stability of thin Hyflon-based membranes, can be also improved by supporting the catalytic membrane on porous PTFE film (Fig. 30 ).

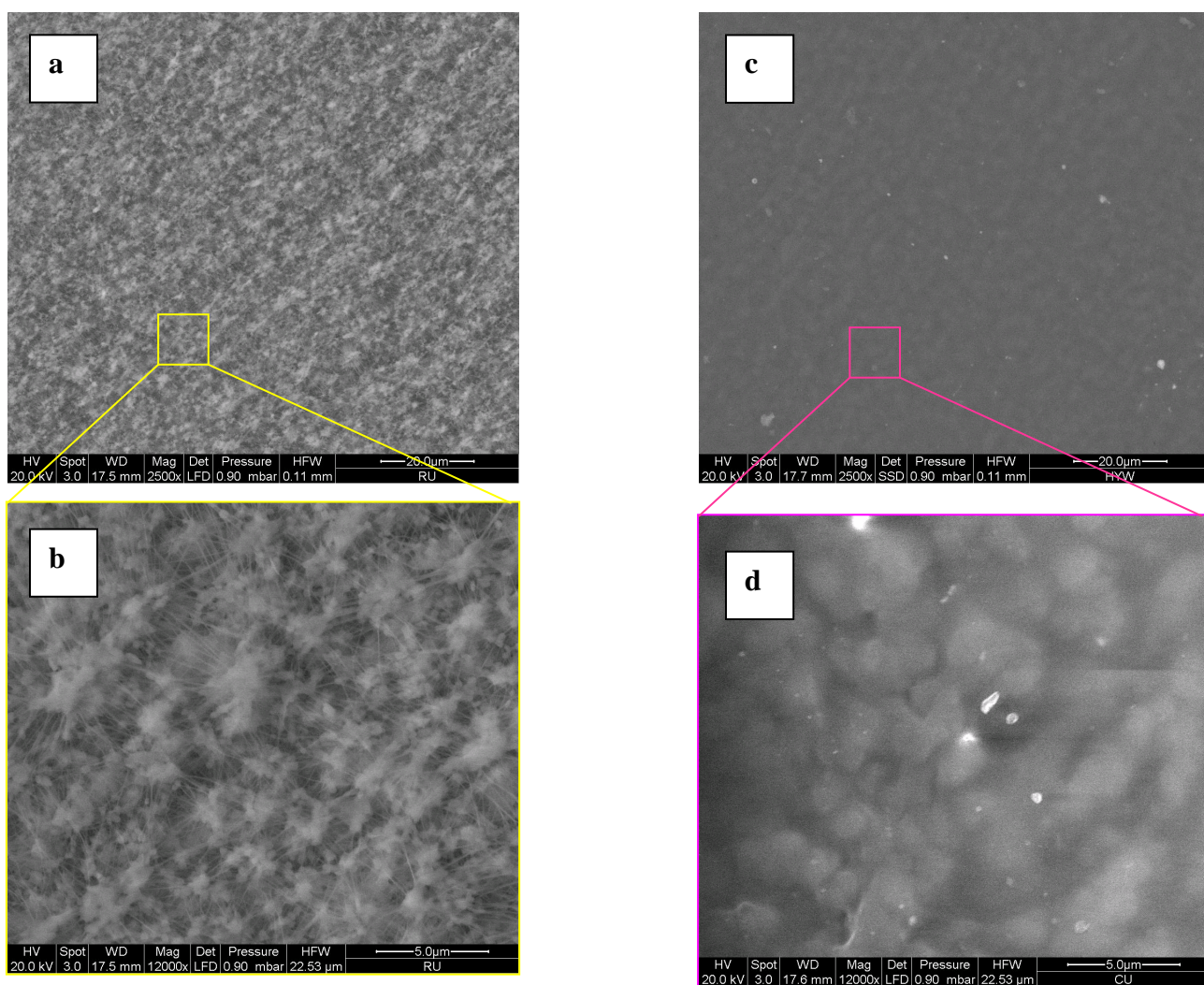


**Figure 30.** SEM image of the surface of the Teflon support (a-b) and a catalytic Hy-Tef-(R<sub>f</sub>N)<sub>4</sub>W10-membrane (c-d)

DR-UV and FT-IR analyses carried out on the membrane surfaces of both porous and dense catalytic membranes, self-supported or supported on Teflon, confirmed that the catalyst did not suffered any modification during the membrane preparation process.

The presence of the charge transfer band at 324 nm typical of the decatungstate was evident in the DR-UV spectra of the catalytic membranes (Figs. 31).

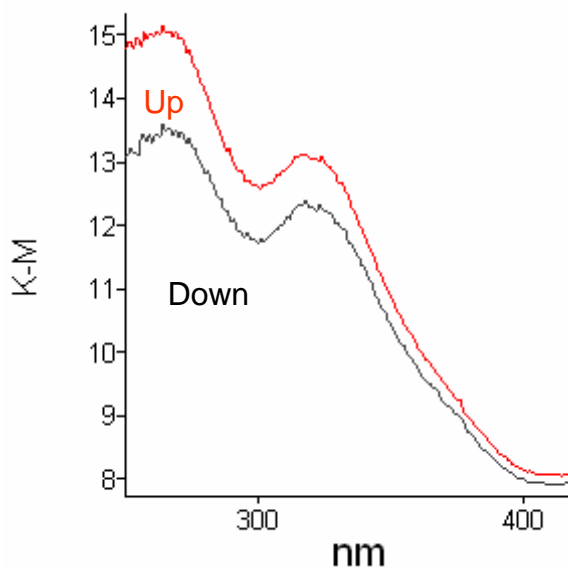


**Figure 31.** UV spectra in diffuse reflectance of the up surface and the down surface of the Hy-(R<sub>f</sub>N)<sub>4</sub>W10 membrane (catalyst loading 25 wt%; thickness 12 μm)

In the Hyflon catalytic membranes, the catalyst is present in the entire membrane. However for the self-supported membranes we observed a little bit higher catalyst concentration near the upper surface, in contact with the air during evaporation of the solvent, in comparison with the bottom surface, in contact with the glass support during membrane formation process (Fig. 31). The origin of this difference might be due to the higher density of the polymer solution (Hyflon:  $d=1.93$ , Galden;  $d=1.66-1.73$  g/ml), in comparison with the catalyst and its solvent (hexafluoro-2-propanol;  $d= 1.596$ ). Although the polymer/galden/hexafluoro-2-propanol/catalyst mixture is initially homogeneous, if partial demixing of the two solvents would occur during the membrane formation process, this would most likely lead to a higher Galden concentration and a higher polymer concentration on the bottom side.

Another possible explanation is that co-diffusion of dissolved catalyst, together with the evaporating solvent, that leads to a net transport of the dissolved catalyst towards the surface, where the solvent evaporates and the catalyst remains at a relatively higher concentration also thank to the stabilizing effect of the water molecules from the atmosphere.

The typical signals of the decatungstate at  $800\text{ cm}^{-1}$  (W-O<sub>b</sub>-W stretching) and at  $960\text{ cm}^{-1}$  (W=O stretching) are present in the FT-IR-ATR spectra(Fig. 32).

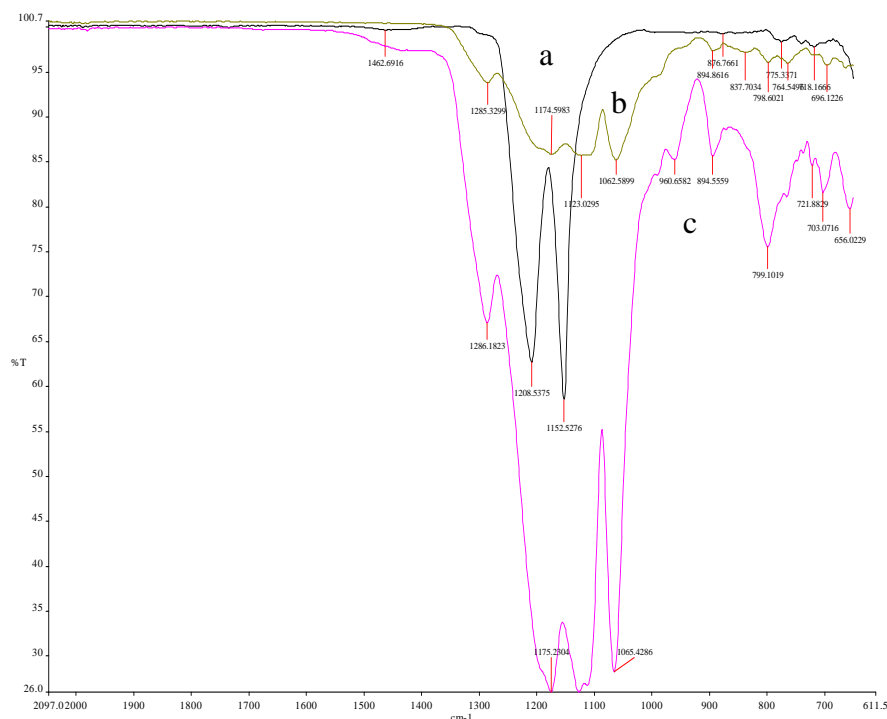


**Figure 32.** FT-IR-ATR spectra of the Teflon support (a), a pure Hyflon (b) and the supported catalytic Hy-Tef-(R<sub>f</sub>N)<sub>4</sub>W10 (c)

The catalytic Hyflon-based membranes have been tested in batch solvent-free oxygenation of benzylic C-H bonds of the ethylbenzene (Fig. 33) at 25 °C under O<sub>2</sub> (membrane cut in small piece and placed on the internal wall of a quartz cuvette opposite to the light<sup>30</sup>).

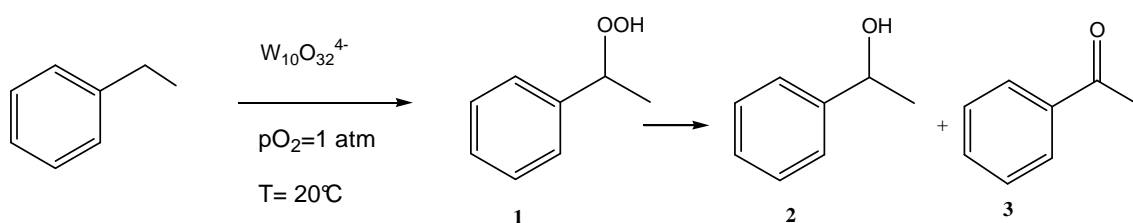


**Figure 33.** Photooxygenation of ethylbenzene. The products are : hydroperoxide (1), alcohol (2) and acetophenone (3)

It is important to stress that this type of experiments have been useful for a fast screening of the heterogeneous catalytic membranes, but they are not complete, because in these conditions the membrane acts only as support for the catalysts and their selective transport properties are not fully exploited.

Although in the batch experiments, carried out principally with dense membrane operating without flux through, only a part of the catalyst can be reached by the substrates, very interesting results have been obtained.



The key observation was provided by an increase of the selectivity towards the alcohol (product of interest) and turnover number when the catalyst is heterogenised in Hyflon membrane (entries 4-7) in comparison with homogeneous catalysts (entries 1-2) or the catalyst heterogenized in PVDF (entry 3) (Tab. 7). Moreover, the use of the fluorus-tagged decatungstate (entries 5-7) well dispersed in Hyflon membrane improve the TON in comparison with the TBAW10 only physically entrapped in Hyflon (entry 4)

**Table 7.** Photocatalytic oxygenation of ethylbenzene by homogeneous decatungstate or heterogeneous catalytic membranes made of PVDF or Hyflon (HF) (data from ref. 30)

	Catalyst	Solvent	Cat. mmol	Products, mM (% 1:2:3)	TON
1	<sup>a</sup> TBAW10	CH <sub>3</sub> CN	0.20	64 (36: 32:32)	351
2	<sup>a</sup> R <sub>f</sub> N <sub>4</sub> W10	HFP	0.18	95 (56: 23:21)	581
3	PVDF-TBAW10	neat	0.32	23 (45: 23:32)	78
4	Hy- TBAW10 (dense membrane, thickness 50 μm)	neat	0.20	81 (14: 66:20)	443
5	Hy-R <sub>f</sub> N <sub>4</sub> W10 (dense membrane, thickness 7 μm)	neat	0.03	94 (16: 46:38)	3447
6	Hy-R <sub>f</sub> N <sub>4</sub> W10 (dense membrane, thickness 50 μm)	neat	0.18	196 (25: 41:34)	1198
7	Hy-R <sub>f</sub> N <sub>4</sub> W10 (dense membrane, thickness 94 μm)	neat	0.70	270 (15:48:37)	424

1: peroxide, 2: alcohol, 3: keton. Reaction conditions: ethylbenzene, 1.1 ml; pO<sub>2</sub>, 1 atm; λ > 345 nm; T = 25°C; 4 h irradiation time. Turnover number calculated as: products (mol)/catalyst (mol).

<sup>a</sup>pseudo-neat conditions by addition of 20 ml of solvent (HFP=hexafluoroisopropanol)

However operating in batch with dense membranes only part of the catalyst is really active in the catalytic process

The turnover dependence on the R<sub>f</sub>N<sub>4</sub>W10 loading and accessibility in Hyflon membrane was studied with membranes at 25% of catalyst loading and thickness in the range 7-90 μm (entries 5-7). Although a steady increase in the total oxidation products is observed as a function of the overall photocatalyst content, the reverse correlation between turnover efficiency and the membrane thickness, indicates a preferential activity of the surface layers with respect to the material bulk when operating in batch modality.

For this reason, using a photocatalytic membrane reactor operating with flow through the membrane, a further optimization of the membrane performance can be predicted.

Concerning the stability of the catalytic membranes, we observed that the polymeric films do not dissolve or release the photoactive component in hydrocarbon media as proved by UV-Vis, FT-IR and reactivity tests.<sup>30</sup>

The use of an hydrophobic material for catalyst heterogenization has been particularly appropriate in order to carry out reactions with organic substrates because the high affinity that can be realized between the polymeric matrix and the substrates.

The water contact angle (WCA) measured on the surface of a dense Hyflon membrane is  $108^\circ \pm 1$ . For comparison, we also carried out the same measurement on a dense membrane prepared using a partially fluorinated polymer, polyvinylidene fluoride (PVDF), and the WCA is  $91^\circ \pm 4$ .

The higher hydrophobic properties of the Hyflon in comparison with PVDF is the first factor which contribute to explain the better performance of the catalytic Hyflon-based membranes in comparison with the catalytic PVDF-based membranes (Tab. 7) in the ethylbenzene heterogeneous photooxidation.

We also measured the swelling of a dense Hyflon membrane and a dense PVDF membrane in liquids of interest for the reaction investigated: ethylbenzene (reagent), 2-phenylethanol (product) and acetophenone (product).

The membranes were dried at  $70^\circ\text{C}$  under vacuum for 24 hours before measurement of weight of the dry membrane. The membranes were then soaked in the testing liquid at  $30^\circ\text{C} \pm 1$  for 72 hours. After, the membranes were removed and wiped to remove any trace of liquid adsorbed on the surface. Immediately, the weight increase of the swollen membranes was measured. The membrane swelling (SW%) defined as:

$$SW\% = \frac{W_w - W_d}{W_d} \cdot 100 \quad (8)$$

where  $W_w$  and  $W_d$  are the weight of swollen and dry membrane, respectively.

The logarithm of the partition coefficient between n-octanol and water (LogP) was used in order to compare the compound's hydrophobicity (the LogP value increases with the hydrophobicity).

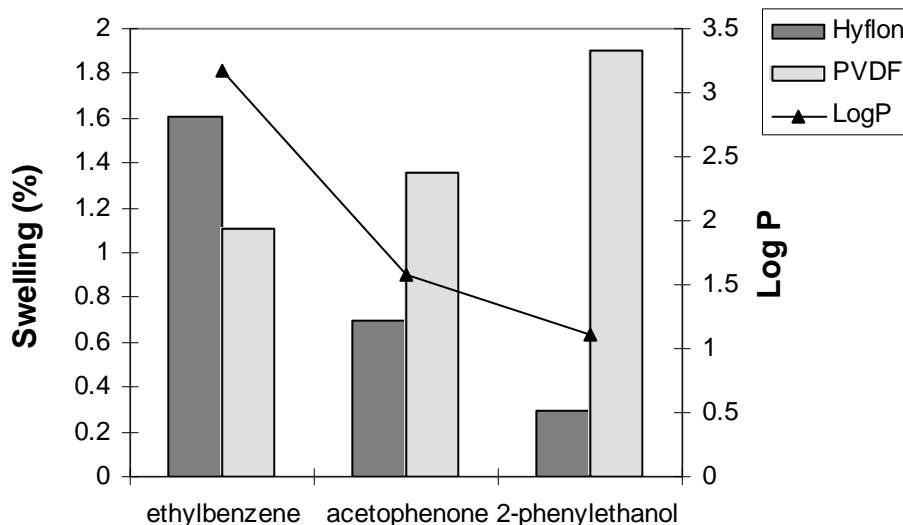


**Figure 34.** Swelling of a dense Hyflon and a dense PVDF membrane in pure liquid at  $30^{\circ}\pm 1$  and logarithm of the partition coefficient between n-octanol and water (LogP) of the pure testing liquid.

The more hydrophobic polymeric material, i.e. Hyflon, has a higher affinity towards the more hydrophobic (higher LogP value) liquid: ethylbenzene. On the contrary it has a low affinity for the more hydrophilic liquid: 2-phenylethanol (Fig. 34). These data can contribute to explain the high reactivity of the catalyst heterogenized in Hyflon membranes (high affinity for the reagent) and the high selectivity (low affinity for the product of interest, i.e. the alcohol, which limits the possibility of over-oxidation of the same).

The better performance of the catalytic Hyflon membranes, in comparison with the catalyst in homogeneous phase or heterogenized in different polymeric material, can depend also from electronic effect of the perfluorinated polymer (electron attractor) and the catalyst.

Moreover it is also well known that fluorinated environment can promote oxidation reactions.<sup>52</sup>

We have compared the oxygen solubility in Hyflon membranes with the oxygen solubility in a polydimethylsiloxane (PDMS) dense membrane, chosen as reference, because PDMS is one of the polymeric materials characterized by an higher solubility of the  $O_2$  (more high than PVDF), although is necessary to remember that the PDMS is a rubbery polymer and the Hyflon and PVDF are glassy polymers (amorphous the first one and semi-crystalline the second one).<sup>53</sup>

The main transport parameters (permeability, diffusion and solubility coefficients) of different gases in the PDMS membrane, Hyflon membrane and Hy-R<sub>f</sub>N<sub>4</sub>W10 (16.7 wt%) were determined by time-lag and steady state permeation experiments.

The Hyflon-based membranes are characterized by an higher O<sub>2</sub> solubility than the PDMS membrane (Tab. 8).

Also this result contribute, to explain the higher activity of the Hyflon based catalytic membranes in the batch experiments.

**Table 8.** Oxygen solubility in PDMS and Hyflon membranes at 25±1°C

O <sub>2</sub> Transport Membrane	Permeability barrer <sup>a</sup>	Select. (P <sub>i</sub> /P <sub>N2</sub> )	D cm <sup>2</sup> /s	S cm <sup>3</sup> /cm <sup>3</sup> bar
PDMS	560	2.06	420	0.21
Hyflon <sup>b</sup>	58.3	2.84	134	0.33
Hyflon-R <sub>f</sub> N <sub>4</sub> W10 (16.7 wt%)	52.5	2.44	39	0.29

<sup>a</sup>1 barrer = 10<sup>-10</sup> cm<sup>3</sup>(STP) cm<sup>-1</sup> s<sup>-1</sup> cmHg<sup>-1</sup>

<sup>b</sup>data from ref. 54

### Conclusions 2/3

The morphological analyses of Hyflon membrane containing the lipophilic salt of decatungstate (TBAW10) clearly revealed the presence of irregular catalyst aggregates.

On the contrary the use of fluorinated cations linked to the decatungstate anion ((R<sub>f</sub>N)<sub>4</sub>W<sub>10</sub>O<sub>32</sub>) improves the affinity between catalyst and polymer and the catalyst can be thoroughly dispersed in the membrane as spherical particles with uniform size.

The presence of the cationic amphiphilic R<sub>f</sub>N<sup>+</sup> groups induces a supramolecular self-assembly of surfactant-encapsulated catalyst clusters (R<sub>f</sub>N<sup>+</sup> groups capped on W<sub>10</sub>O<sub>32</sub><sup>4-</sup>).

A supramolecular self-assembly of these surfactant-encapsulated catalyst clusters allows the formation of the spherical catalyst aggregates with dimensions dependent from the membrane preparation conditions.

Moreover the coexistence of hydrophobic F-containing chains and hydrophilic ionic clusters in the Hyflon-R<sub>f</sub>N<sub>4</sub>W10 systems can be used for the formation of porous membrane by the templating effect of the water molecules.

In batch experiments of ethylbenzene (neat) oxidation, the Hyflon-R<sub>f</sub>N<sub>4</sub>W10 membranes showed super catalytic performance (higher turnover number and better selectivity) compared

to homogeneous catalyst or the catalyst heterogenized in different forms including in PVDF membranes.

This results depend not only from the specific electro-chemical environment of the catalytic site, but also from the high O<sub>2</sub> solubility and the favorable selectivity towards reagents and products of the perfluorinated polymeric material used for the catalyst heterogenization.

### **3.2 Heterogenization of heteropolyacids in proton exchange membranes for energy conversion**

Beside the catalysis, another strategic field for a sustainable growth is the energy production. The increasing energy demand worldwide and environment protection need prompt to study more and more efficient and clean energy conversion technologies. In this frame, the fuel cells (FCs) technology plays an important role because it allows to generate electricity by direct electrochemical conversion of a fuel and an oxidant with both a low pollution level emission and an high efficiency.

However, before fuel-cell technology can gain a significant share of the electrical power market, important issues have to be addressed. These issues include for the polymer electrolyte membrane fuel cell (PEMFCs, principally used in stationary and mobile devices) the development of alternative materials for the proton conducting membranes (PEMs).

Commercialization aspects, including cost and durability, and technical aspects, including high water and methanol crossover and dehumidification problems, have revealed inadequacies of the Nafion and related materials, still today, commonly used in fuel-cell.<sup>55</sup>

Much effort has been applied to the development of cheaper, fluorine-free, membrane materials and polyarylenetherketones-based membranes have been extensively investigated as possible alternative to Nafion for their low cost, high conductivity, good chemical and thermal stability.<sup>56</sup>

As reported in the chapter II, the starting polyetheretherketone (PEEK) presented in many literature works as possible alternative to Nafion for PEMFCs, is a semicrystalline thermoplastic polymer known as Victrex<sup>®</sup> PEEK.<sup>57</sup>

However, a modified PEEK indicated as PEEK-WC or poly(oxa-p-phenylene-3,3-phthalido-p-phenylene-oxa-p-phenylene-oxy-p-phenylene) is a more promising candidate for PEMs development because it is amorphous and the sulfonation reaction can be carried out in shorter time and in completely homogeneous phase in comparison with PEEK Victrex.<sup>58, 59</sup>

The higher glass transition of the PEEK-WC in comparison with the PEEK Victrex, both as starting polymers and sulfonated derivatives, opens the possibility to use the first one at higher temperature than the second one (e.g. the Tg of SPEEK-WC at DS=0.8 is 247°C<sup>60</sup>, the Tg of the SPEEK at the same DS is about 217°C<sup>61</sup>).

Moreover the SPEEK-WC membranes are characterized by an higher stability in water and methanol in comparison with traditional SPEEK membranes at similar degree of sulfonation (DS).<sup>62</sup>

The water and methanol permeability of the SPEEK-WC membranes, are lower than Nafion 117. The proton conductivity of the SPEEK-WC membranes are good and increases with the DS value, however the values were lower than those obtained with a Nafion 117 membrane.<sup>63</sup>

In order to improve the proton conductivity of the SPEEK-WC based membranes, in this work, we have developed new composite membranes entrapping different inorganic proton conductors in the polymeric matrix.

**Table 9.** Some properties of the heteropolyacids used in this work

	$\text{H}_3\text{PW}_{12}\text{O}_{40} \cdot n \text{H}_2\text{O}$ (PW12)	$\text{H}_4\text{SiW}_{12}\text{O}_{40} \cdot n \text{H}_2\text{O}$ (SiW12)	$\text{H}_3\text{PMo}_{12}\text{O}_{40} \cdot n \text{H}_2\text{O}$ (PMo12)	Ref.
<b>Molecular weight (g/mol)</b>	2880.2	2878.3	1825.3	-
<b>Number of crystallization water molecules (n)</b>	29	30	29	64
<b>Proton conductivity at room temperature (S/cm)</b>	$8 \cdot 10^{-2}$	$2 \cdot 10^{-2}$	$1 \cdot 10^{-1}$	65
<b>pK<sub>1</sub><sup>(a)</sup></b>	1.6	2.0	2.0	66
<b>pK<sub>2</sub><sup>(a)</sup></b>	3.0	3.6	3.6	66
<b>pK<sub>3</sub><sup>(a)</sup></b>	4.0	5.3	5.3	66
<b>Acid strength</b>	PW12 > SiW12 ≥ PMo12			66, 67
<b>Oxidation potential</b>	PMo12 >> PW12 > SiW12			66
<b>Thermal stability</b>	PW12 > SiW12 > PMo12			66
<b>Hydrolytic stability</b>	SiW12 > PW12 > PMo12			66

<sup>(a)</sup> Dissociation Constants in acetone at 25°C

Tungstophosphoric acid  $H_3PW_{12}O_{40}$  (PW12), silicotungstic acid  $H_4SiW_{12}O_{40}$  (SiW12) and phosphomolybdic acid  $H_3PMo_{12}O_{40}$  (PMo12) have been used as super acid additives in the composite membranes (Table 9).

These additive have superacid properties because the large size of the heteropolyanion;<sup>66,67</sup> they have been widely used not only as acid catalysts, but also in order to improve the properties of polymeric proton exchange membranes because, they can contribute to the proton transport in the solid state.<sup>68</sup>

The chemical-physical and electrochemical characterization carried-out on the polymeric and composite membranes SPEEK-WC-based, with different DS, was compared with the same values obtained with a commercial Nafion 117 membrane chosen as reference.

#### Membrane preparation and chemical-physical characterization

Sulfonated PEEK-WC with degree of sulfonation (DS) from 0.1 to 1.04 has been kindly supplied by Prof. Francesco Trotta (University of Turin). These samples have been prepared by reaction with  $ClSO_3H$  at room temperature for reaction times from 0.5 to 5 hours.<sup>58</sup>

Commercially available HPAs (PW12, SiW12 and PMo12), solvents and reagents were used as received from Sigma, without further purification.

Nafion 117 membranes (EW 110, thickness 178 $\mu$ m) have been purchased from Quintech (Germany).

Polymeric and composite SPEEK-WC membranes were prepared by phase inversion technique induced by solvent evaporation.

For the polymeric membranes, a 16 wt% of polymer in DMA solution was stirred at room temperature overnight. The solution was cast onto a glass plate (initial thickness from 250 to 1000  $\mu$ m). in a thermostatic box at  $25\pm 1^\circ C$  and  $20\pm 1\%$  of relative humidity (RH) for two days. Then, the SPEEK-WC-based membranes were peeled off in a water bath at room temperature. After, they were immersed for additional 24 hours in a new water bath in order to remove eventual residual traces of solvent, the membranes were dried at room temperature for 24 hours and finally in a vacuum oven at  $70^\circ C$  for additional 24 hours.

Polymeric membranes in the following test are indicated as SPWC(DS value).

For the composite membranes preparation, the same protocol has been used with the exception of the adding to the homogeneous SPEEK-WC solution in DMA, of a 4 wt% of the HPA in order to obtain 20 wt% of the inorganic additive loading in the final membrane.

Composite membranes are indicated in the following test as SPWC(DS value)+HPA code.

Characterization of the membranes by FT-IR (also in ATR), UV-vis and SEM spectroscopies, pure gas permeation experiments, have been carried out as described in the previous sections. Also in this case the pure gas permeability of the membranes has been calculated from the pressure increase of the fixed permeate volume and the gas solubility by the time lag method; however because the sulfonated PEEKWC can absorb up to about 20 wt.% of water upon exposure to the air, each membrane was dried for at least 5 h under vacuum to remove all absorbed water before the permeation measurement. The membrane was kept under vacuum in the permeation cell by a two-stage rotary pump until the baseline slope was significantly below the steady state pressure increase rate. Between two subsequent gases the system was evacuated for a period of at least 5 times the time lag of the previous gas in order to guarantee the complete removal of the previous gas from the system and from the membrane. Water and methanol vapours permeation tests were performed using the cell described in figure 35.

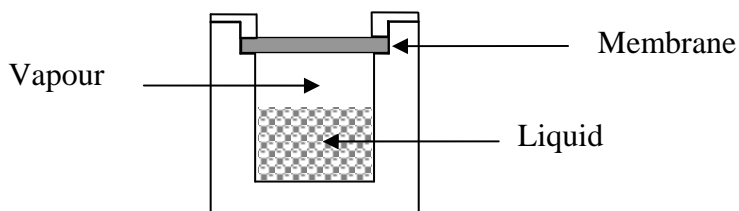


**Figure 35.** Permeation cell used for water and methanol vapors permeation experiments

The membrane was clamped over the cell containing the pure liquid (water or methanol) and keep in contact with the vapour saturated atmosphere. The cell was placed in a box with temperature and relative humidity control. The experiments were performed at  $50 \pm 1^\circ\text{C}$  and the weight variation of the cells was measured until the steady state permeation rate was reached. The partial pressure gradient is given by the difference between the internal ( $P_{\text{int}}$ ) and external ( $P_{\text{ext}}$ ) vapour pressure. The  $P_{\text{int}}$  is assumed equal to the saturated vapour pressure of the liquid at the operative temperature;  $P_{\text{ext}}$  in the case of the methanol is assumed to be zero (box volume  $\gg$  cell volume), in the case of water is calculated considering the relative humidity value in the box ( $50 \pm 1\%$ ).



Stress/strain mechanical tests have been carried using a Z2.5 Zwick Roell instrument and the test data have been elaborated by the TestXpert V11.0 Master software.

Conditions used: size of specimen 40x10 mm, test speed: 4 mm/min; temperature 25°C and humidity 52 RH%.

For each testing reported, at least four specimens were taken and average value was calculated.

#### Determination of Electrochemical Properties of Membranes

The performance of an ion-exchange membranes in the various electro-membrane processes is determined to a very large extent by their electrochemical properties. Therefore, a major task in characterizing PEM is the determination of their electrochemical properties such as the ion-exchange capacity (IEC) and the proton conductivity.

The IEC of the membrane has been measured by acid-base titration method (Fig.36).

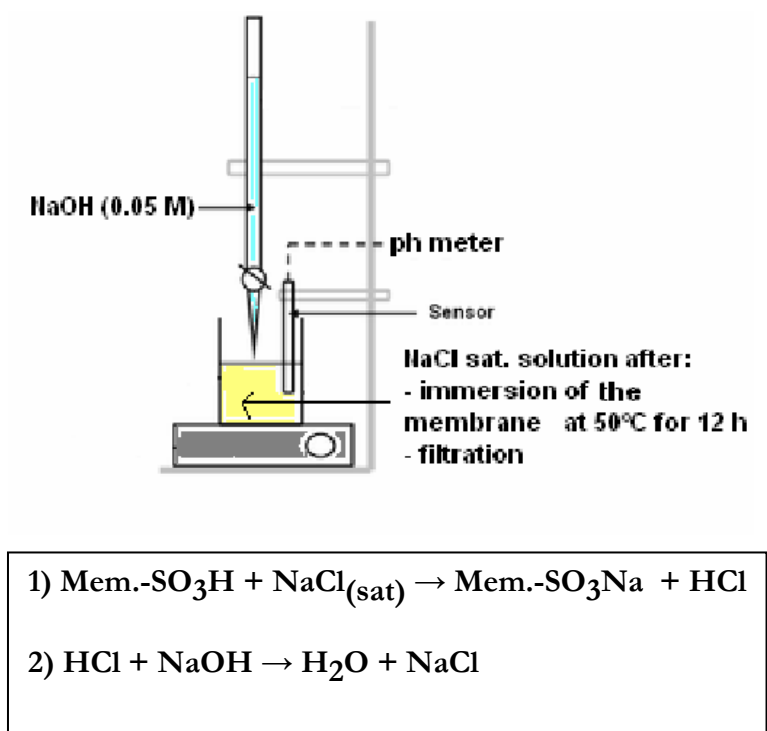


**Figure 36.** Titration procedure used to measure the ion exchange capacity of the membranes

A weighted sample of dry membrane (cut in small pieces) has been immersed in a saturated NaCl solution in water at 50°C for 12 hours under magnetic stirring; the resulting solution has been filtrated and titrated at room temperature with a solution of NaOH (0.05 mol/L) until neutrality (pH meter immersed in solution).

The IEC is calculated as:

$$\text{IEC} = \frac{\text{mol. H}^+ \text{exchanged}}{\text{membrane mass}} = \frac{\text{mol. OH}^- \text{reacted}}{\text{membrane mass}} \quad [\text{mol/g}] \quad (9)$$

For each type of membrane the procedure has been repeated three times.

Proton conductivity has been measured via impedance spectroscopy using a impedance/gain phase analyzer Solartron 1260 (AC amplitude 100 mV; Initial frequency 10 MHz, Final frequency 1 Hz) and the results were elaborated by the Zplot software (Scribner Associates, Inc., USA).

The impedance data were correct for the contribution of the empty and the short-circuit cell. Before the test, the membrane (disc with  $\phi = 9$  mm) was soaked in water for at least 5 hours and then dried on the surface, then, the sample was placed in a home made two-compartment conductivity measurement cell.

The membrane was clamped between two porous stainless steel disc electrodes in the membrane compartment.

The relative humidity (RH) has been controlled by a second compartment containing water keep at temperatures equal or lower than the first compartment by using a tubular oven (Fig. 37).

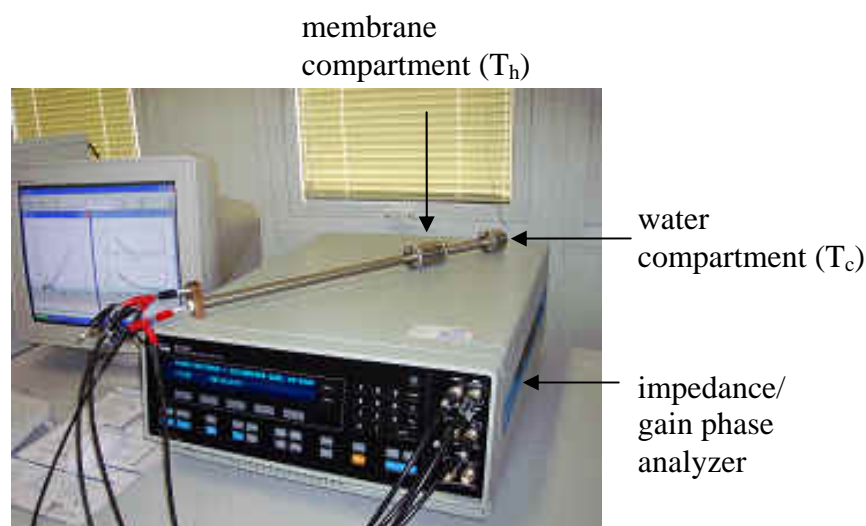


**Figure 37.** Photo of the two compartment cell (inserted inside a tubular oven during the measurement) and the Impedance/gain phase analyzer used for the proton conductivity determination

The RH can be calculated from the ratio between the pressures of saturated water vapor ( $p$ ) at the temperatures of the cold ( $T_c$ ) and hot ( $T_h$ ) compartment<sup>69</sup>:

$$RH = \frac{p(T_c)}{p(T_h)} \cdot 100 \quad (10)$$

The conductivity values reported are refer to measurements carried out after the conductivity had reached a constant value for at least 2 h.

The conductivity of the samples in the transverse direction was calculated from the impedance data, using the following relationship:

$$\sigma = \frac{d}{R \cdot S} \quad (11)$$

Where  $\sigma$  is the conductivity ( $S \text{ cm}^{-1}$ ),  $d$  (cm) and  $S$  ( $\text{cm}^2$ ) are respectively the thickness and area of the sample, and  $R$  ( $\Omega$ ) is the membrane resistance.  $R$  was derived from the intersect at high frequency with real axis of the impedance in the Niqsit plot (imaginary component vs real component of the impedance).

The impedance<sup>70</sup> is defined, in analogy to Ohm's law, as:

$$Z_{(\omega)} = \frac{U_{(\omega)}}{I_{(\omega)}} \quad (12)$$

with:

$$U_{(\omega)} = U_o \sin \omega t \quad (13)$$

and

$$I_{(\omega)} = I_o \sin \omega t + \varphi \quad (14)$$

Here  $Z$  is the impedance,  $U$  is the voltage and  $\omega$  is the frequency of the alternating current  $I$ ,  $t$  is the time,  $\varphi$  is the phase shift between voltage and current, and the subscript  $o$  refers to the amplitude of voltage and current, and  $(\omega)$  refers to a certain frequency.

The frequency  $\omega$  is given by  $2 \pi \nu$ , where  $\nu$  is the circular frequency.

For  $n$  impedances in series the total impedance is:

$$Z_{\text{total}} = Z_1 + Z_2 + \dots + Z_n \quad (15)$$

for  $n$  impedances in parallel the total impedance is:

$$\frac{1}{Z_{\text{total}}} = \frac{1}{Z_1} + \frac{1}{Z_2} + \dots + \frac{1}{Z_n} \quad (16)$$

The impedance is composed of two parts, i.e. the real part given by  $Z' = Z_o \sin \varphi$  and the imaginary part given by  $Z'' = iZ_o \cos \varphi$ :

$$Z_{(\omega)} = \frac{U_{(\omega)}}{I_{(\omega)}} = Z_o e^{-i\varphi} = Z_o \sin \varphi - iZ_o \cos \varphi \quad (17)$$

The impedance related to an resistance (R) and to a capacitance (C) are different. For a resistance the imaginary part of the impedance is zero since the current and voltage are in phase and the real part is independent from the frequency.<sup>70</sup>

$$Z = \frac{U_o}{I_o} = R \quad (18)$$

For a capacitance the impedance is :

$$Z = \frac{1}{i \omega C} \quad (19)$$

A real system like an ion-exchange membrane in an electrolyte is a combination of these elements in series or in parallel.<sup>70</sup>

The total impedance for a resistance and a capacitance in series is given by<sup>70</sup>

:

$$Z_{(\omega)\text{total}} = R + \frac{1}{i \omega C} \quad (20)$$

According to eq. 20 the imaginary part will disappear at very high frequencies if resistance and capacitance are in series and the impedance is identical to the ohmic resistance.

At very low frequencies the resistance of the capacitance increases with decreasing frequency and becomes infinitely high in direct current.

For resistance and capacitance in parallel the total impedance is given by<sup>70</sup>  
:

$$Z_{(\omega)\text{total}} = \frac{R}{1 + \omega^2 R^2 C^2} - i \frac{\omega R^2 C}{1 + \omega^2 R^2 C^2} \quad (21)$$

As indicated by the eq. 21, the imaginary part of the impedance disappears at very low and very high frequencies.<sup>70</sup>

At very low frequency all current is passing through the resistance and the impedance is identical to the ohmic resistance.

At very high frequencies both the imaginary and the real part of the impedance approach to zero.

Moreover, with increasing frequency the phase shift between current and voltage is increasing and with the phase shift the imaginary part of the impedance is increasing and reaches a maximum at a frequency  $\omega=1/RC$ . A further increase in frequency will increase the phase shift but will decrease the imaginary part of the impedance

In a membrane electrode assembly (MEA) may be both resistances and capacitances in series and in parallel and the membrane resistance to the transport of the protons is usually obtained by extrapolating in the Niqsit plot ( $Z''$  vs  $Z'$ ) the intercept at high frequency with the real axis.<sup>70</sup>

### Result and discussion

All the SPEEK-WC-based membranes prepared are transparent, flexible and homogeneous (Fig. 38).

SEM images showed a dense structure for both polymeric and composite membrane (Fig. 39). The good affinity between the organic and inorganic phase allowed the self-assembly of homogeneous hybrid membranes.



**Figure 38.** Photograph of SPEEK-WC membranes with various DS ((A) in order from left to right: 0.10, 0.22, 0.36, 0.60, 0.70, 0.80, 1.04) and a composite membrane containing  $H_3PW_{12}O_{40}$  ((B) DS=0.8)

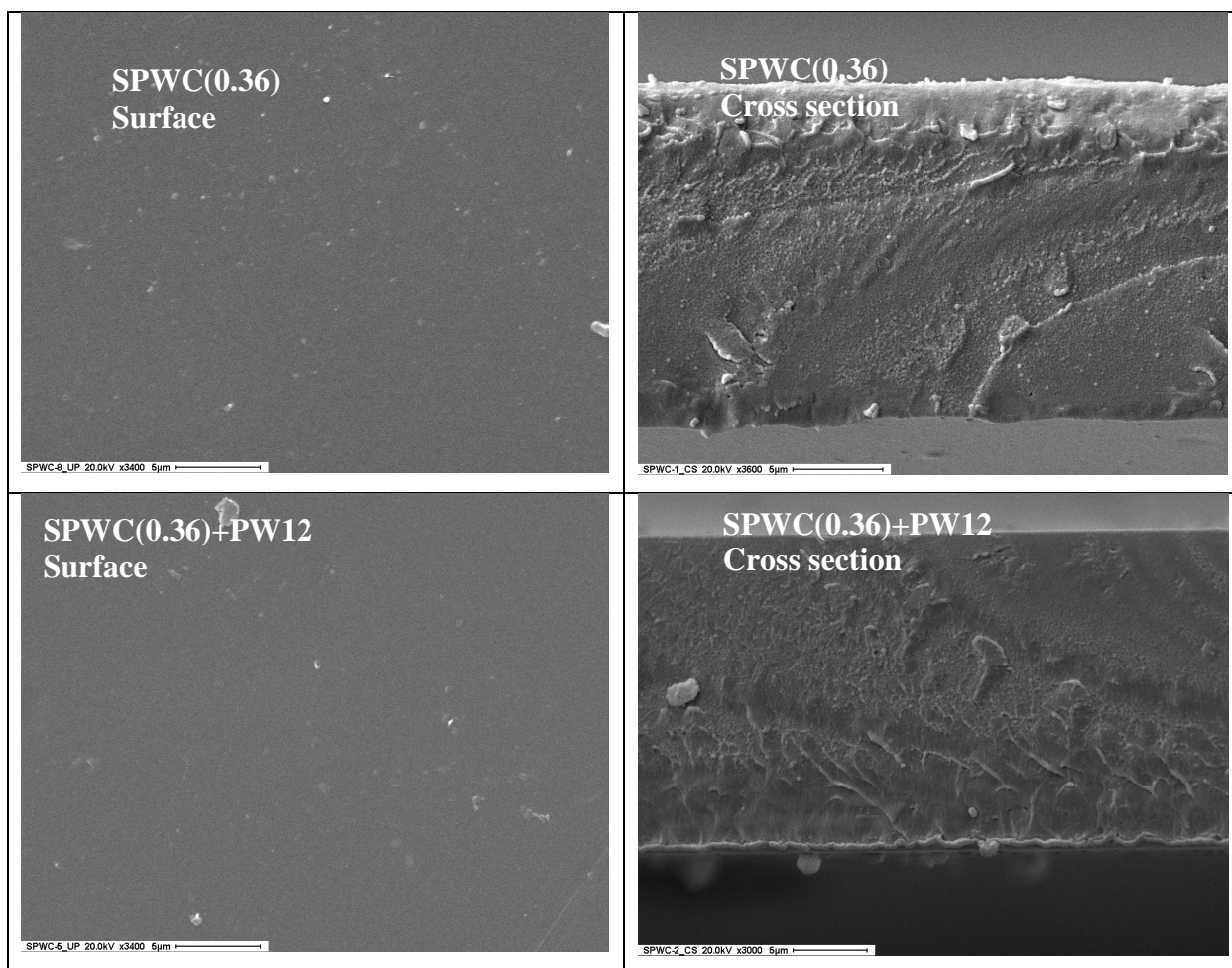


**Figure 39.** SEM images of the polymeric SPEEK-WC membrane with DS 0.36 (SPWC(0.36)) and the composite membranes containing  $H_3PW_{12}O_{40}$  at the same sulfonation level (SPWC(0.36)+PW12)

The good adhesion between the inorganic additives and the polymeric matrix and the homogeneous distribution on nanometric scale of the inorganic phase in the polymeric matrix, has been confirmed also by BSE images of the composite membranes (Fig. 40).

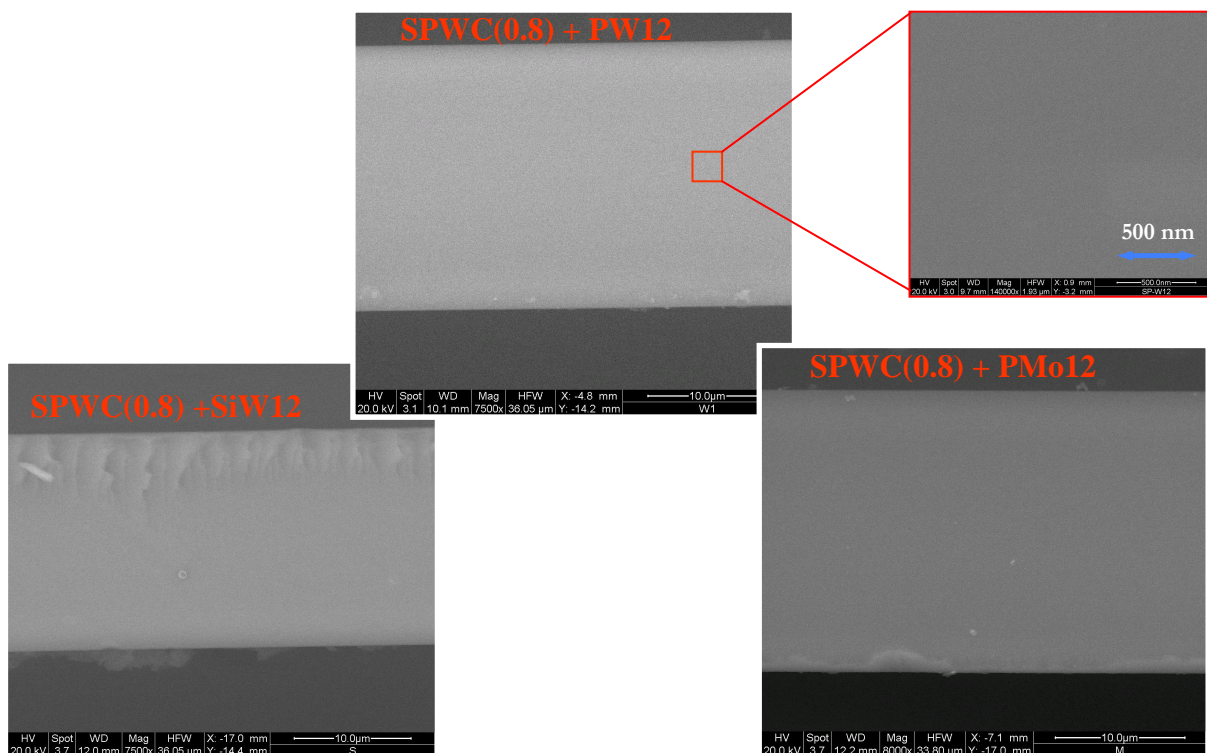


**Figure 40.** SEM images in BSE modality of the composite SPEEK-WC membranes (DS=0.8)

The polymeric membrane prepared using the SPEEK-WC polymer with various DS (from 0.1 to 1.04) have been characterized by FT-IR spectroscopy and compared with a membrane prepared using the unmodified PEEK-WC.

In the spectra of the SPEEK-WC membranes, in addition to the wide band at  $3430\text{--}3460\text{ cm}^{-1}$  due to the stretching of the hydroxyls groups of the  $\text{SO}_3\text{H}$  and the hydration water molecules, a new band appears at  $1480\text{ cm}^{-1}$ , not present in the spectra of the PEEK-WC membrane (fig. 41).

The intensity of this last band assigned to the  $\text{C}\equiv\text{C}$  skeletal vibrations of the tri-substituted aromatic rings, increases with the DS. On the contrary, the intensity of the band at  $1500\text{ cm}^{-1}$  of the  $\text{C}\equiv\text{C}$  skeletal vibrations of the di-substituted aromatic rings decreases with the DS (Fig. 41).

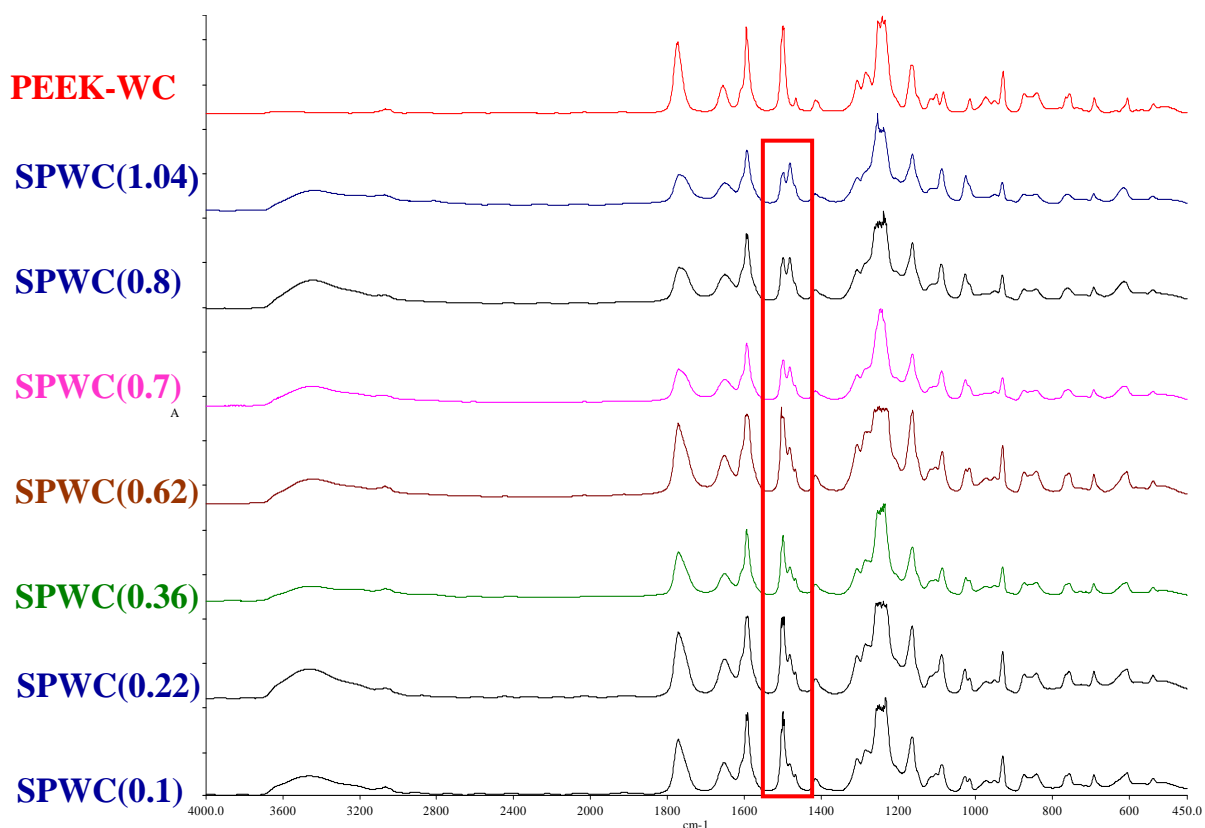


**Figure 41.** FT-IR spectra (absorbance) of a PEEK-WC and S-PEEK-WC membranes (DS from 0.1 to 1.04)

FT-IR analyses confirmed the structural integrity of the HPAs in the polymeric matrix. The typical bands of the Keggin HPAs (Fig. 42 and Tab. 10) are present also in the spectra of the composite membranes. However, HPAs interact with the SPEEK-WC matrix by hydrogen bonds and Coulombic interactions and a small shift of the M=O and O-M-O (M is Mo for PMO12 and W for PW12 and SiW12) bands has been observed: the first is shifted at lower wavenumbers and the second at higher (Fig. 43).



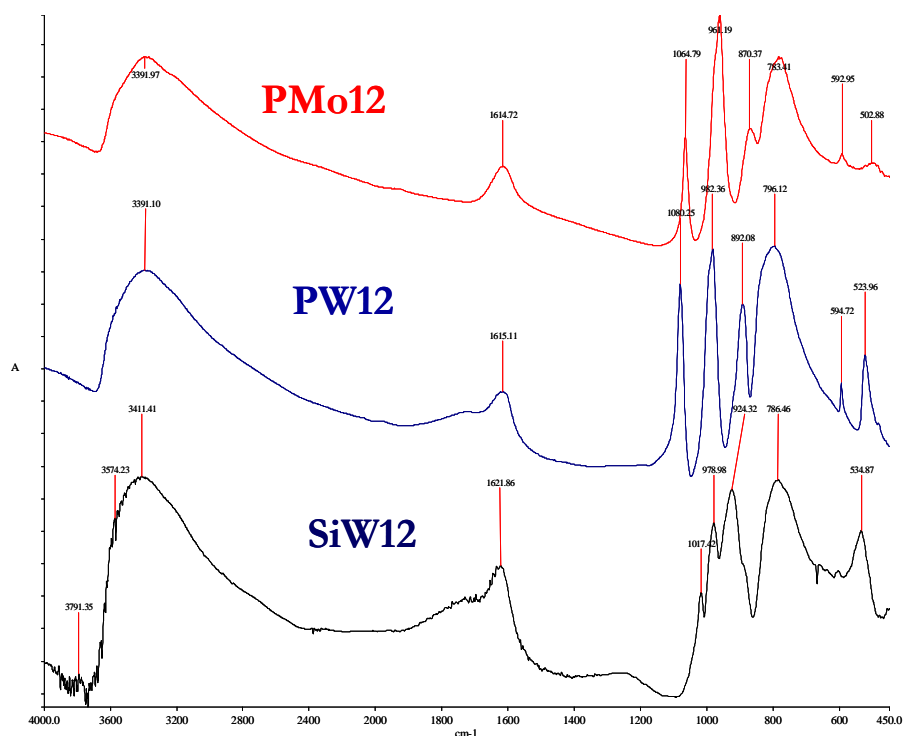
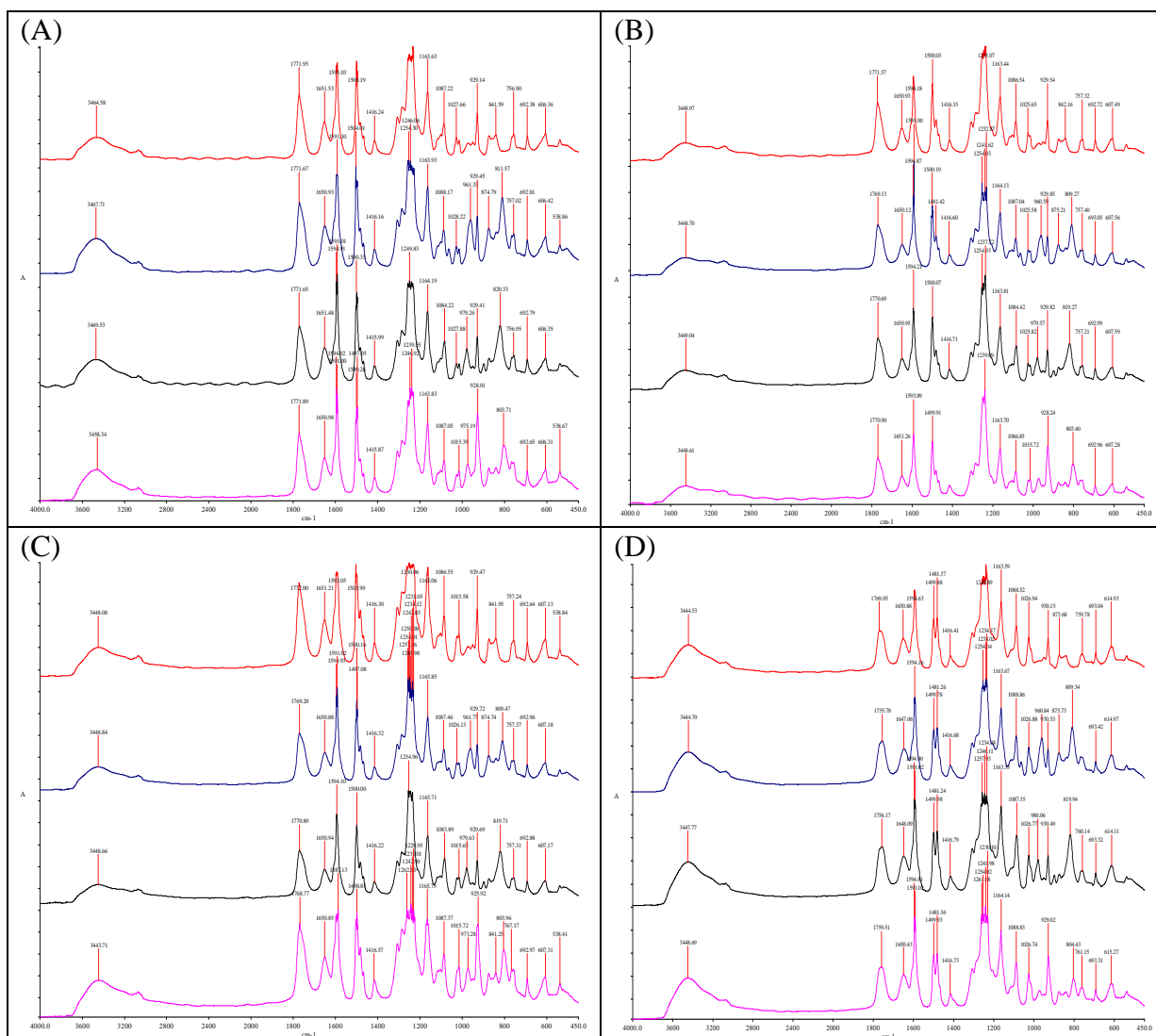


Figure 42. FT-IR spectra of the pure HPA

Table 10. Typical bands of the heteropolyacids used in this study

H <sub>3</sub> PMo <sub>12</sub> O <sub>40</sub>		
Wavenumber (cm <sup>-1</sup> )	Signal	Group
1065	Strech. asym.	P-O
961	Strech. asym.	Mo=O <sub>t</sub>
870	Strech. asym.	Mo-O <sub>b</sub> -Mo
783	Strech. asym.	Mo-O <sub>c</sub> -Mo
593	Bend.	O-P-O
503	Strech. sym.	Mo-O <sub>c</sub> -Mo
H <sub>3</sub> PW <sub>12</sub> O <sub>40</sub>		
Wavenumber (cm <sup>-1</sup> )	Signal	Group
1080	Strech. asym.	P-O
982	Strech. asym.	W=O <sub>t</sub>
892	Strech. asym.	W-O <sub>b</sub> -W
796	Strech. asym.	W-O <sub>c</sub> -W
595	Bend.	O-P-O
532	Strech. sym.	W-O-W
H <sub>4</sub> SiW <sub>12</sub> O <sub>40</sub>		
Wavenumber (cm <sup>-1</sup> )	Signal	Group
979	Strech. asym.	W=O <sub>t</sub>
924	Strech. asym.	Si-O
786	Strech. asym.	W-O <sub>c</sub> -W
534	Strech. sym.	W-O-W



**Figure 43.** FT-IR spectra of the membranes at DS 0.1 (A), 0.36 (B), 0.62 (C) and 0.8 (D).

For each series from the top is reported: the polymeric membrane, the composite containing PMO12, the composite containing PW12 and the composite containing SiW12.

As can be easily predicted, we observed an increase of ion exchange capacity of the SPEEK-WC membranes with the increase of the DS, i.e. with the increase of the number of acid groups per gram of membrane (Fig. 44). The membranes with higher DS have a IEC similar to Nafion.

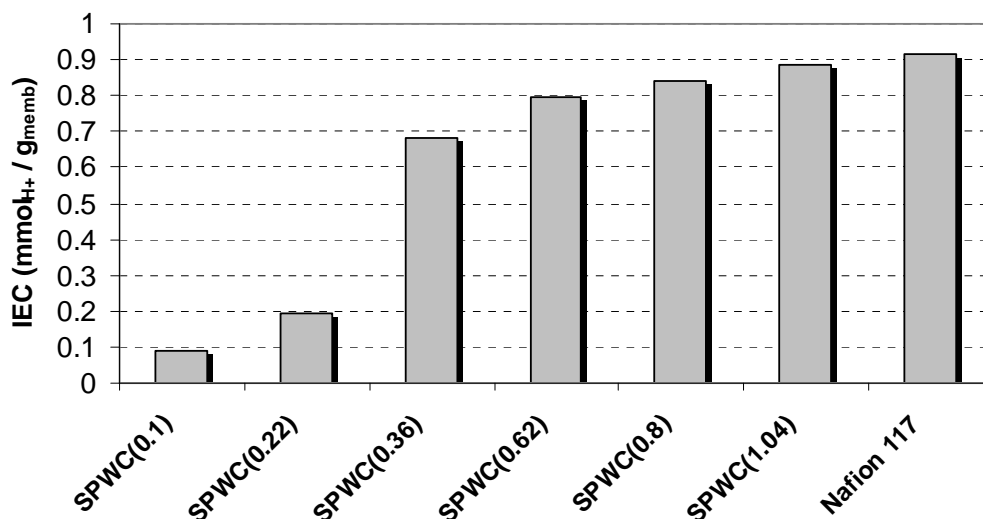


**Figure 44.** Ion exchange capacity measured on the polymeric SPEEK-WC membranes at various DS and a commercial Nafion 117 membrane

The presence of the superacid additives increase the IEC values. In particular the composite membranes incorporating  $H_3PMO_{12}O_{40}$ , showed the higher IEC values (Fig. 45). This can be explained considering the lower molecular weight of this additive (Tab. 9) and, as a consequence, the higher number of moles per gram of membrane (all the composite membranes are at 20 wt%).

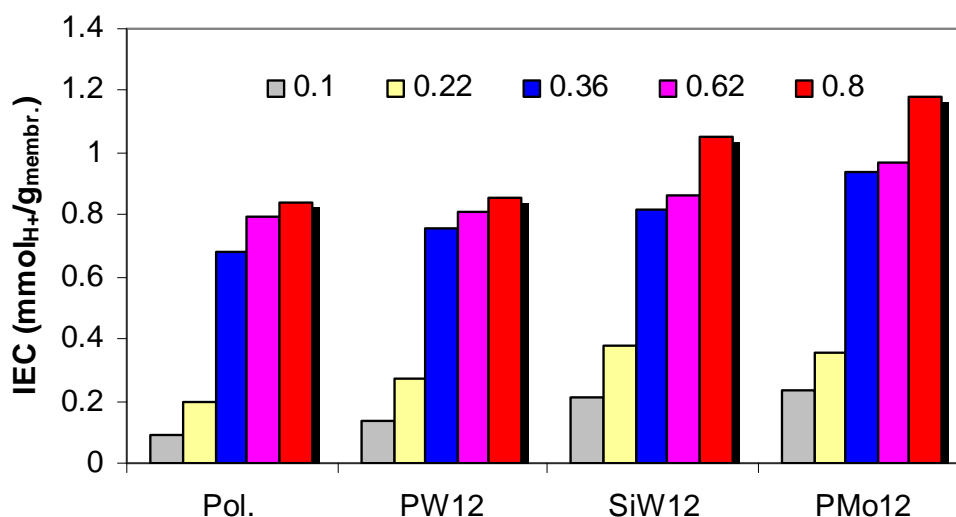
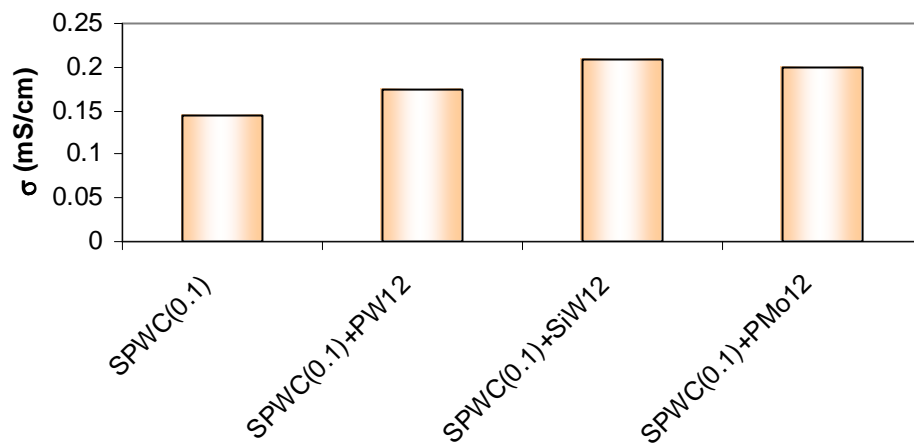


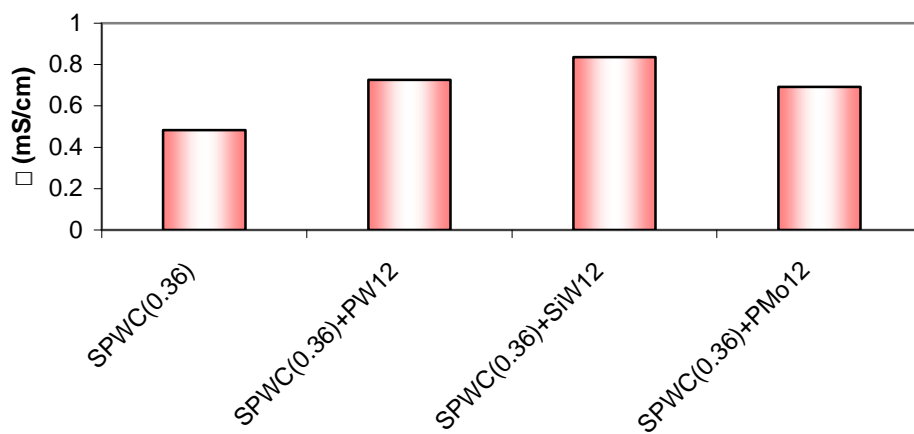
**Figure 45.** Ion exchange capacity of the polymeric and composite membrane (on the x axis is indicated the code of the additive used) at various DS

Also the proton conductivity increase with the DS and the composite membrane contribute to reduce the resistance to the proton transport (Fig. 46).

(A)



(B)



(C)

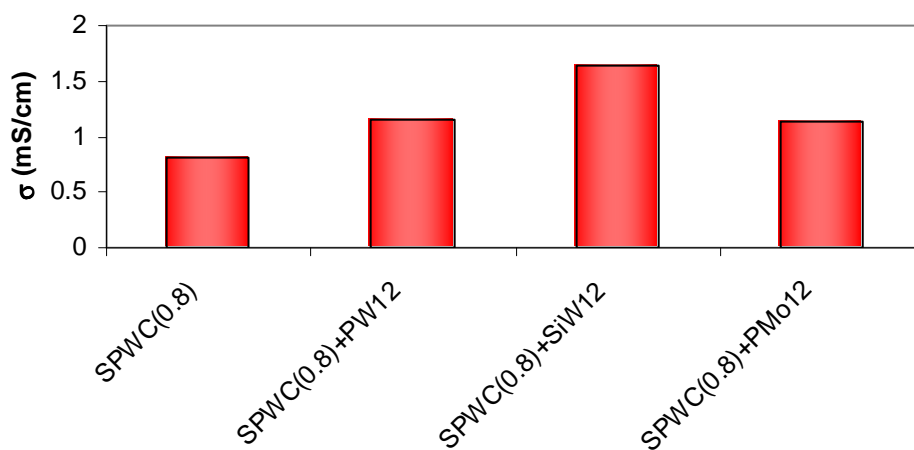


**Figure 46.** Proton conductivity at  $25 \pm 1^\circ\text{C}$  and 100%RH of the polymeric and composite membranes at DS 0.1 (A), 0.36 (B) and 0.8 (C)

The effect of the additives on the proton conductivity is due to their water hydration molecules and dioxonium ions that are used to better interconnect the ionic cluster of the polymeric matrix providing a better pathway for proton hopping.

As reported in chapter II, in the Keggin type HPAs, hydrogen bonds exist between each acid proton and two water molecules, hydrogen bonds are also present between water molecules and the terminal oxygen atoms of the HPAs and, finally, hydrogen bonds involving water molecules can exist between different Keggin units.<sup>71</sup>

FT-IR spectra of the composite membranes (Fig. 43) confirmed the instauration of an interaction between the HPAs and the SPEEK-WC.

Because the HPAs are dispersed on nanometric scale in the proton exchange membrane, the water hydration molecules and the dioxonium ions of the additive have been used to better interconnect the ionic cluster of the polymeric matrix providing a better pathway for proton hopping.<sup>72</sup>

The better additive resulted to be the  $H_4SiW_{12}O_{40}$  heteropolyacid. Moreover operating at higher temperature and lower relative humidity its positive effect on proton transport is more evident and the proton conductivity of the composite membranes approaches the value of the Nafion (Fig. 47).

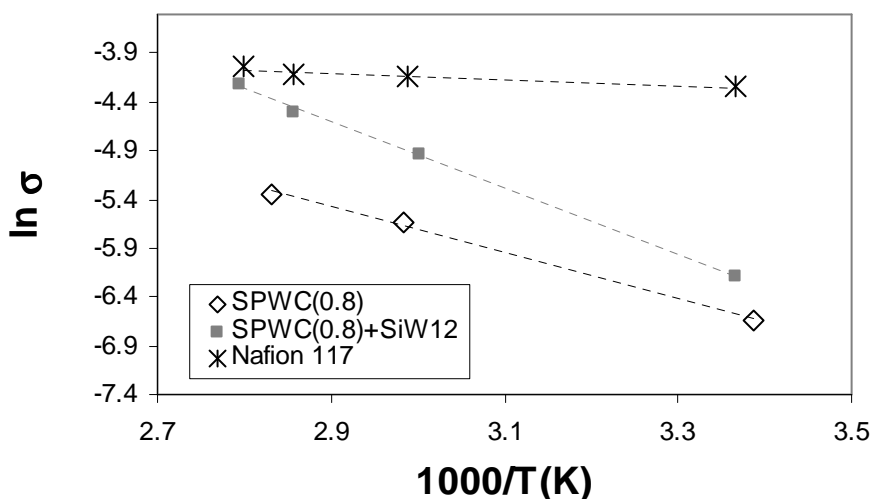


**Figure 47.** Arrhenius plot of the proton conductivity at 75% relative humidity of the Nafion 117 and the SPEEK-WC(DS=0.8) polymeric and composite (containing SiW12) membranes

Concerning the mechanical properties, we observed the decrease of the elastic modulus when DS increases for SPEEK-WC based membranes because the increase of hydration water molecules which swell the hydrophilic regions of the membrane and reduce the membrane rigidity (Tab. 11).

A little increase of the elastic modulus was observed in the presence of the inorganic additive which reinforced the structure, but the values are still higher compared to Nafion 117

Moreover, the S-PEEK-WC based membranes are characterized by a relatively low, in comparison with Nafion, and constant elongation at break (%) (Tab. 11).

These difference depends by the different microstructure of the perfluorinated Nafion and non fluorinated SPEEK-WC membranes.<sup>73</sup>

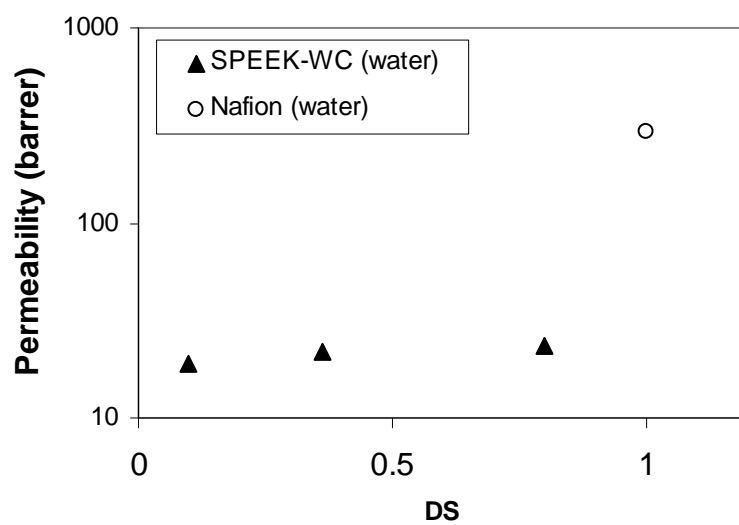
**Table 11.** mechanical properties in stress/strain elongation test carried out on Nafion and SPEEK-WC-base membranes at 25°C and 52 RH%

Membrane	Elastic modulus (N/mm <sup>2</sup> )	Breaking Modulus (N/mm <sup>2</sup> )	Elongation at break (%)
Nafion 117	193	22.5	281
SPWC(0.36)	1658	69.2	5.5
SPWC(0.6)	833	41.4	7.3
SPWC (0.88)	567	28.0	4.7
SPWC (0.88)+SiW12	587	44.7	5.3

Interesting results have been obtained considering the transport of water and methanol in these SPEEK-WC membranes that have a lower methanol and water permeability respect to Nafion 117 (at least one order of magnitude).

No relevant differences between the polymeric and the composite membranes were observed (Figs. 48, 49).

(A)



(B)

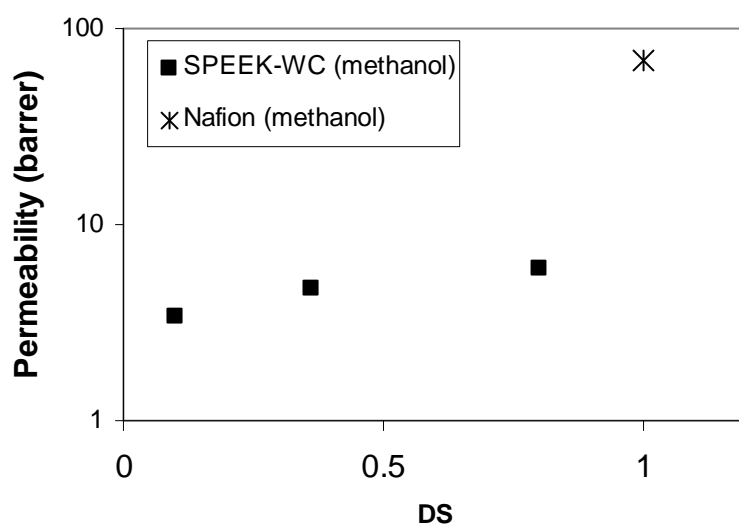
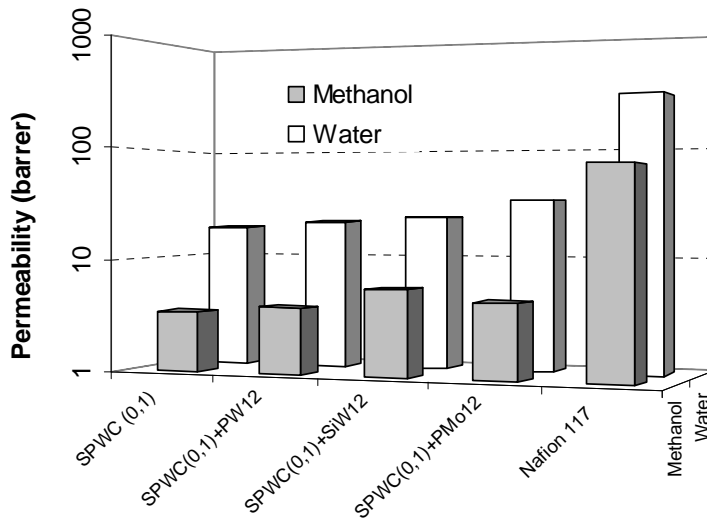
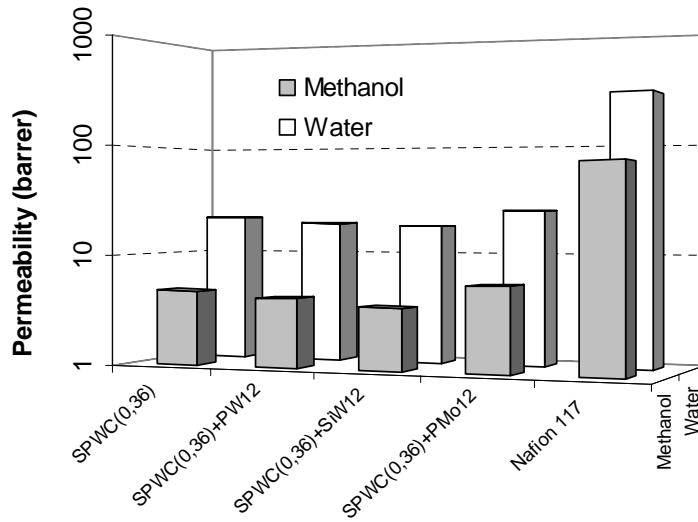


**Figure 8.** Water (A) and methanol (B) vapour permeability of the SPEEK-WC membranes, as a function of the degree of sulfonation (DS), and of the Nafion 117 (we arbitrarily assumed DS=1) at  $50\pm 1^\circ\text{C}$  ( $1 \text{ barrer} = 10^{-10} \text{ cm}^3(\text{STP}) \text{ cm}^{-1} \text{ s}^{-1} \text{ cmHg}^{-1}$ ).

(A)



(B)



(C)

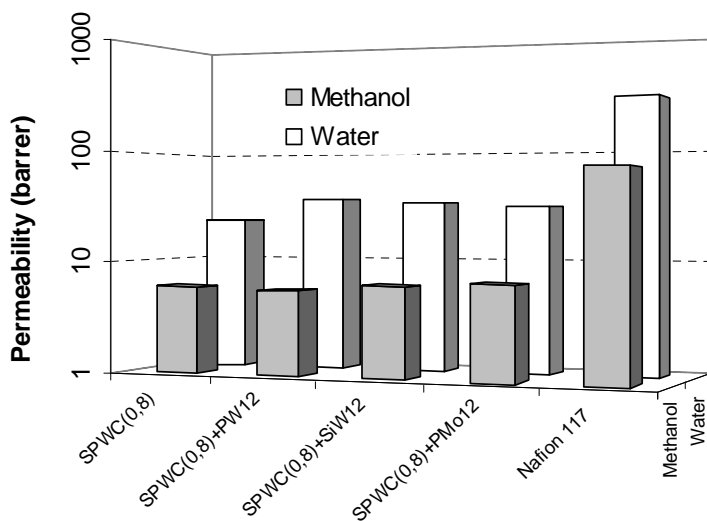


**Figure 9.** Water and methanol vapour permeability through the polymeric and composite SPEEK-WC membranes ((A) DS=0.1; (B) DS=0.36; (C) DS=0.8) and Nafion 117 at 50±°C (1 barrer = 10<sup>-10</sup> cm<sup>3</sup>(STP) cm<sup>-1</sup> s<sup>-1</sup> cmHg<sup>-1</sup>).



Also the gas permeability through the SPEEK-WC membranes was better, because lower, in comparison with Nafion 117 (Tab. 12).

In particular the lower permeability of O<sub>2</sub> and H<sub>2</sub> allows a minor loss of fuel and oxidant in the PEMFC operative conditions. The presence of the inorganic additives further reduce the permeability.

**Table 12.** Gas permeability at 25±1°C measured with the membranes in the dry state

Gas	SPWC (0.8)	SPWC(0.8)+SiW12	Nafion 117
	Permeability (barrer)	Permeability (barrer)	Permeability (barrer)
O <sub>2</sub>	0.109	0.079	0.817
H <sub>2</sub>	3.73	2.83	5.57
He	5.53	4.60	28.9
CO <sub>2</sub>	-	0.290	2.08

T=25±1°C

1 barrer = 10<sup>-10</sup> cm<sup>3</sup>(STP) cm<sup>-1</sup> s<sup>-1</sup> cmHg<sup>-1</sup>

### Conclusions 3/3

Polymeric SPEEK-WC-based dense membranes have been prepared by phase inversion induced by solvent evaporation.

These systems have promising properties for applications in PEMFCs. They have a lower water, methanol, O<sub>2</sub> and H<sub>2</sub> permeability in comparison with a Nafion 117 commercial membranes.

The proton conductivity of the SPEEK-WC membranes increases with the degree of sulfonation, however, as expected for a non fluorinated PEM, the proton conductivity is lower in comparison to Nafion.

The heterogenization of inorganic proton conductors (HPAs), in particular the H<sub>4</sub>SiW<sub>12</sub>O<sub>40</sub>, in SPEEK-WC membranes improves the proton conductivity. The HPAs, are uniformly distributed on nanometric scale and interconnect better the ionic cluster of the polymeric matrix providing a favoured pathway for protons hopping.

Operating at higher temperature and lower relative humidity the advantages to use the composite membranes is more evident because the high capacity of these inorganic systems to retain water and reduces the resistance to the proton transport in these conditions.

FT-IR spectra of the composite membranes confirmed the instauration of interactions between the HPAs and the SPEEK-WC, however the Keggin structure was preserved.

The water, methanol and gases permeability of the composite membranes was similar to those of the polymeric with similar DS. In fact, the good adhesion between the inorganic particles and the polymeric chains allows to obtain hybrid systems without pinholes or defect.

## REFERENCES

- <sup>1</sup> K. Szaciłowski, W. Macyk, A. Drzewiecka-Matuszek, M. Brindell, G. Stochel, *Chem Rev.* 105 (2005) 2647–2694.
- <sup>2</sup> A. Maldotti, A. Molinari, R. Amadelli, *Chem. Rev.* 102 (2002) 3811-3836.
- <sup>3</sup> M. Bonchio, M. Carraro, M. Gardan, G. Scorrano, E. Drioli, E. Fontananova, *Top. Catal.* 40 (2006) 133
- <sup>4</sup> P. Pandit, S. Basu, *Ind. Eng. Chem. Res.* 43 (2004) 7861- 7864.
- <sup>5</sup> W. Liu, J.A. Howell, T.C. Arnot, J.A.Scott, *J. Membrane Sci.* 181 (2001) 127-140.
- <sup>6</sup> K.A. Krishnan, T.S. Anirudhan, *J. Hazard. Mater.* B92 (2002) 161-183.
- <sup>7</sup> S.H .Lin, C.H. Wang, *Ind. Eng. Chem. Res.* 42 (2003) 1648-1653.
- <sup>8</sup> M. H. Heggemann, H.-J. Warnecke, H. J. Viljoen, *Ind. Eng. Chem. Res.* 40 (2001) 3361-3368.
- <sup>9</sup> F.J. Rivas, V. Navarrete, F.J. Beltrán, J.F. García-Araya, *Appl. Catal., B.* 48 (2004) 249-258.
- <sup>10</sup> P. Battistoni, R. Boccadoro, D. Bolzonella, S. Pezzoli, *Ind. Eng. Chem. Res.* 40 (2001) 4506-4512.
- <sup>11</sup> D. Rajkumar, K. Palanivelu, *Ind. Eng. Chem. Res.* 42 (2003) 1833-1839.
- <sup>12</sup> Q. Wang, A.T. Lemley, *J. Agric. Food Chem.* 51 (2003) 5382-5390
- <sup>[13]</sup> P.G. Gogate, A.B. Pandit, *Adv. Environ. Res.* 8 (2004) 553-597.
- <sup>14</sup> M. Pera-Titus, V. Garcya-Molina, M.A. Baños, J. Giménez, S. Esplugas, *Appl. Catal., B.* 47 (2004) 219–256
- <sup>15</sup> A. Mylonas, E. Papaconstantinou, *Polyhedron* 15 (1996) 3211-3217.
- <sup>16</sup> P. Kormali, D. Dimoticali, D. Tsiipi, A. Hiskia, E. Papaconstantinou, *Appl. Catal. B-Environ.* 48 (2004) 175.
- <sup>17</sup> S. Antonaraki, E. Androulaki, D. Dimotikali, A. Hiskia, E. Papaconstantinou, *J. Photoch. Photobio. A.-C.* 148 (2002) 191.
- <sup>18</sup> I.V. Kozhevnikov, *Chem. Rev.* 98 (1998) 171
- <sup>19</sup> M. Misono, I. Ono, G. Koyano, A. Aoshima, *Pure Appl. Chem*, 72 (2000) 1305
- <sup>20</sup> V. Ramani, H.R. Kunz, J.M. Fenton, *J. Membrane Sci.* 232 (2004) 31-44.
- <sup>21</sup> M. T. Pope, *Heteropoly and Isopoly Oxometalates*, Springer-Verlag: New York, 1983.
- <sup>22</sup> M. Bonchio, M. Carraro, G. Scorrano, E. Fontananova, E. Drioli, *Adv. Synth. Catal.* 345 (2003) 1119-1126.
- <sup>23</sup> I. Texier, C. Giannotti, S. Malato, C. Richter, J. Delaire, *Catal. Tod.* 54 (1999) 297.
- <sup>24</sup> E. Fontananova, E. Drioli, L. Donato, M. Bonchio, M. Carraro, G. Scorrano, *The Chinese Journal of Process Engineering* 6 (2006) 645-650 (
- <sup>25</sup> E. Fontananova, E. Drioli, L. Donato, M. Bonchio, M. Carraro, M. Gardan, G. Scorrano, *Desalination* 200 (2006) 705-707
- <sup>26</sup> E. Fontananova et al., Heterogenization of decatungstate in polymeric membranes: an efficient and environmental friendly photocatalytic system, In preparation

- 
- <sup>27</sup> A. Mylonas, E. Papaconstantinou, *Polyhedron* 15 (1996) 3211-3217.
- <sup>28</sup> P. Kormali, D. Dimoticali, D. Tsipi, A. Hiskia, E. Papaconstantinou, *Appl. Catal. B-Environ.* 48 (2004) 175.
- <sup>29</sup> S. Antonaraki, E. Androulaki, D. Dimotikali, A. Hiskia, E. Papaconstantinou, *J. Photoch. Photobio. A.-C.* 148 (2002) 191.
- <sup>30</sup> M. Carraro, M. Gardan, G. Scorrano, E. Drioli, E. Fontananova, M. Bonchio, *Chemical Communications* 43 (2006) 4533
- <sup>31</sup> J. Burdeniuc, M. Sanford, R.H. Crabtree, *J. of Fluorine Chem.* 91 (1998) 49.
- <sup>32</sup> A. Berkessel, M.R.M. Andreae, *Tetrahedron Lett.* 42 (2001) 2293.
- <sup>33</sup> S. de Visser, J. Kaneti, R. Neumann, S. Shaik, *J. Org. Chem.* 68 (2003) 2903.
- <sup>34</sup> D.W. Van Krevelen, *Properties of polymers*, third ed., Elsevier Science, Amsterdam, 1990.
- <sup>35</sup> A.F.M. Barton, *Handbook of Polymer-Liquid Interaction Parameters and Solubility Parameters*, CRC Press, Boca Raton, Florida; 1990.
- <sup>36</sup> D.C Duncan., T.L. Netzel, C.L. Hill, *Inorg. Chem.* 34 (1995) 4640.
- <sup>37</sup> M. Macchione, J.C. Jansen, G. De Luca, E. Tocci, M. Longeri, E. Drioli, *Polymer* 48 (2007) 2619-2635,
- <sup>38</sup> *J Macromol Sci Phys* 517 2001
- <sup>39</sup> H. Strathmann, L. Giorno, E. Drioli, *An introduction to membrane science and technology*, Publisher CNR, Roma, 2006.
- <sup>40</sup> E. Fontananova, J.C. Jansen, A. Cristiano, E. Curcio and E. Drioli, *Desalination* 192 (2006) 190–197.
- <sup>41</sup> A. Chemseddine, C. Sanchez, J. Livage, J.P. Launay, M. Fournieric, *Inorg. Chem.* 23 (1984) 2609-2613
- <sup>42</sup> T.Boccaccio, A. Bottino, G. Capannelli, P. Piaggio, *Journal of Membrane Science*, 210 (2002) 315-329.
- <sup>43</sup> K. Tashiro, *Crystal structure and phase transition of PVDF and related copolymers*, in: H.S. Nalwa (Ed.), *Ferroelectric Polymers*, Marcel Dekker, New York, NY, 1995, pp. 65-69.
- <sup>44</sup> E.Drioli, E. Curcio, E. Fontananova (2006), *Mass Transfer Operation–Membrane Separations*, in *Chemical Engineering*, [Eds. John Bridgwater, Martin Molzahn, Ryszard Pohorecki], in *Encyclopedia of Life Support Systems (EOLSS)*, Developed under the Auspices of the UNESCO, Eolss Publishers, Oxford ,UK, [<http://www.eolss.net>].
- <sup>45</sup> D. R.Dillon., K.K. Tenneti, C.Y. Li, F.K. Ko, I. Sics, B. S. Hsiao, *Polymer* 2006; 47: 1678.
- <sup>46</sup> M. Minglin, H. M. Randal, *Curr. Opin. Colloid. Interface Sci.* 11 (2006) 193.
- <sup>47</sup> J.C. Jansen, F. Tasselli, E. Tocci, E. Drioli, *Desalination*, 192 (2006) 192, 207
- <sup>48</sup> V. Arcella, P. Colaianna, P. Maccone, A. Sanguineti, A. Gordano, G. Clarizia, E. Drioli, *J. Membr. Sci.* 163 (1999) 203.
- <sup>49</sup> Crank J, Park GS, *Diffusion in Polymers*, Academic Press, London, 1986.

- 
- <sup>50</sup> W. Bu, H. Li, H. Sun, S. Yin, L. Wu, *J. Am. Chem. Soc.* 127 (2005) 8016
- <sup>51</sup> H. Li, H. Sun, W. Qi, M. Xu, L. Wu, *Angew. Chem. Int. Ed.* 46 (2007) 1300
- <sup>52</sup> P. G. Boswell, P. Buhlmann, *J. Am. Chem. Soc.* 127 (2005), 8958-8959.
- <sup>53</sup> D.W. Van Krevelen *Properties of Polymers-* Elsevier Third edition 1990
- <sup>54</sup> J.C. Jansen, F. Tasselli, E. Tocci, E. Drioli *Desalination* 192 (2006) 207-213
- <sup>55</sup> B.C.H. Steele, A. Heinzl, *Nature* 414 (2001) 345-352
- <sup>56</sup> K.D. Kreuer, *Journal of Membrane Science*, 185 (2001) 29-39
- <sup>57</sup> [http://www.victrex.com/en/peek\\_poly/properties.php](http://www.victrex.com/en/peek_poly/properties.php)
- <sup>58</sup> F. Trotta, E. Drioli, G. Moraglio, E. Baima Poma, Sulfonation of Polyetheretherketone by Chlorosulfuric Acid. *J. Appl. Polym. Sci.*, 70 (1998) 477-482
- <sup>59</sup> E. Drioli, A. Regina, M. Casciola, A. Oliveti, F. Trotta, T. Massari, *J. Membrane Sci.*, 228 (2004) 139-148.
- <sup>60</sup> E. Fontananova et al. Polymeric and composite SPEEK-WC membranes: promising systems for application in Proton Exchange Membrane Fuel Cells (PEMFCs), In preparation
- <sup>61</sup> S.M.J. Zaidi, S.D. Mikhailenko, G.P. Robertson, M.D. Guiver, S. Kaliaguine, *J. Membrane Sci.* 173 (2000) 17-34.
- <sup>62</sup> E. Fontananova, E. Drioli, A. Regina, J.C. Jansen, S.C. Mio, F. Trotta, Development of new non fluorinated polymeric and composite membranes for applications in fuel cells, 3rd Korea-Italy S&T Forum, April 19-20, 2007, Seoul, Korea (p. 40)
- <sup>63</sup> A. Regina, E. Fontananova, E. Drioli, M. Casciola, M. Sganappa, F. Trotta, *J. Power Sources* 160 (2006) 139-147
- <sup>64</sup> U.B. Mioč, M.R. Todorović, M. Davidović, Ph. Colombari, I. Holclajtner-Antunović, *Solid State Ionics* 176 (2005) 3005-3017
- <sup>65</sup> G. Alberti, M. Casciola, *J. Membr. Sci.*, 145 (2001) 3-16
- <sup>66</sup> I.V. Kozhevnikov, *Catalysis by Heteropoly Acids and Multicomponent Polyoxometalates in Liquid-Phase Reactions*, *Chem. Rev.* 1998, 98, 171-198
- <sup>67</sup> T. Okuhara, Water-tolerant solid acid catalysts, *Chem. Rev.* 102 (2002) 3641-3666
- <sup>68</sup> V. Ramani, H.R. Kunz, J.M. Fenton, *J. Membrane Sci.* 232 (2004) 31-44.
- <sup>69</sup> G. Alberti, M. Casciola, L. Massinelli, B. Bauer, *Journal of Membrane Science* 185 (2001) 73
- <sup>70</sup> H. Strathmann, *Ion exchange membrane separation processes*, Elsevier 2004
- <sup>71</sup> J.B. Moffat, *Polyhedron* 5 (1986) 261
- <sup>72</sup> V. Ramani, H.R. Kunz, J.M. Fenton, *Journal of Membrane Science* 232 (2004) 31-44
- <sup>73</sup> K. D Kreuer. On the development of proton conducting polymer membranes for hydrogen and methanol fuel cells. *J. Membrane Sci.* 185 (2001) 29-39

## Conclusions

Membrane operations have already numerous successfully applications ranging from water desalination, medical engineering, wastewater treatments, food applications and, in general, in every process where a separation is needed.

However, not only the new areas of application of membrane processes, including artificial organs and Micro Electro Mechanical Systems (MEMS), but also those already well established such as catalytic membrane reactors (CMRs) and polymer electrolyte fuel cells (PEMFCs), are creating new materials demands that traditional ones can't fulfill.

One of the most promising strategies to respond to these requests is the combination of two or more materials in a synergistic mode to obtain new composite membranes with better separation properties and/or with new functionalities.

In this thesis, we have investigated the heterogenization of inorganic polyoxanions within various polymeric membranes for applications in catalysis and fuel cells.

In particular novel catalytic membranes have been designed and developed by the heterogenization of the photocatalyst decatungstate ( $W_{10}O_{32}^{4-}$ ) in polymeric membranes.

The photocatalytic composite membranes are characterized by different and tuneable properties depending on the nature of the polymeric micro-environment in which the catalyst is confined.

Decatungstate in the form of a lipophilic tetrabutylammonium salt ( $(n-C_4H_9N)_4W_{10}O_{32}$  indicated as TBAW10) has been well dispersed in porous membranes made of PVDF.

Solid state characterization techniques confirmed that the catalyst' structure and spectroscopic properties have been preserved within the membranes.

The catalytic membranes were successfully applied in the aerobic photo-oxidation of the phenol, one of the main organic pollutants in wastewater, providing stable and recyclable photocatalytic systems.

The dependence of the phenol degradation rate by the catalyst loading in membrane and the transmembrane pressure has been also investigated, allowing to identify the catalytic membrane, with catalyst loading 25.0 wt.% and operating at 1 bar, as the more efficient system.

Catalyst' stability has been positively influenced by the polymeric environment in which the catalytic system is confined, moreover the selective separation function of the membrane results in an enhanced of the phenol mineralization in comparison with homogeneous reaction.

Decatungstate has been also heterogenized in Hyflon membrane. Hyflon is an amorphous perfluoropolymer that offers several advantages when compared to other polymeric materials. Besides its outstanding thermal and oxidative resistance, the peculiar nature of the C-F bonds confers to this materials some unique physical-chemical properties, in particular an high dioxygen solubility.

Initially, we tried to heterogenize the fluorine-free TBAW10 in the Hyflon membranes. However the low affinity between the catalyst and the polymeric matrix induced the formation of irregular catalyst aggregates not well dispersed in the polymeric matrix.

We have demonstrated the possibility to improve the affinity between the polymer and the catalyst by an appropriate functionalizations of the second one, this in order to avoid the catalyst leaching, to have a good adhesion between polymer and catalyst and a good dispersion of the same.

In particular the fluorine-tagged decatungstate,  $([\text{CF}_3(\text{CF}_2)_7(\text{CH}_2)_3]_3\text{CH}_3\text{N})_4\text{W}_{10}\text{O}_{32}$  indicated as  $(\text{R}_f\text{N})_4\text{W}_{10}$  has been well dispersed in the Hyflon membranes as spherical clusters with uniform size.

The decatungstate self-assembling process has been tuned by a proper choice of the membrane preparation conditions.

Moreover the coexistence of hydrophobic F-containing chains and hydrophilic ionic clusters in the  $(\text{R}_f\text{N})_4\text{W}_{10}\text{O}_{32}$ /Hyflon systems can be used for the formation of porous membrane by using the templating effect of the water molecules.

Also the methods used to prepared porous or dense functionalized Hyflon membranes, has guaranteed, not only the catalyst heterogenization by a good dispersion in the polymeric matrix, but also its structural and spectroscopic integrity.

The new multifunctional membranes prepared have been used to catalyze the photooxidation of the ethylbenzene (neat).

These systems showed super catalytic performance (higher turnover number and better selectivity) compared to homogeneous catalyst.

The higher activity of the fluoro-containing decatungstate dispersed in the Hyflon matrix depend on the specific electro-chemical environment of the catalytic sites, the high  $\text{O}_2$  solubility and the selectivity towards reagents and products of the perfluorinated polymeric material.

Finally electrostatic self-assembled composite membrane have been prepared for possible application in PEMFCs.

Commercial available Keggin type heteropolyacids have been dispersed on nanometric scale in polyelectrolytes membranes made of sulfonated PEEK-WC.

SPEEK-WC membranes are promising systems for applications in PEMFCs because of their good proton conductivity and the high resistance opposed to the water, methanol, H<sub>2</sub> and O<sub>2</sub> transport. In particular, in comparison with a commercial Nafion 117 membrane, the SPEEK-WC membranes are at least 10 times less permeable to water and methanol, but, as expected for a non fluorinated ion exchange material, also the proton conductivity of these systems is lower. However, the heterogenization of the inorganic proton conductors in SPEEK-WC membranes improves the proton conductivity without significantly modify the other transport properties.

The positive effect of the inorganic additives on proton conductivity is more evident operating at higher temperature and lower humidity values.



Relazione del Collegio dei Docenti del Dottorato di Ricerca in  
***Ingegneria Chimica e dei Materiali***  
Facoltà di Ingegneria, Dipartimento di Ingegneria Chimica e dei Materiali  
Università degli Studi della Calabria  
XX Ciclo

La dottoranda Enrica FONTANANOVA, laureata in Chimica, ha affrontato il Dottorato di Ricerca in Ingegneria Chimica e dei Materiali allo scopo di completare le conoscenze nella scienza dell'Ingegneria Chimica e dei Materiali, con particolare riferimento all'applicazione di processi di separazione a membrana accoppiati a reazioni chimiche (reattori catalitici a membrana) o a trasformazioni energetiche (celle a combustibile).

La dottoranda, oltre ad avere acquisito i fondamentali delle tematiche in oggetto, ha saputo affrontare le problematiche emerse nel corso degli studi con spirito critico dimostrando come l'integrazione di operazioni a membrana in processi di interesse industriale possa avere un positivo effetto in termini sia di efficienza che di impatto ambientale, nella logica del *process intensification* per uno sviluppo sostenibile.

La dottoranda Enrica FONTANANOVA ha condotto nel suo triennio di Dottorato uno studio sulla funzionalizzazione di membrane polimeriche con additivi inorganici dotati di attività catalitica e/o conducibilità protonica per applicazioni rispettivamente in reattori catalitici a membrana e celle a combustibile ad elettrolita polimerico.

Nel primo caso l'eterogenizzazione del componente inorganico in membrana ha conferito una nuova funzionalità alla stessa (membrana catalitica), nel secondo la coesistenza della fase organica e di quella inorganica ha avuto un effetto sinergico nel migliorare le proprietà di trasporto della membrana (conducibilità protonica).

I risultati ottenuti sono stati oggetto di 6 pubblicazioni su riviste internazionali, 8 presentazioni orali e 4 presentazioni in forma di poster in congressi internazionali, oltre che 3 presentazioni orali e 3 presentazioni poster in convegni nazionali (AICIng e SCI).

Nel lavoro di tesi sono stati approfonditi argomenti quali:

- eterogenizzazione del decatungstato (poliossometallato (POM) attivabile per via fotochimica) in membrane di polivinilidene fluoruro (PVDF) e di Hyflon, caratterizzazione chimico-fisica delle membrane catalitiche, loro applicazione in reazioni di ossidazione;
- eterogenizzazione di tre diversi eteropoliacidi (POM in forma acida:  $H_3PW_{12}O_{40}$ ,  $H_4SiW_{12}O_{40}$  e  $H_3PMo_{12}O_{40}$ ) in membrane di PEEK-WC solfonato, caratterizzazione chimico-fisica ed elettrochimica delle membrane e analisi dell'influenza di diverse variabili, quali grado di solfonazione, natura e concentrazione degli additivi inorganici, sulle proprietà di trasporto.

Nel corso di tutto il suo lavoro la dottoranda FONTANANOVA ha dimostrato doti di entusiasmo per la ricerca, dedizione allo studio e capacità di approfondimento, privilegiando sia i fondamentali chimici che gli aspetti di maggiore interesse ingegneristico delle problematiche affrontate.

Durante il triennio di dottorato la Dottoranda FONTANANOVA ha svolto attività didattica consistente nello svolgimento delle esercitazioni nei corsi di Chimica per Ingegneria A.A. 2004/2005, 2005/2006 e 2006/2007, partecipando anche agli esami come membro di commissione.

Il Collegio dei Docenti, visto l'impegno profuso e la qualità della sua attività, esprime un giudizio molto favorevole ai fini dell'ammissione della Dott.ssa Enrica FONTANANOVA all'esame finale per il conseguimento del titolo di Dottore di Ricerca in Ingegneria Chimica e dei Materiali.

Addì, 09.11.2007



Il Coordinatore del Collegio  
Prof. Rosario Aiello

*Rui*